Expression of the plant Photosystem II core proteins in the cyanobacterium *Synechocystis* sp. PCC6803 and characterization of the DEAD-box RNA helicase RH50 of *A. thaliana*

Dissertation der Fakultät für Biologie der Ludwig-Maximilians-Universität München

vorgelegt von: Francesca PAIERI

Munich, 2018

Expression of the plant Photosystem II core proteins in the cyanobacterium *Synechocystis* sp. PCC6803 and characterization of the DEAD-box RNA helicase RH50 of *A. thaliana*

Dissertation

zur Erlangung des Doktorgrades der Fakultät für Biologie

der Ludwig-Maximilians-Universität München

Francesca Paieri

Erstgutachter: Prof. Dr. Dario Leister

Zweitgutachter: Prof. Dr. Jörg Nickelsen

Tag der Einreichung: 12.04.2018

Tag der mündlichen Prüfung: 26.07.2018

Summary

In plants and algae, oxygenic photosynthesis occurs in chloroplasts, subcellular structures that originate from the endosymbiosis of a cyanobacterium. The study of the photosynthetic apparatus of higher plants, its assembly and regulatory mechanism is of great importance for understanding the flexibility of photosynthesis. The investigation of the photosynthetic proteins and assembly factors, however, is hampered by the technical and biological limits of plants as model organism. The generation of model prokaryote organism, carrying a plant-like photosynthetic apparatus, offers a new strategy for studying and improving plant photosynthesis. To this aim, the photosynthetic apparatus of *A. thaliana* could be introduced in the cyanobacterium *Synechocystis*, where it would be easier to be studied and manipulated. The focus of my thesis is to assemble a functional plant PSII in *Synechocystis*. For this purpose two synthetic constructs, RC1, encoding the PSII plant proteins D1, D2, CP43 and PsbI, and RC2, encoding $Cytb_{559}$, PsbL, PsbJ, CP47, PsbT and PsbH, were generated and independently cloned into *Synechocystis*. The strain *ΔpsbA2DC RC1*, KO for the endogenous *psbA2* and *psbDC* genes, was able to grow photoautotrophically and accumulate the plant proteins CP43 and PsbI, carried by the RC1 construct. This strain could also accumulate the transcripts of the synthetic plant genes *AtpsbA2* and *AtpsbD* but further analysis are needed to determine whether the protein is present. In contrast, the *psbEFLJ RC2* strain, KO for the endogenous *psbEFLJ* operon, could not accumulate the transcripts of the RC2 construct, probably due to transcript instability or activation of a transcriptional regulatory mechanism.

DEAD-box RNA helicases (DBRHs) modify RNA secondary structures and are involved in RNA metabolism. Many DBRHs are targeted to the chloroplast, but the role of the majority of them is still unknown. RH50 is a chloroplast-located DBRH that co-localizes and is co-expressed with GUN1, a key factor in chloroplast-to-nucleus signaling. When mutations in *rh50* and *gun1* genes were introduced into genetic backgrounds impaired in plastid gene expression (*prors1-1, prpl11-1, prps1-1, prps21-1, prps17-1 and prpl24-1*) *rh50* and *gun1* show similar phenotypic patterns at physiological and molecular level. Moreover, the double mutant of *rh50-1 gun1-102* exhibit a reduction in size, supporting the idea that RH50 and GUN1 are functionally related. RH50 is involved in PRORS-triggered-plastid-to-nucleus retrograde signaling as PHANGs repressor like GUN1. The *rh50* mutant showed sensitivity to

erythromycin and cold-stress and is impaired in processing of the 23S-4.5S intergenic region. The RH50 protein co-migrates with ribosomal particles and can bind the 23S-4.5S intergenic region *in vivo* and *in vitro*. Based on these results, I conclude that RH50 is a plastid rRNA maturation factor.

Zusammenfassung

In Pflanzen und Algen findet die oxygene Photosynthese in den Chloroplasten statt. Diese Organellen sind subzelluläre Strukturen, die aus der Endosymbiose eines Cyanobakteriums hervorgegangen sind. Die Erforschung des Photosynthese-Apparates höherer Pflanzen, seine Zusammensetzung und Regulationsmechanismen sind von großer Bedeutung für das Verständnis der Flexibilität der Photosynthese. Die Untersuchung photosynthetischer Proteine und deren Assemblierungsfaktoren wird jedoch limitiert durch technische und biologische Grenzen in Bezug auf genetische Manipulation in höheren Pflanzen. Die Entwicklung eines prokaryotischen Modellorganismus, der einen pflanzenähnlichen Photosynthese-Apparat trägt, bietet eine neue Strategie zur Untersuchung und Verbesserung der Photosynthese von Pflanzen. Die grundlegende Idee dahinter ist es den photosynthetischen Apparat von *A. thaliana* in das Cyanobakterium *Synechocystis* einzufügen, wodurch Funktionen einfacher zu untersuchen und zu manipulieren wären. Daher lag der Schwerpunkt meiner Arbeit auf der Assemblierung eines funktionellen Photosysthem II (PSII) von höheren Pflanzen in *Synechocystis*. Für diesen Zweck wurden zwei synthetische Konstrukte, RC1, das die PSII-Pflanzenproteine D1, D2, CP43 und PsbI kodierten, und RC2, welches $Cytb_{559}$, PsbL, PsbJ, CP47, PsbT und PsbH kodiert, erzeugt und jeweils in *Synechocystis* kloniert. Der Stamm *ΔpsbA2DC RC1* ist in der Lage photoautotroph zu wachsen und die Pflanzenproteine CP43 und PsbI zu akkumulieren. Die Akkumulation der Transkripte *AtpsbA2* und *AtpsbD* konnte nicht gezeigt werden, daher sind weitere Analysen erforderlich, um die Anwesenheit der Proteine zu bestimmen. Im Gegensatz dazu konnte der *psbEHLJ-RC2*-Stamm die Transkripte des RC2-Konstrukts nicht akkumulieren, wahrscheinlich aufgrund von Transkript-Instabilität oder Aktivierung eines Transkriptionsregulationsmechanismus.

DEAD-Box-RNA-Helikasen (DBRHs) modifizieren RNA-Sekundärstrukturen und sind am RNA-Metabolismus beteiligt. Viele DBRHs werden in Chloroplasten importiert, aber die Rolle der meisten von ihnen ist noch unbekannt. RH50 ist ein Chloroplasten-lokalisierter DBRH, der mit GUN1, einem Schlüsselfaktor bei der Signalübertragung vom Chloroplasten zum Nukleus, co-lokalisiert und co-exprimiert wird. Die Mutationen der Gene *rh50-* und *gun1*wurden in Mutanten mit unterschiedlichen genetischen Hintergründen eingeführt, welche in der Plastidengenexpression (*prors1-1, prpl11-1, prps1-1, prps21-1, prps17-1 und prpl24-1*) beeinträchtigt sind. Dies ergab ein ähnliches phänotypisches

Pattern für *rh50* und *gun1* auf physiologischer und molekularer Ebene. Darüber hinaus zeigt die Doppelmutante von *rh50-1 gun1-102* eine Verringerung der Größe, was die Idee unterstützt, dass RH50 und GUN1 funktionell verwandt sind. RH50 ist an der PRORS-getriggerten retrograden Signalübertragung vom Plastiden zum Nukleus als PHANG-Repressor wie GUN1 beteiligt. Des Weiteren zeigt die *rh50*-Mutante eine Empfindlichkeit gegenüber Erythromycin und Kältestress und ist bei der Verarbeitung der 23S-4.5S-intergenischen Region beeinträchtigt. Das RH50-Protein migriert mit ribosomalen Partikeln und kann die 23S-4.5S-intergenische Region *in vivo* und *in vitro* binden. Basierend auf diesen Ergebnissen folgerte ich, dass RH50 ein Plastid-rRNA-Reifungsfaktor ist.

Index

Summary ..... **i**

Zusammenfassung ..... **iii**

Index ..... **v**

List of Figures ..... **viii**

List of Tables ..... **x**

Abbreviations ..... **xi**

1 Introduction **1**

1.1 Oxygenic photosynthesis in plants and cyanobacteria 1

1.2 PSII structure, assembly and repair 5

1.3 *Synechocystis* PCC6803 as a model organism to study and improve plant photosynthesis 8

1.4 Chloroplast evolution and chloroplast gene expression 10

1.5 DEAD-box RNA helicases 12

1.6 Aim of the work: 14

1.6.1 Replacement of *Synechocystis* PSII core complex 14

1.6.2 Characterization of the DEAD-box RNA helicase RH50 of *A. thaliana* 16

2 Materials and Methods **17**

2.1 Materials and methods of *Synechocystis* 17

2.1.1 Chemicals, enzymes, radioactive substances and antibodies 17

2.1.2 Database analysis and software tools 17

2.1.3 Bacterial cell culture and growth conditions 18

2.1.4 Synthetic construct design 19

2.1.5 *Synechocystis*' natural transformation 20

2.1.6 Conjugation of cyanobacteria with pUR2LT donor RC2 20

2.1.7 PCR (standard and High fidelity) 21

2.1.8 Genomic DNA isolation 23

2.1.9 RNA isolation 23

2.1.10 *Arabidopsis* cDNA Synthesis 24

2.1.11 Northern blot analysis 24

2.1.12 Protein extraction 25

2.1.13 Thylakoid preparation 26
2.1.14 Immunoblot analysis 26
2.1.15 Bacterial whole cell absorbance spectra 26
2.1.16 Low temperature (77K) fluorescence emission spectra 26
2.1.17 Accession Numbers 27
2.2 Materials and methods *A. thaliana* 28
2.2.1 Chemicals, enzymes, radioactive substances and antibodies 28
2.2.2 Database analysis and software tools 28
2.2.3 Plant material, propagation and growth measurements 28
2.2.4 Transient co-expression in *A. thaliana* leaf protoplasts 30
2.2.5 Chlorophyll *a* fluorescence measurements 31
2.2.6 Co-expression analysis performed by Dr. Tatjana Kleine 31
2.2.7 Transcriptome sequencing and analysis 31
2.2.8 Nucleic acid analysis 32
2.2.9 Immunoblot analyses 32
2.2.10 Protein complex and polysome analysis 33
2.2.11 *In vivo* translation assay 33
2.2.12 Co-immunoprecipitation and slot blot analysis performed by Dr. Manavski 33
2.2.13 Production of recombinant protein and EMSA performed by Dr. Manavski 34
2.2.14 Size exclusion chromatography (SEC) performed by Dr. Manavski 34
2.2.15 Accession Numbers 34
3 Results 36
3.1 Replacement of the *Synechocystis* PSII core complex 36
3.1.1 Construction of synthetic vectors carrying an *A. thaliana* PSII core 36
3.1.2 Generation of *Synechocystis* RC1 mutant 37
3.1.3 Generation of *Synechocystis* the *RC2* mutant 40
3.1.4 Generation of a *ΔpsbA2DC RC1* mutant 44
3.1.5 Characterization of *psbA2 RC1-7* and *ΔpsbA2DC RC1* mutant strains 46
3.2 Characterization of the DEAD-box RNA helicase RH50 51
3.2.1 *RH50* is co-expressed with the *GUN1* regulon 51
3.2.2 RH50 is a subunit of the GUN1-containing subdomain of pTAC-complexes 52

3.2.3 The *rh50* mutation suppresses transcriptional downregulation of PhANGs 53
3.2.4 *RH50* genetically interacts with components of the 50S plastid ribosomal subunit 55
3.2.5 RH50 interacts with the plastid ribosomal large subunit 58
3.2.6 RH50 is required for cold stress acclimation 61
3.2.7 RH50 is involved in plastid RNA metabolism 65
3.2.8 Lack of RH50 affects plastid translation in the *prpl11* genetic background 69
3.2.9 RH50 associates with 23S-4.5S intergenic region 70
4 Discussion 72
4.1 Introduction of a plant photosystem II into the cyanobacterium *Synechocystis* 72
4.2 Characterization of the DEAD-box RNA helicase RH50 76
4.2.1 RH50 is involved in PGE-triggered plastid-to-nucleus retrograde signaling and shows comparable genetic interaction with GUN1 76
4.2.2 RH50 promotes the biogenesis of the plastid ribosome large subunit by assisting in the 23S-4.5S rRNA processing 79
Appendix 81
Bibliography 84
Acknowledgment 96
Curriculum vitae 97
Declaration / Eidesstattliche Erklärung 99

List of Figures

Figure 1.1: Schematic overview of oxygenic photosynthesis in plants. 2
Figure 1.2: Photosynthetic apparatus of (A) the higher plant *Arabidopsis thaliana* and (B) the cyanobacterium *Termosynechococcus elongatus*. 3
Figure 1.3: Crystal structure of PSII of the cyanobacterium *Thermosynechococcus elongatus*. 4
Figure 1.4: Assembly of PSII in (A) plants and (B) cyanobacteria. 6
Figure 1.5: Communication between Chloroplast, Mitochondria and Nucleus. 11
Figure 1.6: Schematic overview of the substitution of the *Synechocystis* PSII core with a plant type PSII. 15
Figure 3.2: Scheme of RC1 (B) and RC2 (C) synthetic constructs and the respective regions of insertion in the *Synechocystis* genome. 37
Figure3.3: Analysis of the *ΔpsbA2 RC1* mutant strain. 38
Figure 3.4: Generation of *ΔpsbA2 KO* mutant line. 39
Figure 3.5: Expression analysis of *Synechocystis ΔpsbA2 RC1-7* mutant. 40
Figure 3.6: Analysis of the *ΔpsbEFLJ RC2* mutant strain. 41
Figure 3.7: Expression analysis of *Synechocystis ΔpsbEFLJ RC2* mutant 42
Figure 3.8: Generation and transcription analysis of the *RC2.2* mutant. 43
Figure 3.9: Generation of *ΔpsbDC KO* and *ΔpsbA2DC RC1* mutants 45
Figure 3.10: Growth rate analysis of the *ΔpsbA2DC RC1* strain. 47
Figure 3.11: PSII characterization. 49
Figure 3.12: Immunoblot analysis of CP43 and D2 proteins 50
Figure 3.13: RH50 is co-expressed with the GUN1 regulon. 52
Figure 3.14: RH50 and GUN1 co-localize in chloroplasts 53
Figure 3.15: The *rh50* mutant is not a *gun* mutant but is involved in PRORS1-triggered retrograde signaling. 54
Figure 3.16: Genetic interaction between *rh50*, *gun1* and several mutation (*prors1-1, prpl11-1, prps1-1, prps21-1, prps17-1* and *prpl24-1*) affecting plastid gene expression (PGE). 56
Figure 3.17: Investigation of protein-protein interactions via Yeast-2-Hybrid assay. 58

Figure 3.18: RH50 is associated with chloroplast ribosomes. 60
Figure 3.19: The *rh50-1* mutant is cold-stress sensitive. 61
Figure 3.20: The *rh50-1* mutant is sensitive to cold stress. 62
Figure 3.21: *rh50-1* shows translation impairments. 63
Figure 3.22: Differential enrichment of plastid-encoded genes. 66
Figure 3.23: RH50 is required for the processing of the 23S-4.5S rRNA polycistronic transcript. 68
Figure 3.24: The *rh50-1* mutation impairs plastid translation in *prpl11-1* genetic background. 69
Figure 3.25: RH50 is associated with the 23S-4.5S intergenic region in vivo. 70
Figure 3.26: RH50 binds to the 23S-4.5S intergenic region in vitro. 71

List of Tables

Table 1.1: List of proteins and genes coding for the PSII core of *A. thaliana* and *Synechocystis*..... 5
Table 2.1: Bacterial strains used in this study..... 18
Table 2.2: Plasmids used in this study 19
Table 2.3: Primers used in this study 22
Table 2.4. Primer used in this study..... 29
Table 3.1: RNA-seq analysis 64

Abbreviations

°C	Degree Celsius
µ	Micro
Å	Ångström
A. thaliana	*Arabidopsis thaliana*
ADP	Adenosindiphosphate
Amp	Ampicillin
ATP	Adenosintriphosphate
BG11	Blue Green 11 (growth medium)
BSA	Bovine Serum Albumin
cDNA	Complementary DNA
Chl	Chlorophyll
Ci	Curie
Co-IP	Co-Immuno Precipitation
CRISPR-Cas	Clustered regulatory interspaces short palindromic repeats-CRISPR associated
cTP	Chloroplast Transit Peptide
$Cytb_{559}$	Cytochrome b_{559}
$Cytb_6f$	Cytochrome b_6f
Da	Dalton
DEPC	Diethylpyrocarbonate
DNA	Desoxyribonucleic acid
dNTP	Desoxynucleotide Triphosphate
DTT	Dithiothreitol
EDTA	Ethylenediaminetetraacetic acid
EMSA	Electrophoretic Mobility Shift Assay
Et-Br	Ethidium bromide
FD	Ferredoxin
FNR	Ferredoxin-$NADP^+$ Reductase

FPLC	Fast Protein Liquid Chromatography
g	Gram
g	Gravity force
GFP	Green Fluorescent Protein
GT	Glucose Tolerant
H	Hour
H^+	Proton
HEPES	4-(2-hydroxyethyl)-1-piperazineethanesulfonic acid
HF	High Fidelity
Hz	Hertz
K	Kelvin
Kan	Kanamycin
KO	Knockout
L	Litre
LB	Luria-Bertani (growth medium)
Lhc	Light Harvesting Complex
m	Milli
M	Molar
MES	2-(N-morpholino)ethanesulfonic acid
mol	Mole
MOPS	3-(N-morpholino)propanesulfonic acid
mRNA	Messenger RNA
MS	Mass Spectrometry
N	Nano
$NADP^+$	Nicotinamide Adenine Dinucleotide Phosphate
OD	Optical Density
OEC	Oxygen Evolving Complex
PAGE	Polyacrylamide Gel Electrophoresis
PC	Plastocyanin

PCR	Polymerase Chain Reaction
PQH_2	Plastoquinone
PSI	Photosystem I
PSII	Photosystem II
pTAC	plastid transcriptionally active chromosome
PVDF	Polyvinylidene difluoride
RC	Reaction Center
RFP	Red Fluorescence Protein
RNA	Ribonucleic acid
RNA-seq	RNA-deepsequencing
Rpm	Revolutions per minute
RT-PCR	Reverse transcription-PCR
SDS	Sodium Dodecyl Sulphate
Spec	Spectinomycin
Suc	Sucrose
TALEN	Transcription Activator-Like Effector Nuclease
TBS-T	Tris-Buffered Saline with Tween20
TCA	2,4,6-Trichloroanisole
T-DNA	Transfer DNA
v/v	volume per volume
w/v	weight per volume

1 Introduction

1.1 Oxygenic photosynthesis in plants and cyanobacteria

Oxygenic photosynthesis is one of the most important biological process on earth, it is capable of converting sun light into chemical energy generating oxygen and providing the energy to produce most of the biomass of the planet ($nCO_2 + nH_2O + light \rightarrow (CH_2O)_n + O_2$). In particular, the light reactions are the key components that perform photochemistry coupled to water oxidation. In higher plants, photosynthesis takes place in specialized organelles, the chloroplasts, which evolved from an ancient cyanobacterial endosymbiont. In the chloroplast, the photosynthetic machinery is embedded in the thylakoid membranes. As described schematically in Figure 1.1, the chlorophyll P680 of Photosystem II is excited by photons collected by the light harvesting antenna (LHC), one electron is ejected and is rapidly transferred over several electron carriers to the plastoquinone Q_B. The "electron hole" generated at $P680^+$ is filled by an electron from a nearby redox-active tyrosine (Y_Z), which is then reduced by an electron from the oxygen-evolving-complex (OEC) harvested from the oxidation of water. After another photocycle, fully reduced plastoquinol Q_B is released into the membrane and electrons are transferred by the plastoquinone (PQH_2) to the cytochrome b_6f complex (Cyt b_6f). Through the action of the OEC, oxygen and protons are produced. The protons accumulate in the luminal side of the thylakoids, where a proton gradient is generated. Next, the electrons flow from Cyt b_6f to the small soluble protein plastocyanin (PC) and finally to the chlorophyll $P700^+$ of photosystem I (PSI). The electron transfer through the Cyt b_6f further contributes to build up the proton gradient into the lumen. The photochemistry of PSI is initiated by a P700 chlorophyll-*a* (Chl*a*) dimer that transfers electrons to a chlorophyll a monomer (A_o). In the PSI the electrons are transferred sequentially to the phylloquinone A_1, three iron-sulfur complexes, a ferredoxin protein and ultimately to $NADP^+$ for the generation of NADPH. The luminal proton gradient is used by the multi subunit complex of ATP-synthase for the synthesis of ATP. The chemical energy stored in ATP and the reducing power of NADPH is then used for metabolic processes, in particular for carbon fixation.

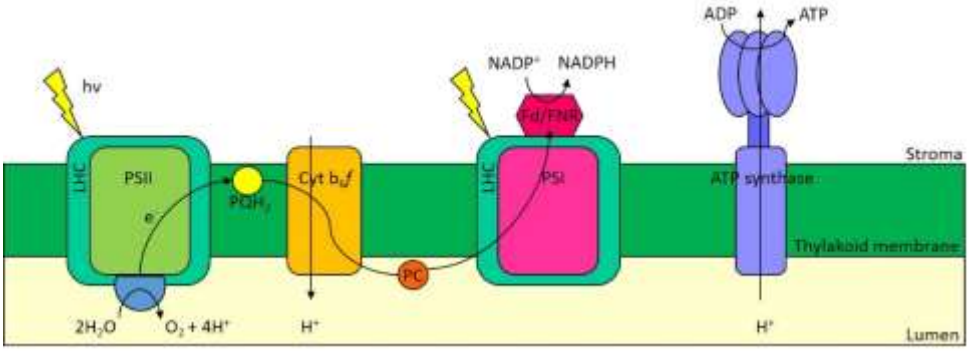

Figure 1.1: Schematic overview of oxygenic photosynthesis in plants.

Major protein complexes of the chloroplast photosynthetic apparatus. Photosystem II, PSII; Light-harvesting complex, LHC; Plastoquinone, PQH_2; Cytochrome b_6f; Plastocyanin, PC; Photosystem I, PSI; Ferredoxin, Fd; Ferredoxin-$NADP^+$ reductase, FNR; Electron, e^-; Proton, H^+. See text for details.

As previously mentioned, chloroplasts derived from an ancient endosymbiotic event between a cyanobacterial endosymbiont and a eukaryotic host. During evolution, the cyanobacterial-derived genome has been drastically reduced in size, mainly because of gene loss and large-scale transfer to the nucleus (Kleine et al., 2009). For this reason, the majority of chloroplast proteins is encoded by the nuclear genome and must be imported post-translationally into the organelle. This is true also for the photosynthetic apparatus, which are a mosaic of nuclear and plastid encoded proteins (Fig. 1.2 A) (Allen et al., 2011). It is interesting to note that the photosynthetic apparatus of plants and cyanobacteria shows little differences (Fig. 1.2 B). The degree of similarity is higher in the core membrane proteins compared to the more soluble and peripheral ones. The high degree of conservation has been proved by the successful exchange of photosynthetic core subunits between different organisms. Six genes of the PSII core of *Chlamydomonas reinhardtii* (*psbA, psbD, psbE, psbF, psbB* and *psbC*) could be successfully replaced by their homologous genes of three different green algae, reconstituting the photosynthetic activity till up to 85 % of the wild-type level (Gimpel et al., 2015). The PSII core protein D1 is highly conserved between species, sharing an approximately 85% identity between the cyanobacterial and higher plant forms (85% with *Poa annua*, 81% with *Arabidopsis*).

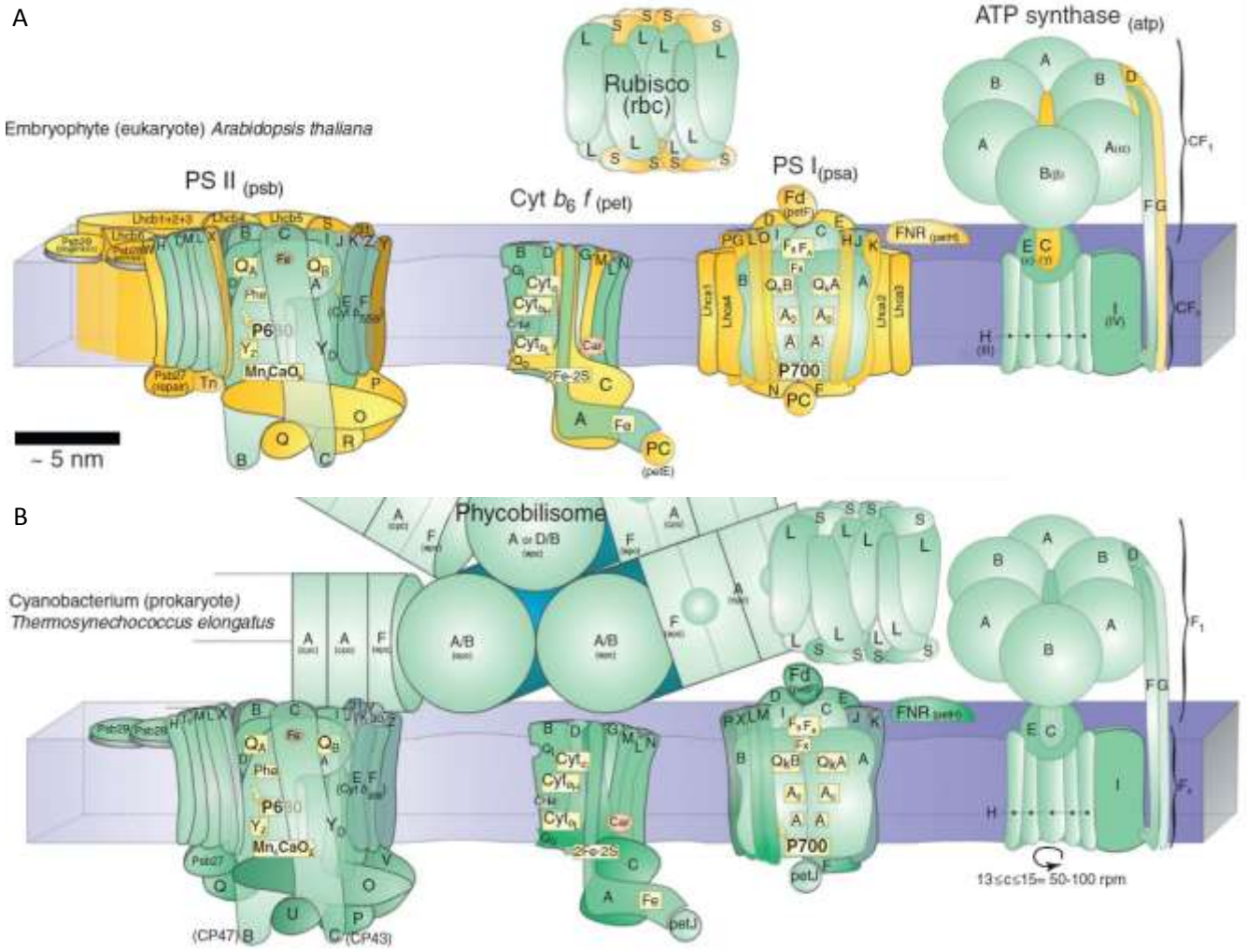

Figure 1.2: Photosynthetic apparatus of (A) the higher plant *Arabidopsis thaliana* and (B) the cyanobacterium *Thermosynechococcus elongatus*. Protein subunits encoded by the plastidial or cyanobacterial genome are colored in green, the one encoded by the nucleus are colored in yellow. Figure adapted from Allen et al, 2011.

It has been shown that D1 from *Synechocystis* could be replaced by the homologous protein of the higher plant *Poa annua*, generating a functional chimeric PSII (Nixon et al., 1991). The low molecular weight protein PsbH of *Synechocystis*, which shares a degree of similarity between 70 and 80 % among different species, could be replaced by the homologous subunit from *Zea mays* resulting in a chimeric PSII, able to perform photosynthesis even though with higher susceptibility to photoinhibition (Chiaramonte et al., 1999). Recently, also the PSI subunit PsaA of *Synechocystis* could partially be replaced by the homologous protein of *Arabidopsis* (Viola et al., 2014). Although the photosystems of

plants and cyanobacteria are highly conserved, they display differences in their structure and assembly (Fig. 1.2). The antenna systems of cyanobacteria and land plants present a great variety of protein structures and pigments, suggesting that they diverged during evolution to adapt to different light environments. Many cyanobacteria, like *Synechocystis*, have water-soluble light-harvesting phycobiliproteins organized in large structures, the phycobilisomes, which are attached to the stromal side of the thylakoid membranes (Liu et al., 2013). The plant light-harvesting-complex (LHC) proteins instead, are composed of three transmembrane helices and are embedded into the thylakoid membrane, where they are associated with the core complexes. Some variation can be observed in the subunit composition of the PSII, in particular of the OEC (Fig. 1.2) where plants and green algae bind the PsbP and PsbQ proteins, while red algae and cyanobacteria bind the PsbU and PsbV proteins (De Las Rivas and Barber, 2004). Differences are also found in the plant-specific factors involved in PSII assembly that might have evolved as functional substitutes for cyanobacterial equivalents (Nickelsen and Rengstl, 2013).

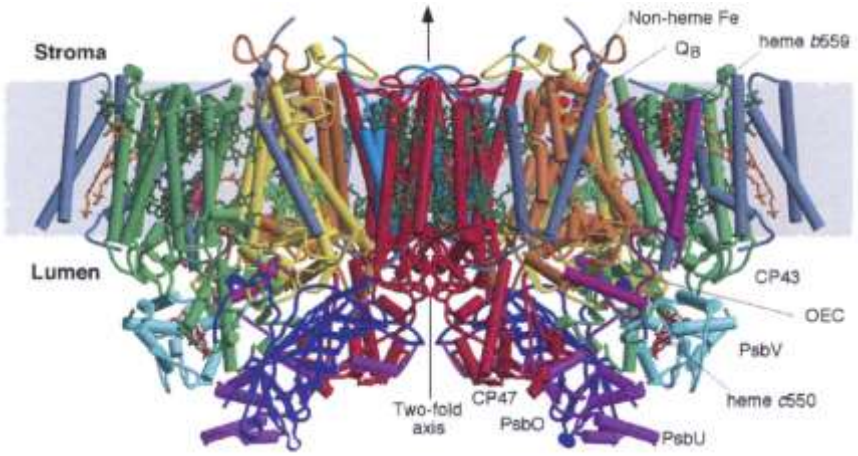

Figure 1.3: Crystal structure of PSII of the cyanobacterium *Thermosynechococcus elongatus*. Overview of the PSII dimer perpendicular to the thylakoid membrane. Helices are represented as cylinders with D1 in yellow, D2 in orange, CP43 in green, CP47 in red, cyt b_{559} in wine red; PsbM, PsbL and PsbT in medium blue; PsbH, PsbK, PsbI, PsbJ, PsbX, PsbZ and PsbN in grey. The extrinsic proteins are PsbO in blue, PsbU in magenta and PsbV in cyan. Chlorophyll of the D1/D2 RC are light green, pheophytins are blue, chlorophylls of the antenna complexes are dark green, β-carotenes are in orange, hemes are in red, nonheme Fe is red, Q_A and Q_B are purple. The OEC is shown as red (oxygen atoms), magenta (Mn ions) and cyan (Ca^{2+}) balls. The Figure is taken from (Ferreira, 2004)

1.2 PSII structure, assembly and repair

PSII is a water-plastoquinone photo-oxidoreductase, a highly conserved multi-subunit pigment-protein complex found in plants and cyanobacteria. PSII mediates the initial charge separation to generate the high-energy electrons for photosynthetic electron transport. The PSII core monomer has a molecular mass of 350 kDa, it consists of at least 20 protein subunits, 35 chlorophylls, two pheophytins, eleven β-carotenes, two plastoquinones, one heme (two hemes in cyanobacteria), one nonheme iron, and the Mn_4CaO_5 cluster that catalyzes the splitting of water and the production of O_2 (Fig. 1.3) (Umena et al., 2011). The structure of PSII has been extensively studied thanks to several crystallography studies conducted in the last years. Of particular interest is the crystal structure of PSII from *Thermosynecococcus elongatus* resolved at 3.5 Å (Fig. 1.3) (Ferreira, 2004) which reveals the arrangement of protein subunits and cofactors. A more recent high resolution crystal structure of PSII from *T. vulcanus* at 1.9 Å (Umena et al., 2011) could further uncover the structure of the oxygen-evolving-complex. The protein components of the PSII core complex of A. thaliana and their homologous in Synechocystis are listed in Table 1.1.

Table 1.1: List of proteins and genes coding for the PSII core of *A. thaliana* and *Synechocystis*

PSII core proteins	*A. thaliana* PSII core genes	*Synechocystis* PSII core genes	Protein similarity
D1	*psbA-AtCg00020*	*psbA1, psbA2, psbA3- slr1181, srl1311,sll1867*	88,3% -92,5% -92,5%
D2	*psbD-AtCg00270*	*psbD1, psbD2- sll0849, srl0927*	92,4% - 92,4%
CP43	*psbC-AtCg00280*	*psbC- sll0851*	87,1%
CP47	*psbB-AtCg00680*	*psbB- srl0906*	89,2%
$Cytb_{559}$ α	*psbE-AtCg00580*	*psbE- ssr3451*	86,7%
$Cytb_{559}$ β	*psbF-AtCg00570*	*psbF- smr0006*	75,0%
PsbL	*psbL-AtCg00560*	*psbL- smr0007*	76,9%
PsbJ	*psbJ-AtCg00550*	*psbJ- smr0008*	82,9%
PsbI	*psbI-AtCg00080*	*psbI- sml0001*	81,6%
PsbT	*psbT-AtCg00690*	*psbT- smr0001*	63,3%
PsbH	*psbH-AtCg00710*	*psbH- ssl2598*	67,9%

PSII is assembled in a highly ordered process, and large numbers of additional factors are involved in forming this multiprotein complex. PSII assembly occurs in three phases: early, later and final phase (Fig. 1.4). The early phase takes place directly at the membrane where the nascent polypeptide can integrate into the lipid bilayer (Zhang et al., 1999). The first subcomplex accumulating is the so called-

RC complex, which consists of D1, D2, cytb$_{559}$ (PsbE and PsbF) and PsbI (Fig. 1.4). The formation of the cytb$_{559}$ is a prerequisite for the accumulation of D2. The D2- cytb$_{559}$ subcomplex is the platform for the incorporation of a dimer of the precursor of D1 (pD1) and PsbI. During the formation of the RC complex, CtpA (C-terminal processing protease) processes pD1 at the C-terminus. During this step, the cyanobacterial PSII-specific assembly factor PratA interacts directly with the C-terminus structure of pD1 and seems to load the early PSII complex with Mn^{2+} (Fig. 1.4 B) (Stengel et al., 2012).

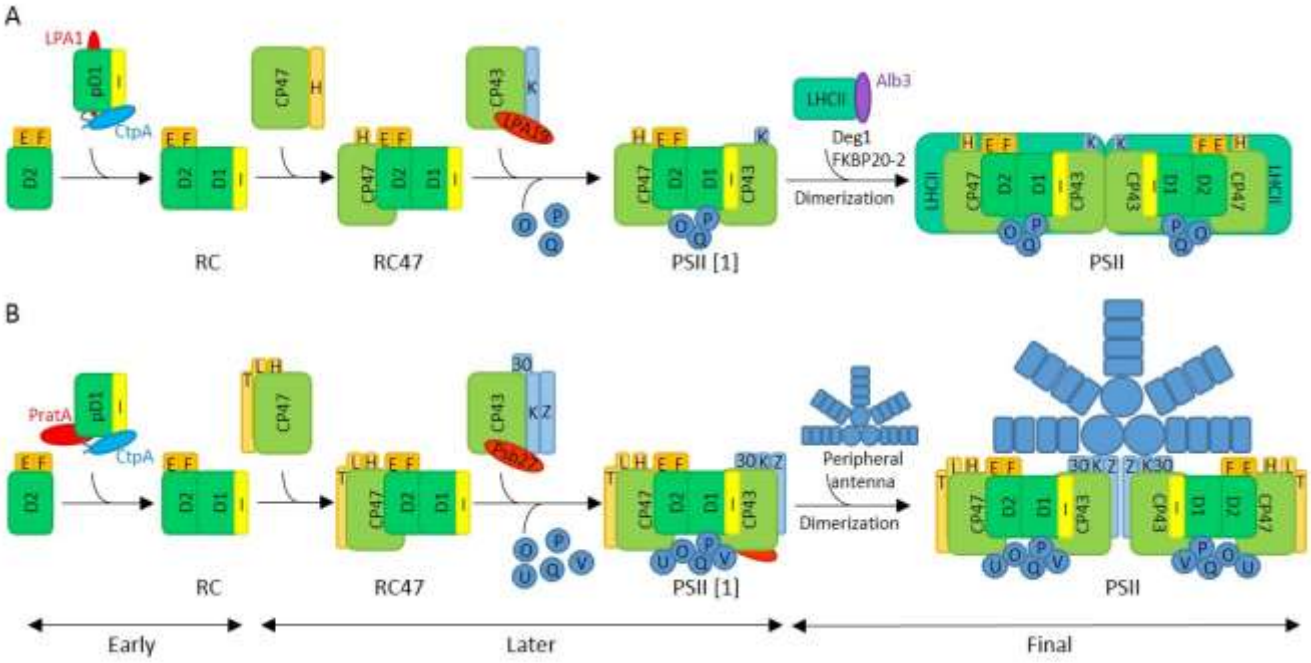

Figure 1.4: Assembly of PSII in (A) plants and (B) cyanobacteria. The assembly of PSII in plants and cyanobacteria occurs in three main steps indicated by the arrows at the bottom (early, later and final phase). Transiently interacting factors are indicated by ovals. Homologous proteins have the same color. PSII core subunits are indicated with their common name (D1, D2, CP47 and CP43). PSII subunits are indicated with the letter or number of their protein names (for example PsbI, I). Abbreviations: E and F, cytochrome *b*$_{559}$; pD1, precursor form of D1; RC, reaction center complex lacking CP47 and CP43; RC47, reaction center complex lacking CP43; PSII [1], monomeric; PSII, dimeric; LHCII, light-harvesting complex II.

In plants, LPA1 showed a similar function (Fig. 1.4 A)(Ma et al., 2007). The later phase consists in the conversion of the RC complex into the PSII monomer with the sequential attachment of the two inner antenna proteins CP47 and CP43 as well as the assembly of the extrinsic subunits that shield the Mn_4CaO_5 cluster (Fig. 1.4). CP47 is first integrated into the membrane as a precomplex with several low molecular-mass PSII subunits, which include PsbH, PsbL, and PsbT in cyanobacteria (Fig. 1.4 B) and just PsbH in spinach chloroplasts (Boehm et al., 2012; Rokka et al., 2005). Next, a preformed complex of CP43 (the second inner antenna protein) together with PsbK, PsbZ and Psb30 in cyanobacteria or only PsbK in chloroplasts (Boehm et al., 2011; Sugimoto and Takahashi, 2003) incorporates in the RC47 complex with the help of an assembly factor called Psb27 in cyanobacteria and LPA19 in chloroplast. With the attachment of CP43, PSII monomer is formed. PSII monomer carries all the amino acid residues necessary for the photoactivation of the OEC (Dasgupta et al., 2008). Furthermore, the extrinsic subunits PsbO, PsbP, PsbQ, PsbU and PsbV are attached at the luminal side of the cyanobacterial PSII monomer generating a shielding cap for the stabilization of the Mn_4CaO_5 cluster. In chloroplasts the shielding cap is formed by PsbO, PsbP and PsbQ (Bricker et al., 2012). The final step of the biogenesis of PSII consist in the dimerization and the attachment of the peripheral antenna with the help of Alb3, Deg1 and FKBP20-2 in plants (Lima et al., 2006; Moore et al., 2000; Sun et al., 2010).

Being responsible for the water splitting reaction, PSII is essential for photosynthesis, however, it is also the rate limiting protein component, due to the fact that it is extremely susceptible to light. When exposed to high light, PSII activity declines rapidly, facing photoinhibition (Aro et al., 2005, 1993; Barber and Andersson, 1992). The core protein D1 is the main target of photodamage. For this reason, D1 has an unusually high turnover rate, in order to replace the damaged D1 with a newly synthesized one and in this way avoid the complete inactivation and disassembly of PSII (Mulo et al., 2012). During the PSII repair cycle, damaged PSII is disassembled to the level of the RC47 complex. In chloroplasts but not in cyanobacteria the damaged D1 is phosphorylated and migrates from the grana stacks to the stroma lamellae where it is then dephosphorylated and degraded (Tikkanen et al., 2008). In chloroplast and cyanobacteria, the damaged D1 is removed by FtsH metalloproteases (Nixon et al., 2010). Finally newly synthetized pD1 is assembled following the usual PSII assembly pathway (Nickelsen and Rengstl, 2013).

1.3 *Synechocystis* PCC6803 as a model organism to study and improve plant photosynthesis

Photosynthesis is a relatively inefficient process, being able to convert just 8-10% of the sunlight into biochemical energy and biomass (Zhu et al., 2010). Therefore, photosynthesis as it is cannot meet the increasing demand of food, feed and biofuel that will occur over the next decades (Ort et al., 2015). In the last years the scientific community is developing ideas for photosynthesis improvement, being convinced that there are processes that can be ameliorated (Blankenship et al., 2011; Jensen and Leister, 2014a; Leister, 2012; Ort et al., 2015). Genetic engineering and synthetic biology can help in reaching this goal. New genetic engineering methods have been developed in plants, such as the genome editing mediated by CRISPR/Cas9 (Feng et al., 2013) or the TALEN (Christian et al., 2013) system. However, due to the complexity of both higher plants and the photosynthetic process, photosynthesis improvement remains difficult to achieve in plants. Plants can do homologous recombination but at very low frequency, it is therefore not possible to introduce or remove specific mutations or genes in short time. The plastid genome of several land plants can be transformed and progress has been made in the last years in order to make plastid transformation more efficient in recalcitrant plants, like for example in *A. thaliana* (Yu et al., 2017). The CRISPR/Cas9 system, that recently revolutionized genome editing thanks to its efficiency and simplicity, can still not be used to target the chloroplast genome. In comparison to plants, cyanobacteria are an easier platform for genetic manipulation, thanks to various techniques and toolkits, which allow large-scale genetic modifications in a reasonable time frame (Jensen and Leister, 2014a). Compared to *A. thaliana*, *Synechocystis* is a less complex photosynthetic organism. *Synechocystis* has a short life cycle with a duplication time of 6 hours, it is naturally competent, it is able to perform homologous recombination and it has a small genome, which is completely sequenced. Moreover, glucose-tolerant strains of *Synechocystis* are available, which can grow heterotrophically in the dark (Williams, 1988), thus making it possible to study mutants of plastidial genes that are lethal or albinotic in plants. All these features, together with the available molecular tools, make *Synechocystis* an ideal model organism to study and improve plant oxygenic photosynthesis (Jensen and Leister, 2014a). The generation of a new model prokaryote carrying a plant-like photosynthetic apparatus is a new strategy for studying and improving it (Rühle and Leister, 2015). With this aim, the *Synechocystis* endogenous PSI, PSII (Rühle and Leister,

2015), cyt b_6f and ATP-Synthase complexes would be replaced with plant ones and subsequently plant specific proteins and assembly factors would be introduced. Marker-less gene deletion and replacement strategies needing only a single transformation step (Viola et al., 2014) as well as novel approaches for chromosomal integration and expression of synthetic gene operons (Bentley et al., 2014) are some of the strategies that will help in making large scale replacement. Several attempts in the introduction of plant proteins in *Synechocystis* have already been carried out. The PSII core protein D1 of the land plant *Poa annua* has been introduced in a *Synechocystis* strain lacking the endogenous D1, generating a strain with an hybrid PSII that was able to grow photoautotrophically and oxidize water at a rate comparable with the wild type (Nixon et al., 1991). *Synechocystis* lacks the capability to synthetize chlorophyll b and LHCII (the chlorophyll a/b-binding light-harvesting complex of photosystem II). Therefore the chlorophyll(ide) a oxygenase gene (cao) of *A. thaliana*, which is responsible for the conversion of chlorophyll a into chlorophyll b , was introduced in *Synechocystis* PSI-less strain, containing only 15–20% of the amount of chlorophyll a present in wild type. Chlorophyll b could accumulate in high amount in the mutant, replacing chlorophyll a in PSII, only when LHCII from pea was introduced in the strain (Xu et al., 2001). The plant LHCII alone was also introduced in *Synechocystis*, where it could transiently accumulate but was rapidly degraded and could not be assembled in the thylakoids (He et al., 1999). The reason was probably the lack of some plant specific assembly factors like SRP54 and HSP70, usually present in the stroma to assist in the integration of a protein in the thylakoid membrane (Li et al., 1995; Yalovsky et al., 1992). All these attempts drive to the idea that the generation of a *Synechocystis* strain carrying a plant-like photosynthetic apparatus can be achieved and that probably unknown plant auxiliary factors will be necessary to stabilize the complex.
The generation of a novel synthetic organism, carrying the Arabidopsis photosynthetic apparatus in a cyanobacteria cell background would allow us: (1) the adaptation of photosynthesis to different environmental stress conditions through in vitro adaptive evolution (Leister, 2017); and (2) the generation of more stable chimeric complexes with direct protein manipulation (Jensen and Leister, 2014a).

1.4 Chloroplast evolution and chloroplast gene expression

It is well accepted by the scientific community that some organelles of eukaryotic cells originated from prokaryotic organisms. In particular, the chloroplast generated from an endosymbiotic event occurred between an eukaryotic cell and a cyanobacterium. During the evolution, most of the cyanobacterial genome was transferred to the nuclear genome and only a small part was retained by chloroplasts (Kleine et al., 2009). The chloroplast genome of *A. thaliana* contains only 120-130 genes, which encode for 75-90 proteins most of which are subunits of the transcription and translation machinery and of the photosynthetic apparatus (Wang et al., 2014). About 95% of the plastid proteins are nuclear encoded and have to be imported post-translationally into the chloroplast (Jarvis and Lopez-Juez, 2013; Martin et al., 2002). In order to modulate the expression of nuclear genes according to developmental and physiological needs of chloroplasts, communication mechanisms between organelles and nucleus is necessary (Fig. 1.6) (Koussevitzky et al., 2007; Leister, 2005). This is evident when it comes to plastid transcription. Plastid transcription is performed by two RNA polymerases: the plastid encoded polymerase (PEP) and the nuclear encoded polymerase (NEP). PEP transcribes plastid-encoded photosynthetic genes. Non-photosynthetic housekeeping genes are transcribed by both PEP and NEP, whereas a few genes, such as *rpoB* and *accD*, are transcribed exclusively by NEP (Hajdukiewicz et al., 1997). The communication pathway from the nucleus to the organelles is called anterograde signaling. It is a really important communication pathway since many chloroplast proteins are encoded in the nucleus and must be imported into the organelle after their translation in the cytosol, where they can modify the function and expression of plastidial genes. The signaling from organelle-to-nucleus is called retrograde signaling and the nature of this mechanism is still under investigation. Several putative retrograde signals have been identified: i.e. tetrapyrrole intermediates (Pogson et al., 2008;Woodson et al., 2011), reactive oxygen species (ROS) (Kim and Apel, 2013) and the redox state of the organelle (Pfannschmidt et al., 2003). Recently, secondary metabolites like the phosphonucleotide 3'-phosphoadenosine 5'-phosphate (PAP) involved in drought and high light response and the methylerythritol cyclodiphosphate (MEcPP) a precursor of isoprenoids which induces under stress conditions, like excess light or a wound (Estavillo et al., 2011; Ramel et al., 2013; Xiao et al., 2012), have been discovered to be involved in the retrograde plastid signaling pathway (Fig. 1.5).

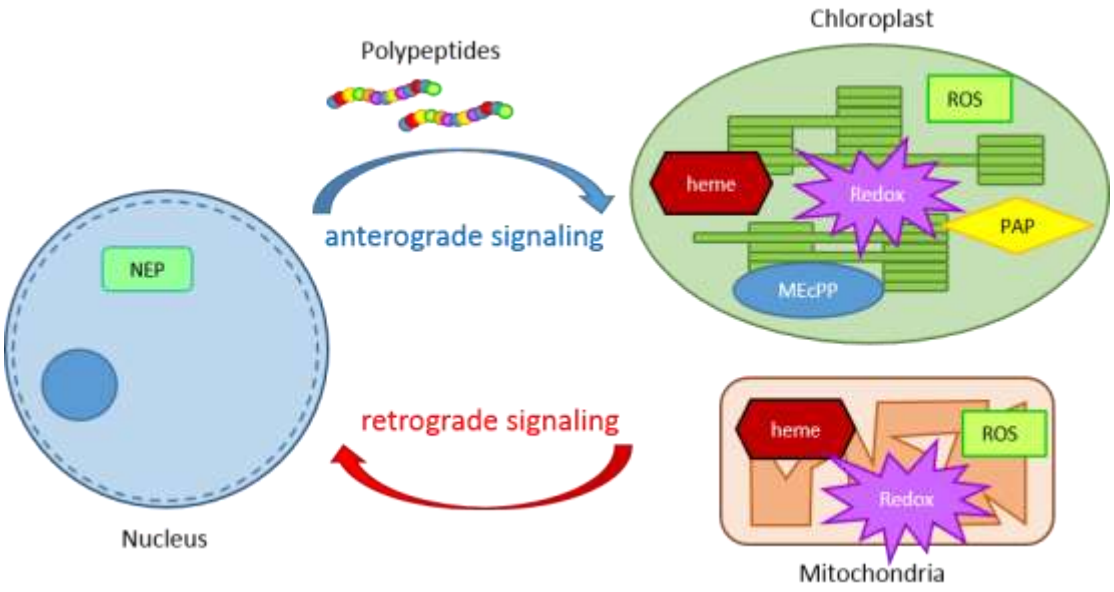

Figure 1.5: Communication between Chloroplast, Mitochondria and Nucleus.

Details of anterograde and retrograde signaling between the nucleus and the organelles are discussed in the text. Anterograde signaling is indicated by the blue arrow, retrograde signaling by the red arrow. Abbreviations: NEP, nuclear encoded polymerase; ROS, reactive oxygen species; PAP, 3'-phosphoadenosine 5'-phosphate; MEcPP, methylerythritol cyclodiphosphate; Redox, redox state.

In the chloroplast, multiple copies of highly condensed cpDNA, RNA and several proteins are organized in nucleoids (Powikrowska et al., 2014). Nucleoids contain the molecular machinery necessary for transcription replication and segregation of the plastid genome (Sakai et al., 2004). Plastid transcription occurs in the transcriptionally active part of the nucleoids, the pTAC complex. The pTAC is membrane attached and consists of multimeric protein complexes (Pfalz et al., 2006). It has been shown that pTAC can transcribe rRNA, tRNA and plastid protein-coding genes (Suck et al., 1996). Forty different polypeptide have been identified as part of the pTAC complex among them are subunits of the PEP.

As part of the pTAC complex also helical repeat proteins, like octatricopeptide (OPRs), pentatricopeptide (PPRs) or tetratricopeptide-repeat (TPRs) have been identified, in agreement with their primary role in modulating gene transcription and RNA editing, maturation or stability. In addition,

GUN1 (GENOME UNCOUPLED 1), a member of the PPR protein family, has been also described as pTAC component (Koussevitzky et al., 2007). GUN1 integrates several retrograde signaling pathways (Koussevitzky et al., 2007), modulates the accumulation of PRPS1 and genetically interacts with plastid ribosomal proteins (Tadini et al., 2016). COE1 (Chlorophyll A/B-Binding Overexpression 1)/mTERF4 was recently proposed to be part of GUN1-mediated retrograde signaling pathway (Sun et al., 2016). Because the *coe1* mutant accumulates high levels of unprocessed RNAs, it was speculated that these unprocessed RNAs might represent a retrograde signal for the down-regulation of nuclear photosynthetic gene expression (Sun et al., 2016).

1.5 DEAD-box RNA helicases

DEAD-box RNA helicases (DBRHs) participate in many cellular processes, including RNA metabolism (synthesis, modification, cleavage and degradation), ribosome biogenesis and translation initiation (Cordin et al., 2006; Silverman et al., 2003). In fact, non coding RNA molecules (tRNA and rRNA) must fold into a correct conformation in order to interact with proteins, and DBRHs are responsible for rearranging the RNA secondary structure, by unwinding duplexes in a local strand separation reaction (Jarmoskaite and Russell, 2011). To this end, helicases bind directly to the duplex region, where the interaction occurs, and exploit the energy from the hydrolysis of ATP to move directionally along one of the strands (Jarmoskaite and Russell, 2011). DBRHs contain at least nine conserved motifs that constitute the helicase core domain, in particular a stretch of highly conserved Asp-Glu-Ala-Asp (D-E-A-D) residues in motif II (Caruthers and McKay, 2002; Cordin et al., 2006). In *A. thaliana*, ten out of 58 annotated DBRHs (Mingam et al., 2004) are predicted to be plastid-localized (RH3, 11, 17, 22, 26, 33, 41, 50, 52, 58) (Asakura et al., 2012). Mass spectrometry analyses have identified seven DBRHs in *A. thaliana* chloroplasts, namely RH3, 22, 26, 39, 47, 50 and 58 (Majeran et al., 2012; Olinares et al., 2010). Phylogenetic analyses cluster the plastid DBRHs in different groups: RH3 together with mitochondrial and nuclear orthologous; RH26 is part of a clade with proteins with unknown function, whereas RH22, RH39, RH47, RH50 and RH58 form a separate group (Asakura et al., 2012; Chi et al., 2012). Some of the plastid helicases have been functionally characterized. The *rh39* mutant accumulates precursors of the 23S rRNA, indicating that RH39 is involved in plastid rRNA maturation by introducing the hidden break

into the 23S rRNA (Nishimura et al., 2010). Also RH22 is involved in the assembly of the 50S ribosomal subunit in the chloroplast: complete loss of RH22 causes a lethal phenotype, while a knockdown line displayed delayed cotyledon greening and defects in chloroplast rRNA accumulation, in particular of the precursor of the 23S and 4.5S rRNA (Chi et al., 2012). Yeast two-hybrid and pull-down assays indicated that RH22 can interact with the plastid 50S ribosomal protein PRPL24 and with a small fragment of 23S rRNA. RH3 was characterized in both *A. thaliana* and maize (Asakura et al., 2012; Gu et al., 2014). The *atrh3* null mutant is embryo lethal and a weak allele (*rh3-4*) resulted in pale-green seedlings due to defects in splicing of group-II introns reduced amount of the 50S ribosomal subunit due to the decrease in the accumulation of the 23S and 4.5S rRNA (Asakura et al., 2012; Gu et al., 2014). A tobacco RH58/VDL mutant displayed defects in plastid differentiation and plant morphogenesis (Wang et al., 2000). The rice homologue of *Arabidopsis* RH50 (OsBIRH1) exhibits RNA helicase activity in vitro but no direct target of OsBIRH1 has been identified yet (Li et al., 2008). In *A. thaliana*, RH50 was detected in the pTAC, together with PRPs, the PEP-core enzyme and proteins involved in transcription, translation and RNA metabolism (such as RNAses and DEAD-box RNA helicases) (Majeran et al., 2012; Olinares et al., 2010).

1.6 Aim of the work:

1.6.1 Replacement of *Synechocystis* PSII core complex

The assembly of PSII - and more in general - of the photosynthetic apparatus and its regulation mechanisms it's a complex process. Knowledge on the assembly of this multiprotein complex and the factors involved in this process is still incomplete. Most of the plant and cyanobacteria PSII assembly factors, so far identified, have been studied by a "top-down" approach with forward and reverse genetic by disrupting singular components of the photosynthetic apparatus and of the assembly process and characterizing the phenotypic effect obtained on the generated mutants. These methods are suitable tools for the in-depth study of molecular mechanisms but they will hardly be able to identify the sufficient set of proteins, assembly factors and cofactors required for the assembly and well-functioning of PSII (Rühle and Leister, 2015). A "*bottom-up*" approach, meaning the synthesis and introduction of the subunits of the PSII core complex in a new environment where genetic engineering can be easily applied and later on characterize the protein complex functionality, would be more suitable for the complete understanding of PSII assembly and repair and eventually its improvement. This concept however cannot be completely implemented in higher plants particularly in the model organism *A. thaliana*, given their long life cycle and inefficient genetic engineering technology (Jensen and Leister, 2014b; Rühle and Leister, 2015). On the other hand, cyanobacteria, in particular *Synechocystis*, are a more suitable candidate for this approach. *Synechocystis* has a short life cycle, is fast growing, can grow both in autotrophic and heterotrophic conditions and has a small genome easy to manipulate. All these characteristics make *Synechocystis* a good model organism to be used for a new "*bottom up*" approach.

This work focused on the replacement of the multi-protein complex known as Photosystem II of *Synechocystis* with the one of *A. thaliana*. The main goal is to substitute the cyanobacterial PSII core, first by introducing the synthetic plant PSII complex and then by removing the cyanobacterial endogenous PSII genes (Fig. 1.6). To support plant PSII assembly in *Synechocystis*, plant specific assembly factors would have to be also introduced (Fig. 1.6). In this way, the generation of a hybrid organism carrying plant type PSII and later on the whole plant photosynthetic apparatus would be achieved. This will give us the chance to better understand photosynthesis by revealing unknown plant

specific assembly factors and the precise mechanism of assembly and repair and will give us a chassis to be used as a platform for photosynthetic improvement.

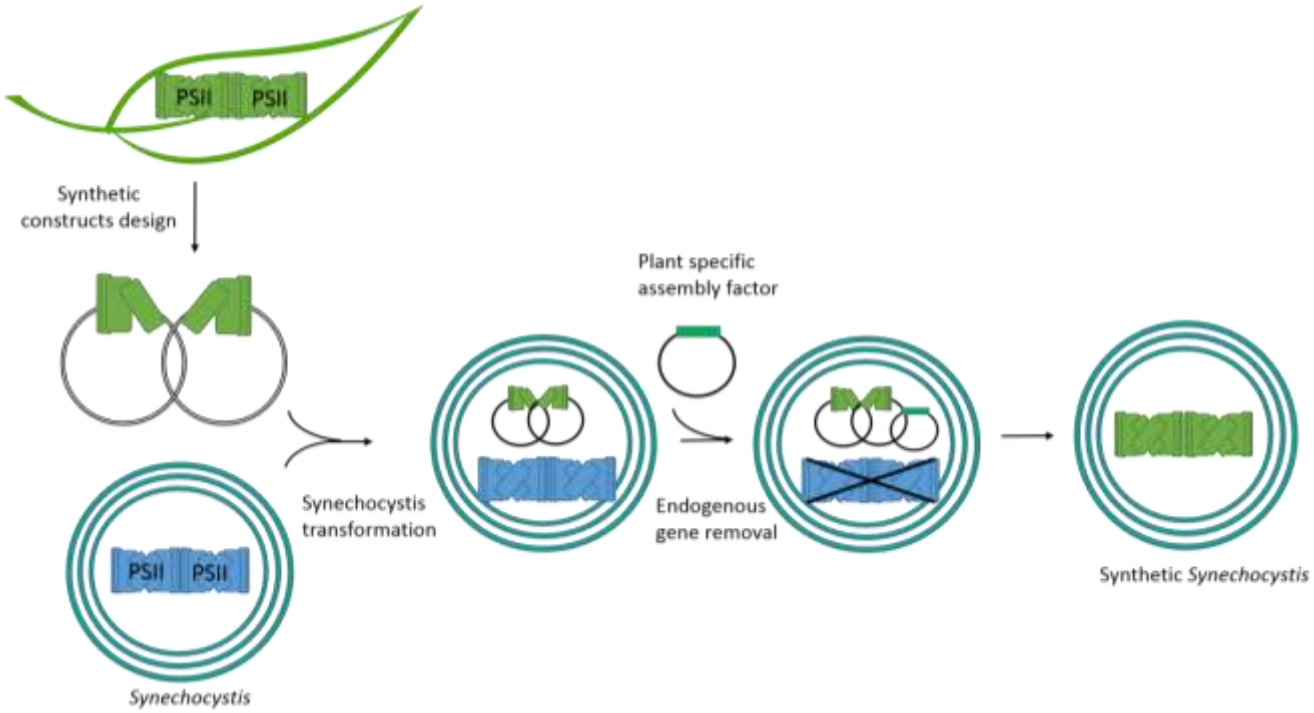

Figure 1.6: Schematic overview of the substitution of the *Synechocystis* PSII core with a plant type PSII.

The *A. thaliana* PSII core complex is represented in green, while the one of *Synechocystis* is in blue. A synthetic construct carrying genes encoding the plant PSII core will be introduced in *Synechocystis* wild type cells through natural transformation. Endogenous PSII core genes will be deleted and at the same time plant specific assembly factor will be introduced in the *Synechocystis* genome. A final strain, Synthetic *Synechocystis*, carrying a fully assembled PSII core complex of *A. thaliana*, will be isolated.

1.6.2 Characterization of the DEAD-box RNA helicase RH50 of *A. thaliana*

DBRHs play an important role in RNA metabolism and ribosome biogenesis (Cordin et al., 2006). Several DBRHs are targeted to the chloroplast and for some the function is still unknown. Ribosome biogenesis is a complex multistep process which requires transcription of the ribosomal gene cluster, rRNA processing and ribosome assembly (Kaczanowska and Rydén-Aulin, 2007). DBRHs, with the ability of unraveling RNA secondary structures, help RNA molecules in reaching the right conformation for the interaction with their target protein. RH50 is a DBRH, which was found in the chloroplast proteome as part of the nucleoids in the pTAC complex, together with OPR, TPR and PPR proteins, involved as well in RNA metabolism. The PPR protein GUN1, the integrator of several retrograde signaling pathway, has been also localized in the pTAC complex (Koussevitzky et al., 2007). The *gun1* mutant fails to repress the expression of nuclear encoded photosynthetic genes like *Lhcb* and *RbcS*, in conditions of plastid translation inhibition (lincomycin-treatment) or chloroplast photo-bleaching (norflurazon-treatment) or in mutant backgrounds where protein import (*ppi2* mutant), plastid transcription (*sig2*) and translation (*prors1-1*) are affected (Kakizaki et al., 2009; Koussevitzky et al., 2007; Tadini et al., 2016; Woodson et al., 2013). Although, GUN1 has been shown to be part of pTACs, not much is known about its functional partners and about the molecular details of its function as an integrator of plastid retrograde signals.

The aim of this work is to elucidate the role of RH50 in RNA metabolism, ribosome biogenesis and chloroplast gene expression, and its possible involvement in the complex network of retrograde signaling. The introgression of RH50 mutation in genetic backgrounds impaired in plastid gene expression, such as *prors1-1* (down-regulated expression of the nuclear gene Prolyl-tRNA Synthetase1), *gun1* (complete loss of retrograde signal regulation) and mutants lacking plastid ribosomal proteins, will allow us to elucidate the role of RH50 in RNA metabolism and its functional relation with GUN1 and the retrograde signaling pathway.

2 Materials and Methods

2.1 Materials and methods of *Synechocystis*

2.1.1 Chemicals, enzymes, radioactive substances and antibodies

Standard chemicals were purchased from Roth (Karlsruhe, Germany), Duchefa (Haarlen, Netherlands), Applichem (Darmstadt, Germany), Serva (Heidelberg, German), Invitrogen (Darmstadt, Germany) and Sigma-Aldrich (Steinheim, Germany).
Restriction enzymes were purchased from New England Biolabs (Ipswich, MA, USA) and Fermentas (Thermo Scientific, Rockford, USA). DNA purification kit, plasmid kits and Taq DNA polymerase from QIAgen (Venlo, Netherlands) and Metabion GmbH (Martinsried, Germany).
Q5 High-Fidelity DNA polymerase and Phusion High-Fidelity DNA polymerase were purchased from New England BioLabs.
Radiochemicals (^{32}P-dCTP,^{35}S-Met) were from Hartmann Analytic (Braunschweig, Germany).

All primers used in this study were purchased from Metabion GmbH. GeneRulerTM 1 kb Plus DNA ladder (Thermo Scientific, Rockford, USA), was used as DNA length standard. The apparent molecular weight of proteins in SDS-polyacrylamide gel electrophoresis was determined according to PageRuler pre-stained molecular weight marker (10 to 170 kDa) from Pierce (Thermo Scientific).
Immuno-decoration of Western blot membranes was done with following antibodies specific for PsbE, PsbI, CP43 and D2 (Agrisera, Vännäs, Sweden).

2.1.2 Database analysis and software tools

Synechocystis sp. PCC6803 sequences were obtained from Cyanobase (http://genome.kazusa.or.jp/cyanobase/Synechocystis) and from NCBI (https://www.ncbi.nlm.nih.gov/nuccore/BA000022), *Arabidopsis thaliana* sequences were obtained from TAIR (https://www.arabidopsis.org/). Vectors were designed with ApeVector (http://biologylabs.utah.edu/jorgensen/wayned/ape/) and VectorNTI

(https://www.thermofisher.com/de/de/home/life-science/cloning/vector-nti-software.html). Melting temperature of primers for PCR analysis was calculated using the Thermo Fisher online Tm calculator tool (https://www.thermofisher.com/de/de/home/brands/thermo-scientific/molecular-biology/molecular-biology-learning-center/molecular-biology-resource-library/thermo-scientific-web-tools/tm-calculator.html#/legacy=www.thermoscientificbio.com).

2.1.3 Bacterial cell culture and growth conditions

The bacterial strains and plastids used in this study are described in Table 2.1 and 2.2. CopyCutter™ EPI400™ Electrocompetent *E. coli* and DH5α *E. coli* bacterial strain were grown in Lysogeny broth (Bertani, 2004) (LB, see abbreviations) medium at 37°C and shaking at 225 rpm or on LB containing 1% w/v agar for growth on plates.

Synechocystis sp. PCC 6803 glucose tolerant wild type strain (GT, H. Pakrasi, Department of Biology, Washington University, St. Louis) and all the mutant generated in this study, unless otherwise indicated, were grown at 25°C in BG11 medium containing 5 mM glucose (Rippka et al., 1979) under continuous illumination at 30 µmol photons m^{-2} s^{-1}. Liquid cultures were shaken at 120 rpm. For growth curves experiments, liquid culture were grown in a Multi-Cultivator MC1000 (Photon System Instrument, PSI, Brno, Czech Republic). For growth on plates, 1.5 % (w/v) agar and 0.3 % (w/v) sodium thiosulfate were added to the BG11 medium. PSII-defective mutant strains were grown in low light conditions (5-10 µmol photons m^{-2} s^{-1}). For positive selection of the mutants, increasing concentrations of kanamycin and/or spectinomycin (10 to 200 µg/ml) were added to the medium. For negative selection of markerless mutant strain, BG11 containing 5 % (w/v) sucrose was used.

Table 2.1: Bacterial strains used in this study

Strain	Characteristics	Selection	Source
E. coli			
DH5α	competent cells used for cloning procedures		
EPI400™	electrocompetent cells used for expression of pUC57_RC2	Amp	GenScript
Synechocystis PCC6803 GT	Glucose tolerant		Prof. H. Pakrasi (Washington University, St. Louis, Missouri)
ΔD1	psbA1, A2 and A3 KO		Prof. P. Nixon (Imperial College, London)

Table 2.2: Plasmids used in this study

Plasmid	Characteristics	Selection	Source
pRL250	nptI-sacB, double selection cassette	Kan, Suc	P. Wolk (Michigan University)
pICH69822	Destination vector for Golden Gate cloning	Kan	E. Weber (Icon Genetics GmbH, Halle)
pUR2LT donor	pVZ derived, mobilizable plasmid, with modified cloning site: ribosomal sliding site (T_{13}) downstream ATG, SfiIA and SfiIB as cDNA cloning	Kan, Spec	unpublished
pUC57_RC1	At psbDC_opt, At psbA_opt, At psb_I	Amp	GenScript, this study
pUC57_RC2	At psbEFLJ_opt, At psbB_opt, At psbT_opt, At psbH_opt	Amp	GenScript, this study
ΔpsbA2 RC1	psbA2 flanking regions + RC1 synthetic construct+ nptI-sacB in pICH69822 destination vector	Kan, Suc	this study
ΔpsbEFLJ RC2	psbEFLJ flanking regions + RC2 syntehtic construct + nptI-sacB in pICH69822 destination vector	Kan, Suc	this study
ΔpsbA2 KO	psbA2 flanking regions + nptI-sacB in pICH69822 destination vector	Kan, Suc	this study
ΔpsbDC KO	psbDC flanking regions + nptI-sacB in pICH69822 destination vector	Kan, Suc	this study
ΔpsbDC KO spec	psbDC flanking regions + spec cassette in pICH69822 destination vector	Spec	this study
pUR2LT donor RC2	RC2 synthetic construct + nptI-sacB in self replicative vector	Kan, Spec, Suc	this study
psbA2 RC1 no cassette	psbA2 flanking regions + RC1 synthetic construct in pICH69822 destination vector	Kan	this study

Selections: Kan, Kanamycin; Suc, sucrose; Spec, spectinomycin; Amp, ampicillin.

2.1.4 Synthetic construct design

S*ynechocystis* sp. PCC6803 sequences were obtained from Cyanobase (http://genome.kazusa.or.jp/cyanobase/Synechocystis) and from NCBI (https://www.ncbi.nlm.nih.gov/nuccore/BA000022) (see before); *A. thaliana* sequences were obtained from TAIR (https://www.arabidopsis.org/). The flanking region sequences of each construct were PCR amplified and then purified from 1 % agarose gel with the QIAgen (Venlo, Netherlands) or Metabion (see before) gel extraction kit following the producer's instructions. All vectors were assembled using the one-step Golden Gate Shuffling cloning strategy (Engler et al., 2008). For all constructs, the plasmid pICH69822 was used as destination vector. The *nptI-sacB* double-selection cassette was amplified from the pRL250 plasmid, the spectinomycin resistance cassette was amplified from pICH30971, using the primers 43 and 44 (Table 2.1). The synthetic constructs, RC1 and RC2, were designed to express the *A. thaliana* core of Photosystem II. In particular, RC1 was carrying the *A. thaliana psbDC*, *psbA*, *psbI* genes and RC2 the *psbEFLJ*, psbB, *psbT*, *psbH* genes. All *A. thaliana* genes were codon optimized using OptimumGene™ - Codon Optimization tool by GenScript (Codon Adaptation Index value >0.8) for expression into *Synechocystis* sp. PCC6803 (*At psbDC_opt, At psbA_opt, At psbI_opt, At psbEFLJ_opt, At psbB_opt, At psbT_opt and At psbH_opt)*, purchased from GenScript (Hong Kong) and cloned into the

EcoRV restriction site of pUC57. The synthetic construct RC2 was amplified with primer 45 and 45 (Table 2.1) designed with a restriction site for *SfiI* restriction enzyme, using Phusion high fidelity DNA polymerase. This was subsequently digested with *SfiI* at 50°C for 2h. pUR2LT expression vector was also digested with *SfiI*. Purified RC2-*SfiI* construct and digested pUR2LT were ligated at 4°C over-night generating the pUR2LT donor RC2 vector.

2.1.5 *Synechocystis*' natural transformation

Synechocysts wild type and mutant strains were transformed with plasmid vectors purified using Plasmid Midiprep kit from Qiagen or Metabion. For each transformation, 10 ml of growing cells at an OD_{730} of 0.6 were harvested by centrifugation at 4000x*g* for 10 min and resuspended in 1/20 volume of BG11. 2 µg of plasmid DNA per transformation were added to the cells. Transformations were incubated in light for 5 hours, the last 3 hours with shaking. For recovery, 1 mL of fresh BG11 was added and the transformations were incubated overnight in the dark with shaking at 25 °C. On the next day, cells were collected by centrifugation at 4500xg for 10 min, resuspended in a small volume of fresh BG11 medium and plated on BG11 agar plates containing low concentration (5-10 ug) of the correct antibiotic. Unless otherwise indicated, plates of transformed cells were incubated in light at 25 °C.

2.1.6 Conjugation of cyanobacteria with pUR2LT donor RC2

Liquid culture of *E.coli* helper strain JM53/RP4 and *E. coli* donor strain (DH5α or F10) carrying the desired target plasmid (pUR2LT donor RC2) were grown in LB medium with appropriate antibiotic with shaking at 180 rpm. The cultures were then diluted 1:40 in LB without antibiotics, to a final volume of 10 mL and grown for 2,5h at 37°C at 180 rpm. The cells were gently harvested by centrifuging for 10 min at 2000xg and resuspended in 1/10 volume (1 mL) of LB. 1 mL of helper and donor strain were collected in a 2 mL tube, centrifuged for 5 min at 2000xg and resuspended in 100 µl LB. The cell mixture was incubated for 1 h at 30°C without shaking and then 800 µl of recipient cyanobacteria strain (*Synechocystis* OD_{750nm} about 0.9) were added. The cell were harvested by centrifuging at 2000x*g* for 5 min and resuspended in 30µl BG11-medium. The solution was dripped onto sterile filter (nitrocellulose) and placed on a BG11 agar plate containing 5% LB medium without antibiotics. The plates were

incubated overnight at 30°C in dim light. The filters were then rinsed with fresh BG11-medium and different volume of this suspension were plated on BG11agar plates containing the appropriate antibiotic. Plates were let at 30°C with 50 µE for 10-14 days. The clones were transferred in new plates with higher concentration of antibiotic.

2.1.7 PCR (standard and High fidelity)

For genotyping of bacterial strains, PCR analysis was performed using 0.5 µl of genomic DNA as template in a total reaction volume of 20 µl. The reaction mix contained 1x PCR-buffer (QIAgen), 100 µM dNTPs, 200 µM primers, 0.5 units of Taq DNA polymerase. The PCR products were then loaded on a 1% agarose TAE (150 mM Tris-HCl, 1.74 M Acetic acid, 1 mM EDTA) gel and visualized by Ethidium bromide staining.

DNA fragments were amplified from *Synechocystis* genomic DNA or *A. thaliana* Col-0 cDNA with the Phusion High-Fidelity DNA Polymerase (New England BioLabs) or Q5 High-fidelity DNA Polymerase (NEB). Reactions were performed in a total volume of 20 µl each containing 1x HF reaction buffer, 200 µM dNTPs, 200 µM of each primer (listed in Table 2.3) and 0.4 units of HF DNA Polymerase. The PCR-products were loaded on a 1% agarose gel and then cut from the gel and purified with the QIAgen gel extraction kit following the producer's instructions.

Table 2.3: Primers used in this study

Primer Name	Sequence 5'-3'	Purpose
HR1 FW	TTT**GGTCTC**T*AGGT*TTCCTTGTCATAGCTCCGAGC	psbA2 RC1 and psbA2 KO constructs HR1
HR1 RV	TTT**GGTCTC**T*GGGT*ACCATAGTTCTGGGCTGTGTAG	psbA2 RC1 construct HR1
HR 1 RV_2	TTT**GGTCTC**T*AACG*ACCATAGTTCTGGGCTGTGTAG	psbA2 KO construct HR1
HR2 FW	TTT**GGTCTC**T*TATG*AGTCCGGGGCAGTTACCATTAG	psbA2 RC1 and psbA2 KO constructs HR1
HR2 FW_2	TTT**GGTCTC**T*CGTT*AGTCCGGGGCAGTTACCATTAG	markerless psbA2 RC1 construct HR2
HR2 RV	TTT**GGTCTC**T*AAGC*ATCGCCTATTGCAACTGCGC	psbA2 RC1 and psbA2 KO constructs HR2
HR3 FW	TTT**GGTCTC**T*AGGT*AGCCGACATCATCCAAAC	psbEFLJ RC2 construct HR3
HR3 RV	TTT**GGTCTC**T*AACG*CTAGGGAACCATTGCCAC	psbEFLJ RC2 construct HR3
HR4 FW	TTT**GGTCTC**T*GGTT*TAAGGTGGGCTTGG	psbEFLJ RC2 construct HR4
HR4 RV	TTT**GGTCTC**T*AAGC*AAATACAGTCCTGGCTCTGC	psbEFLJ RC2 construct HR4
HR5 FW	TTT**GAAGAC**TT*AGGT*ACCTTCAACAGTCTCCACG	psbDC KO construct HR5
HR5 RV	TTT**GAAGAC**TT*AACG*AAATGCAAATCCTCTTGCGTAGC	psbDC KO construct HR5
HR6 FW	TTT**GGTCTC**T*TATG*AACTGGATGGGGATGGC	psbDC KO construct HR6
HR6 RV	TTT**GGTCTC**T*AAGC*TAGAGCGTCGCCATAGGAAATTAG	psbDC KO construct HR6
psbA2 Syn FW	AAACTGACTGACCACTGACC	genotyping
psbA2 Syn RV	TTACCAGCGGCATTAATGGC	genotyping
AtpsbD FW	ACTCATGGATTGGCCTCCAG	PCR, N.B.
AtpsbD RV	AGCACGTAAATTCAAGGCCAGC	PCR, N.B.
AtpsbC FW	TATTTAATGGGACTCTGGCC	PCR, N.B.
AtpsbC RV	AACAGGCAATAAAACCGCAC	PCR, N.B.
AtpsbB FW	GCCATTATTCCCACCAGTGC	PCR, N.B.
AtpsbB RV	ACCGGCTGTTGTTAAAGCTG	PCR, N.B.
AtpsbI FW	ATGTTGACCCTGAAACTGTT	PCR, N.B.
AtPsbI RV	TCCGGCCGGGATCGTTACTC	PCR, N.B.
psbEFLJ Syn FW	AATGGAGCGATGTGATTGCTCC	genotyping
psbEFLJ Syn RV	ATAGGCATCGGGATCTAAACG	genotyping
AtpsbE FW	ACAGCATTACTATTCCCTCTC	PCR, N.B.
AtpsbE RV	TTCGTCTAACTGTTCCAAGGG	PCR, N.B.
AtpsbF FW	ATGACTATTGACCGCACTTATCC	PCR
AtpsbF RV	AAATTGCATGGCACTAATGGAC	PCR
AtpsbL FW	ATGACTCAATCCAATCCCAATG	PCR
AtpsbL RV	TAATTGGAAAACAACACGGC	PCR
AtpsbJ RV	TTACAAACTGGAACCCAGGC	PCR
AtpsbB FW	TTGTGTTTAGCGGGCTGTG	PCR, N.B.
AtpsbB RV	TTGATTTTCAGCCAAGCCGG	PCR, N.B.
AtpsbT FW	TTGTTAGTTTCCACTTTGGG	PCR
A psbT RV	TTTGGTACTAATTTTGGGgg	PCR
AtpsbH RV	TACCATCTAACAACACACTGG	PCR
psbDC Syn FW	GGCTAAAGCGTGATCGTTTC	genotyping
psbDC Syn RV	TGTGGAAGGGGTTCAAAGTC	genotyping

psaA Syn FW	TGGTTCCACTACCACGTCAA	PCR
psaA Syn RV	TAGAGTTCCGCCATCTTGCT	PCR
Spec Fw	TTT**GGTCTC**T*CGTT*TTGAATTCGATCCATGGTCG	psbDCKO spec construct
Spec RV	TTT**GGTCTC**T*CATA*TAGAGCTTGAGTTAAGCCGC	psbDCKO spec construct
SfiI RC2 FW	TTTT**GGCC***ATTA*TGGCCGCGGCTCACAAAATAGTAGAC	pUR2LT donor RC2
SfiI RC2 RV	TTTT**GGCC***GAGG*CGGCCCTGACTAGCCAATGACAG	pUR2LT donor RC2

Bold: restriction site.**GGTCTC**, BsaI; **GAAGAC**, BbsI; **GGCC**, SfiI. italis: sticky end

2.1.8 Genomic DNA isolation

Small-scale genomic DNA isolation was performed according to the xanthogenate-SDS method (Tillett and Neilan, 2000). In brief, 1 ml of exponentially growing cell cultures were pelleted and resuspended in 50 µl of TER buffer (10 mM Tris/HCl pH 7.4, 1 mM EDTA pH 8.0 and 100 µg/ml RNAse A). 750 µl of freshly made XS buffer (1% calciumethylxanthogenate, 100 mM Tris/HCl pH 7.4, 20 mM EDTA pH 8.0, 1% SDS, 800 mM ammonium acetate) were added to each sample which were then mixed by inversion and incubated at 70^{o}C for 2 h in order to dissolve membranes. The samples were vortexed for 10 sec and incubated on ice for 30 min. To remove cells debris, the samples were centrifuged for 10 min at 13,000x*g* . The supernatant was transferred to a new tube containing 750 µl isopropanol for DNA precipitation. The DNA was collected by centrifugation at 12,000x*g* for 10 min and washed with 70% ethanol. Finally, the DNA was air dried and resuspended in 100 µl ddH_2O.

2.1.9 RNA isolation

Total RNA was isolated from *Synechocystis* samples using the TRIzol method. Cells from 50 ml liquid cultures (OD_{730}=0.7) were pelleted at 6,000x*g* for 15 min, resuspended in 1 ml TRIzol (Thermo Fisher) and vortexed thoroughly. The samples were immediately frozen in liquid nitrogen and incubated at 65^{o}C for 15 min, (this step was repeated 2 times). Cell debris was removed by centrifugation at 12,000x*g* for 15 min at 4^{o}C. The supernatant was transferred into a new tube and mixed with 0.2 volumes of chloroform and incubated at room temperature for 15 min. After phase separation by centrifugation at 12,000x*g* for 15 min at 4^{o}C, the aqueous phase was transferred into a new tube. RNA was precipitated with 0.25 volume of isopropanol and 0.25 volume of a high salt solution (1.2 M NaCl and 0.4 M sodium

citrate) and washed with 70% ethanol. The dried RNA pellet was resuspended in 100 µl H_2O and the concentration was measured by Nanodrop (Nanodrop 200, Peqlab).

2.1.10 *Arabidopsis* cDNA Synthesis

Synthesis of *Arabidopsis thaliana* cDNA was performed using the iScript reverse transcriptase kit (Bio-Rad, Hercules, CA, USA, www.bio-rad.com). During the whole procedure, DEPC-treated water was used. For digestion of DNA contaminations, DNAse treatment of 1 µg of RNA was performed in a total reaction volume of 10 µl, containing 1x PCR buffer (Qiagen, Venlo, Netherlands) + $MgCl_2$ and 0.5 units of DNAse I. The reaction mix was incubated at room temperature for 30 min and the enzyme was then inactivated by adding 2.5 mM EDTA and further incubating for 15 min at 65 °C. Each RNA sample was then used in a total reverse transcription reaction volume of 20 µl, containing 1x iScript reaction mix buffer and 1 µl of iScript reverse transcriptase. The first-strand cDNA synthesis was performed according to the following protocol by using a thermocycler (BioRad): 5 min at 25 °C, 40 min at 42 °C and 5 min at 85 °C.

2.1.11 Northern blot analysis

Northern blot analysis was performed according to Green and Sambrook (2001). 10 µg total RNA samples were mixed with 5x RNA loading dye and incubated at 65^{o}C for 15 min and then kept on ice for 5 min. After denaturation, the samples were loaded on an denaturing 2% (w/v) agarose gel, which contains 1x MOPS buffer (200 mM MOPS, 50 mM sodium acetate and 10 mM EDTA, pH 7) and 1% formaldehyde and run for 2-3 h, at 60 V, in a 1x MOPS running buffer.

The gel was then subjected to the following manipulations for the RNA capillary transfer to the membrane. The gel was equilibrated in 10x SSC (1.5M Na-chloride and 150 mM Na-citrate, pH 7). The capillary transfer was performed by placing the gel upside down on the transfer bridge (made of Whatman paper 3MM). The positively charged nylon membrane (Hybond N+; GE Healthcare, Freiburg, Germany) was shortly equilibrated in 2x SSC and layered on top of the gel, as well as three Whatman papers (3MM) also equilibrated in 2x SSC. On top of this stack, paper towels and an extra weight were placed in order to start the capillary transfer. The transfer solution was 10x SSC and the transfer was carried out overnight (16-20 h). The RNAs were cross-linked on the membrane by UV radiation

(Stratalinker® UV Crosslinker 1800, Stratagene, USA) at 1200 µJ cm^{-2}. The membrane was stained in a methylene blue solution (0.02% (w/vol) in 0.3 M Na-acetate (pH 5.5)) until the rRNAs became visible (~3–5 min) and then rinsed with ddH_2O to wash away the excess dye. For the pre-hybridization step, the membrane was placed into a glass cylinder containing 20 ml prehybridization buffer (7% SDS, 0.25 M Na2HPO4 pH 7) and 160 µl denatured herring sperm. The membrane was incubated at 65°C for at least 4 h prior to hybridization. For probe preparation approximately 100 ng of PCR-product were filled up to 12 µl with ddH_2O, denaturated at 95°C for 5 min and cooled down on ice for 5 min. Afterwards, 4 µl of 5x OLB buffer (50 mM Tris pH6.8, 10 mM MgOAc, 50 mM DTT, 0.5 mg/ml BSA, 33 µM of dATP, dTTP and dGTP), 1 µl of Klenow DNA polymerase and 3 µl of radioactive ^{32}P-dCTP were added to the probe and incubated for 3h at 37°C. For probe purification, Illustra MicroSpinTM G-25 Columns were used according to the producer's instructions. The radioactive labeled probe was then added and the hybridization was performed for 16 h at 65°C. Hybridization buffer was discarded and 10 ml of pre-warmed washing buffer (0.1% SDS, 0.2 M NaCl, 20 mM NaH_2PO_4, 5 mM EDTA; pH7.4) was added to the membrane and incubated for 30 min at 65°C. The second washing step was performed with the same buffer but incubated for 15 min at 65°C. The final washing step was carried out with 1x RT buffer (6 mM NaH_2PO_4, 1 mM EDTA, 0.2% SDS; pH 7.0) for at least one hour on a shaker at room temperature. The membrane was then exposed to a radioactive sensitive screen (Storage Phosphor Screen, Fuji) overnight. The signals were detected with the Phosphorimager (Typhoon, GE Healthcare).

2.1.12 Protein extraction

For total protein extraction, *Synechocystis* cultures in the exponential growth phase were collected by centrifugation and resuspended in 1 volume of thylakoid buffer (50 mM HEPES/NaOH pH 7.0, 5 mM $MgCl_2$, 25 mM $CaCl_2$, 10 % glycerin). Cell suspensions were transferred into a 2 ml tube together with 0.5 volumes of glass beads (0.25-0.5 mm diameter), and vortexed 5 times for 20 sec. Samples were placed on ice for 1 min between each vortexing step. Beads and unbroken cells were pelleted by centrifuging at 1600x*g* for 3 min and then the supernatant, corresponding to the total protein fraction, was transferred into a new tube.

2.1.13 Thylakoid preparation

For preparation of thylakoid fractions, the crude extract was diluted in 2 volumes of thylakoid buffer and membranes were pelleted at 16000x*g*, 4 °C, for 30 min. The thylakoid pellet was washed once more in thylakoid buffer and resuspended in a small volume of it.

2.1.14 Immunoblot analysis

For Immunoblot analysis the protein samples were loaded on a Tris-tricine SDS-Polyacrylamide gel (Schagger and von Jagow, 1987) with the desired acrylamide concentration and, afterwards, the proteins were transferred to PVDF membranes (Immobilon-P, Millipore, Germany). After Western blotting according to the manufacturer's instructions using a semi dry blot system (Bio-Rad), membranes were saturated with 5 (w/v) milk proteins dissolved in 1x TBS-T (150 mM NaCl, 10 mM Tris pH 8.0, 0.1 % v/v Tween20) and incubated overnight at 4°C with the specific primary antibody diluted in TBS-T containing 5 % milk proteins. The primary antibody was then removed and the membranes were washed 3 times in TBS-T (10 min each). The membranes were afterwards incubated for 1 hour with the corresponding secondary antibody, diluted in TBS-T containing 5 % milk proteins, conjugated with horseradish peroxidase. Detection of the horseradish peroxidase signal was performed using the Pierce ECL Western Blotting Substrate kit (Thermo Scientific, Rockford, USA).

2.1.15 Bacterial whole cell absorbance spectra

Absorbance spectra of *Synechocystis* cells cultures were recorded using a spectrophotometer (Shimadzu, Kyoto, Japan). The optical density of the suspensions was measured at 730 nm.

2.1.16 Low temperature (77K) fluorescence emission spectra

77K fluorescence was recorded using an in-house built spectrofluorometer. Synechocystis samples of different mutants were used. Cells were harvested, washed and resuspended in BG11 liquid medium to a final OD_{730} of 0.5, dark-adapted for 10 min and then rapidly frozen in liquid nitrogen. To investigate the stoichiometry of the PSI and PSII complexes, their fluorescence emission spectra under the Chl a

excitation at 435 nm were recorded between 600 and 800 nm. Fluorescence emission peaks of PSI (720 nm) of the different strains were compared by normalizing the PSII emission peak (695 nm) to the one from WT.

2.1.17 Accession Numbers

PSII *A. thaliana* genes used in the synthetic constructs: *psbA* (*AtCg00020*), *psbDC* (*AtCg00270-280*), *psbI* (*AtCg00080*), *psbEFLJ* (*AtCg00580-570-560-5550*), *psbB* (*AtCg00680*), *psbT* (*AtCg00690*) and *psbH* (*AtCg00710*).

PSII *Synechocystis* genes: *psbA1* (*slr1181*), *psbA2* (*slr1311*), *psbA3* (*sll1867*), *psbD1C* (*sll0849-0851*), *psbD2* (*slr0927*), *psbEFLJ* (*ssr3451, smr0006-0007-0008*), *psbB* (*slr0906*), *psbH* (*ssl2598*), *psbT* (*smr0001*) and *psbI* (*sml0001*). PSI *Synechocystis* gene *psaA* (*sllr1834*).

2.2 Materials and methods *A. thaliana*

2.2.1 Chemicals, enzymes, radioactive substances and antibodies

Chemicals, enzymes and radioactive substances as described in chapter 2.1.1. Commercially available antibodies were used against RbcL (Agrisera, see before) PRPS1 (Agrisera), PRPS5 (Agrisera), PRPL11 (Meurer et al., 2017) and GFP (Life technologies, Carlsbad, USA). A RH50 antibody (GenScript, New Jersey, United States, www.genscript.com) was raised against the peptide CDNERGLRGGSHSKG.

2.2.2 Database analysis and software tools

Gene and protein sequences were obtained from NCBI and TAIR (www.ncbi.nlm.nih.gov, www.arabidopsis.org). The chloroplast transit peptide lengths were predicted using ChloroP 1.1 (http://www.cbs.dtu.dk/services/ChloroP/). Nucleic acid sequence analysis was performed using the Gene Runner (www.generunner.net) and BioEdit Sequence Alignment Editor (www.mbio.ncsu.edu/bioedit/bioedit.html) software. ImageJ software (rsbweb.nih.gov) was used for growth measurements.

2.2.3 Plant material, propagation and growth measurements

The *A. thaliana* T-DNA insertion mutant line *rh50-1* (GABI_629A10, genetic background Col-0) was obtained from the GABI-KAT collection (Rosso et al., 2003) and the transposon line *rh50-2* (GT_5_111858, genetic background L*er*) from the GT collection (http://gt.jbei.org/arabidopsis.html). The regions flanking the T-DNA and transposon insertions were PCR-amplified and sequenced (primer sequences in Table 2.4). Both *rh50-1* and *rh50-2* contain the T-DNA or transposon insertion in exon 2 (at positions 433 and 429 relative to the start codon, respectively). In addition, the following previously described mutant lines were used in this work: *gun1-102* and *prps21-1* (Tadini et al., 2016), *prors1-1* (Pesaresi et al., 2006), *prpl11-1* (Pesaresi et al., 2001), *prps1-1*, *prps17-1* and *prpl24-1* (Romani et al., 2012). *A. thaliana* plants were grown on soil in a climate chamber as described (Pesaresi et al., 2009). For the norflurazon (NF), lincomycin (LIN) and erythromycin treatments, surface-sterilized mutant and

wild type (WT) seeds were plated on Murashige and Skoog (MS) medium (PhytoTechnology Laboratories, LLC™, USA) containing 1% (w/v) sucrose and 0.8% (w/v) agar supplemented with either 5 µM NF (Sandoz Pharmaceuticals, Vienna, Austria) or 220 µg ml^{-1} of LIN (Sigma, St Louis, MO, USA) or 50 µg ml^{-1} erythromycin (Sigma-Aldrich, Munich, Germany). For the cold stress treatments, surface-sterilized mutant and WT seeds were plated on MS medium containing 1% (w/v) sucrose. The seeds were allowed to germinate in a climate chamber at 4°C under long day conditions (16h light and 8h dark) at either growth or low light (100 and 30 µmol photons s^{-1} m^{-1}, respectively) conditions for 6 weeks and then transferred at 22°C under same long day conditions.

Table 2.4. Primer used in this study.

Locus	Gene	Sense primer (5' to 3')	Antisense primer (5' to 3')	Use	Nucleotide added at 5' end
AT3G06980	*RH50*	TGTTTCGTAACGGCGGAGGAG	CAAAACGCCTATCTTCTCTAC	genotyping	/
AT3G06980	*rh50-1*	CCCATTTGGACGTGAATGTAGACAC	CAAAACGCCTATCTTCTCTAC	genotyping	/
AT3G06980	*rh50-2*	TGTTTCGTAACGGCGGAGGAG	CGAATAAGAGCGTCCATTTTAG	genotyping	/
AT3G06980	*RH50*	**GTGGATCC**TTGTTTCGTAACGGCGGAGG	**GTCGACTTATTTTTCGAACTGCGGGTGGCTCCAAGCGCT**CAAAAGAAGAGGCTGTAAAGCAAAC	EMSA	BamHI/Strep-tag-SalI
AT1G61520	*LHCA3*	AGGCTGGTCTGATTCCAGCA	ACTTGAGGCTGGTCAAGACG	NB	/
AT3G47470	*LHCA4*	TGAGTGGTACGATGCTGGGA	GTGTTGTGCCATGGGTCAGA	NB	/
AT1G29910	*LHCB1.2*	GACTTTCAGCTGATCCCGAG	CGGTCCCTTACCAGTGACAA	NB	/
AT5G01530	*LHCB4.2*	AGCTAGTGGATGGATCATCT	CAGGAGGAAGAGAAGGTATC	NB	/
AT4G02770	*PSAD1*	AAGCCGCCGGGATCTTCAAC	CTAAGCCTTGTCCCCAAAGC	NB	/
AT4G28750	*PSAE1*	ATGGCGATGACGACAGCATC	TGTTGGTCGATATGTTGGCG	NB	/
AT1G08380	*PSAO*	ATGGCAGCAACATTTGCAAC	GTAATCTTCAGTCCTGCCCT	NB	/
AT1G30380	*PSAK*	ATGGTCTTCG AGCCACCAAA	CGTTCAGGTGCATGAGAATA	NB	/
ATCG00490	*rbcL*	CGTTGGAGAGACCGTTTCTT	CAAAGCCCAAAGTTGACTCC	NB	/
ATCG00020	*psbA*	CGGCCAAAATAACCGTGAGC	TATACAACGGCGGTCCTTATG	NB	/
ATCG00920	*rrn16S*	AGTCATCATGCCCCTTATGC	CAGTCACTAGCCCTGCCTTC	NB	/
23S-4.5S intergenic region		CATCCCCGCAGGGGCGGAGAACCCGTTGCTGTCTCGGCTGTGCTACCGGAGGCTCTGGGGAAGTCGGAATCTC****		NB/SB	/
23S-4.5S intergenic region		***TGCTCTCCTATTCCGACTTCC	TACCGGTCTGTTAGGATGCC	EMSA	/
ATCG01180	*rrn23S*	GTTCGAGTACCAGGCGCTAC	CGGAGACCTGTGTTTTTGGT	NB/SB	/
		TAATACGACTCACTATAGGGggacctttccctagtacgagag	GGAGAGCACTCATCTTGGGG	EMSA	/
ATCG00960	*4.5S rRNA*	GAAGGTCACGGCGAGACGAGCC	GTTCAAGTCTACCGGTCTGTTAGG	NB	/

ATCG00970	*5S rRNA*	TATTCTGGTGTCCTAGGCGTAG	G ATCCTGGCGTCGAGCTATTT	NB	/
ATCG00770	*rps8*	ATGGGGAAAGACACCATTGC	TCCGCCGATTCTTTTTAGTC	NB	/
ATCG00830/ ATCG01310	*rpl2*	GAGGAATAATTACCGCAAGG	CTCTACCCAAACTTTTCTGG	NB	/
ATCG00800	*rps3*	AGACTTGGTACAACCCAAAG	TGTAAAGGAACTCTGCCTTC	NB	/
ATCG00840/ ATCG01300	*rpl23*	ATGGATGGAATCAAATATGCAG	TCTAAGAGGTGGAATAGAATAACC	NB	/
AT3G06980	*RH50*	**GTGGATCC**TGTTTCGTAACGGCGGAGGAG	**GTGGATCC**GGTCAAGATGAAGAGTTACTTAGGT TGTG	Yeast 2H	BamHI/BamHI
AT2G31400	*GUN1*	**GTGAATTC**GCTCATCTTTCACAGACTACTC	**GTGGATCC**CACAGAGCCAAACATTGTTAGG	Yeast 2H	EcoRI/BamHI
AT1G32990	*RPL11*	**GTGAATTC**GCCATGGCTCCACCTAAACCC	**GTGGATCC**ATAGAAACTACCAACCAGGC	Yeast 2H	EcoRI/BamHI
AT5G30510	*RPS1*	**GTGAATTC**GTTGCAATGTCTAGCGGTC	**GTGGATCC**CTAAATATCAACTGCAGAAGGAATG	Yeast 2H	EcoRI/BamHI
AT1G79850	*RPS17*	**GTGAATTC**GCCATGAAAACGATGCAGGG	**GTGGATCC**CTACGCCGGCTGCTGAGAC	Yeast 2H	EcoRI/BamHI
AT3G27160	*RPS21*	**GTGAATTC**GAATCAATGGCGGTCGAAG	**GTGGATCC**TCAAGAAGGTACATCTCCACCAG	Yeast 2H	EcoRI/BamHI
AT1G08520	*CHLD*	**GTGGATCC**GTGCCTCCGCGAATGCTAC	**GTGGATCC**GTATTGCAGACAAAATGAGGTCAAG	Yeast 2H	BamHI/BamHI
AT3G06980	*RH50*	*AGATGTTGGCGAGAGCTCCAC	**TTGTGAACTCGTAAGCGTTTGG	Subcellular localization	attB sites
AT2G31400	*GUN1*	*TCCTTTCAATGGCGTCAACG	**ACAAAAGAAGAGGCTGTAAAGCAAACG	Subcellular localization	attB sites

NB, Northern Blot; SB, Slot Blot; attB sites: GGGGACAAGTTTGTACAAAAAAGCAGGCT*; GGGGACCACTTTGTACAAGAAAGCTGGGT**; TAATACGACTCACTATAGGG***; CCCTATAGTGAGTCGTATTA****

2.2.4 Transient co-expression in *A. thaliana* leaf protoplasts

GUN1 and *RH50* cDNA were cloned without their stop codons into the gateway entry vector pDONR207 (Invitrogen; Carlsbad, CA) as described (Tadini et al., 2016). The entry vector was then recombined with pK7RWG2 and pB7FWG2 (Vinti et al., 2000) to generate 35S promoter-driven C-terminal GUN1-RFP and RH50-GFP fusions. Seedlings of 2-week-old wild-type *A. thaliana* plants were cut into small pieces and incubated for 16 h at 24°C in the dark in a protoplasting solution (10 mm MES, 20 mm CaCl2, 0.5 m mannitol, pH 5.8, 0.1 g mL^{-1} macerozyme (Duchefa, Haarlem, Netherlands), and 0.1 g mL^{-1} cellulase [Duchefa]). Protoplasts were then isolated as described (Dovzhenko et al., 2003) and transfected by the PEG–calcium-mediated transfection with the GUN1-RFP and RH50-GFP constructs. Protoplasts were incubated for 24 h to allow gene expression. The samples were then studied with a confocal microscope (Leica TCS SP5 CLSM).

2.2.5 Chlorophyll *a* fluorescence measurements

Five plants of each genotype were analyzed and average values and standard deviations were calculated. In vivo chlorophyll *a* fluorescence of single leaves was measured using the Dual-PAM 100 (Walz, Germany). Pulses (0.5 s) of saturating red light (5,000 µmol photons m^{-2} s^{-1}) were used to determine the maximum fluorescence and the ratio $(F_m - F_0)/F_m = F_v/F_m$, where F_0 is the minimum fluorescence. A 15-min exposure to red actinic light (37 µmol photons m^{-2} s^{-1}) was used to drive electron transport before measuring the effective quantum yield (Φ_{II}) (Armbruster et al., 2010). In vivo Chl a fluorescence of whole plants was recorded using an imaging Chl fluorometer (Imaging PAM; Walz, Germany). Dark-adapted plants were exposed to a pulsed, blue measuring beam (1 Hz, intensity 4; F_0) and a saturating light flash (intensity 4) to obtain F_v/F_m, as the maximum quantum yield of PSII.

2.2.6 Co-expression analysis performed by Dr. Tatjana Kleine

To identify genes represented on the ATH1 Affimetrix microarray (22K) chip that show a significant degree of co-expression with *GUN1*, an expression correlation analysis with the "CoExSearch" tool implemented in ATTED-II (htt://atted.jp/; (Obayashi et al., 2009, 2007) was performed. Hierarchical clustering was done with the single linkage method of the „HCluster" tool in ATTED-II.

2.2.7 Transcriptome sequencing and analysis

Total RNA was extracted from 3-week-old wild type and *rh50-1* plants, using standard TRIzol extraction and purification. RNA was tested for quality using a spectrophotometer, agarose gel visualization and PCR. RNA-Seq library preparation and lnRNA sequencing (LncRNAs) were both performed at Novogene Biotech (Bejing, China) using standard Illumina protocols. The RNA-Seq libraries were sequenced on an Illumina HiSeq 2500 system with the paired-end mode. At least 3 biological replicates were used for each analysis. The quality of the raw data was verified with FASTQC (http://www.bioinformatics.babraham.ac.uk/projects/fastqc/). Sequences were filtered and trimmed using Trimmomatic (http://www.usadellab.org/cms/?page=trimmomatic) (Bolger et al., 2014). Reads were mapped to the *Arabidopsis* reference genome (TAIR10) using HISAT with default parameter settings (https://ccb.jhu.edu/software/hisat/index.shtml). Transcript assembly and FPKM (RPKM)

values were calculated using htseq-count (http://www-huber.embl.de/HTSeq/doc/count.html, version of 2016). Deregulated genes were identified with DESeq2 (https://bioconductor.org/packages/release/bioc/html/DESeq2.html) (Love et al., 2014). These analyses were performed using a local Galaxy server (http://galaxyproject.org) (Giardine et al., 2005). To obtain a more detailed view of the chloroplast genome, the reads of the WT and *rh50-1* were mapped to the chloroplast genome of *A. thaliana* using the Qiagen CLC Genomics Workbench v.8.5.1 (hereafter CLC). Before assembly, the reads were trimmed using CLC with default settings. The trimmed sequence were then mapped to the chloroplast genome *of A. thaliana* (NC_000932.1). Fold change was calculated and visualized with Excel.

2.2.8 Nucleic acid analysis

A. thaliana genomic DNA was isolated as described (Ihnatowicz et al., 2004) and RNA was purified from total leaf frozen tissue as described before (Armbruster et al., 2010). Northern analyses were performed under stringent conditions (Green and Sambrook, 2001) using 5 µg samples of total RNA. Probes complementary to nuclear and chloroplast genes were used for the hybridizations. Primers used to amplify the probes are listed in Table 2.4. Probes used were cDNA fragments except for the 23S-4.5S intergenic region, for which DNA fragments labelled with ^{32}P were used. Signals were quantified by the ImageJ software (http://imagej.nih.gov/ij/index.html).

2.2.9 Immunoblot analyses

Frozen plant material was homogenized in 2X Laemmli buffer (200 mM Tris-HCl pH 6.8, 4% SDS, 20% glycerol, 5% β-mercaptoethanol) and solubilized for 15 min at 65°C. After a centrifugation step (16,000x*g*, 10 min) the supernatant was boiled 5 min to denature the sample. The total protein extraction was then loaded on a Tris-glycine 12% SDS-PAGE (Schagger and von Jagow, 1987), afterwards, proteins were transferred to PVDF membranes (Ihnatowicz et al., 2004) and immuno-decorated with antibodies. Signals were quantified by the ImageJ software (http://imagej.nih.gov/ij/index.html).

2.2.10 Protein complex and polysome analysis

For two-hybrid assays, the coding sequences for the mature proteins (without the chloroplast transit peptides cTP) of interest (see Table 2.4 for primer sequences), were cloned into pGBKT7 (RH50) and pGADT7 (GUN1, PRPS21, PRPS17, PRPL11 and PRPL24) vectors (Clontech Otsu, Japan), or *vice versa*. Interactions in yeast were then analyzed as described before (DalCorso et al., 2008). Polysome loading experiments were conducted as described by Barkan (1993) were performed by Dr. N. Manavski.

2.2.11 *In vivo* translation assay

The *in vivo* translational assay was performed essentially as described (Tadini et al., 2016). Twelve leaf discs of 4 mm diameter were incubated in a buffer containing 20 µg ml^{-1} cycloheximide, 1 mM K_2HPO_4 – KH_2PO_4 (pH 6.3), and 0.1% (w/v) Tween-20 to block cytosolic translation. Then, [^{35}S] methionine was added to the buffer (0.1 mCi ml^{-1}) and the material was vacuum-infiltrated. Leaves were exposed to light (20 µmol photons m^{-2} s^{-1}) and four leaf discs were collected at each time point (5, 15 and 30 min). Total proteins were extracted as described (Martínez-García et al., 1999) and loaded on glycine SDS-PAGE (12% PAA). Signals were detected and quantified using a Phosphoimager (GE Helathcare Life Sciences, Little Chalfont, England, www3.gehealthcare.com) and the program Image Quant (GE Healthcare Life Sciences).

2.2.12 Co-immunoprecipitation and slot blot analysis performed by Dr. Manavski

Chloroplasts from three-week-old WT plants were isolated as described previously (Stoppel et al., 2012). Lysis was achieved by passing the chloroplast-containing solution (30 mM HEPES pH 8.0; 10 mM Mg acetate; 60 mM K acetate; freshly added Protease Inhibitor Cocktail (Roche, Basel, Swiss) 25 times through a 0.45 mm needle. Lysates were cleared by centrifugation at 45.000 g for 30 min at 4°C. One milligram of stroma was diluted with the same volume of Co-IP buffer (20 mM Tris pH 7.5; 150 mM NaCl; 1 mM EDTA; 0.5% Nonidet P40, Protease Inhibitor Cocktail (Roche) and incubated either with RH50-specific antibodies (30µl) or with the pre-serum (2µl) for 1 h at 4°C and for another hour with 50 µl SiMAG-Protein G beads (Chemicell, Berlin, Germany). Washing, RNA extraction and slot-blot analysis were performed as described by Manavski et al. (2015).

2.2.13 Production of recombinant protein and EMSA performed by Dr. Manavski

The RH50 coding region, devoid of the chloroplast transient peptide (cTP), was cloned into pMAL-Tev vector using a restriction enzymes strategy (BamHI-SalI). The coding sequence for Strep-Tag (WSHPQFEK) was added to the reverse primer (see Table 2.4 for primer sequences). The pMAL-Tev vector was kindly provided by Alice Barkan. Expression, purification and proteolytic digestion were conducted as described previously (Chi et al., 2012). The EMSA experiments were essentially performed as described previously (Meurer et al., 2017). Binding reactions (20 µl) contained 40 mM Tris HCl pH 8.0; 30 mM KCl; 1 mM MgCl2; 0.01% w/v NP40; 1 mM DTT, 50 µg/ml heparin, trace amounts of radio-labelled probes and increasing concentrations of recombinant RH50 (100 nM, 200 nM, 400 nM, 800 nM). Probes were generated by in vitro transcription using PCR products as described.

2.2.14 Size exclusion chromatography (SEC) performed by Dr. Manavski

Chloroplasts were isolated from three-week-old plants as described previously (Stoppel et al., 2012). Chloroplasts were lysed in extraction buffer (10 mM HEPES-KOH, pH 8.0, 5 mM $MgCl_2$, and protease inhibitor cocktail (Roche) by passing the suspension 20 times through a 0.5 mm needle. Membranes were pelleted by centrifugation (45.000x*g*, 30 min, 4°C). 3 mg of RNase A-treated (300 µg RNase A, Qiagen, 1 h on ice). or untreated stroma extracts were fractionated by SEC using Superose 6 10/300 GL column (GE Healthcare) and an ÄKTA FPLC system (Amersham Biosciences) as described (Olinares et al., 2010). Fractions (0.5 ml) were precipitated with TCA and separated on 10% SDS-PAGE.

2.2.15 Accession Numbers

The genes co-expressed with RH50 code for: RH11, DEAD-box ATP-dependent RNA helicase 11 (*At3g58510*); RH52, DEAD box ATP-dependent RNA helicase 52 (*At3g58570*); RH58, DEAD box ATP-dependent RNA helicase 58 (*At5g19210*); GUN1, Genome Uncoupled 1 (*At2g31400*); PRPS1, plastid ribosomal protein S1 (*At5g30510*);CHLD, magnesium-chelatase subunit D (*At1g08520*); PPOX, protoporphyrinogen oxidase (*At4g01690*); RH17, DEAD box ATP-dependent RNA helicase 17 (*At2g40700*); RH22, DEAD box ATP-dependent RNA helicase 22 (*At1g59990*); RH26, DEAD box ATP-dependent RNA helicase (*At5g08610*).

The genes analyzed by Northern blots, size exclusion chromatography and polysome analysis were: 16S rRNA (*AtCg00920*), 23S rRNA (*AtCg01180*), 4.5S rRNA (*AtCg00960*), 5S rRNA (*AtCg00970*), *rbcL* (*AtCg00490*), *psbA* (*AtCg00020*), *LHCA3* (*At1g61520*), *LHCA4* (*At3g47470*), *LHCB1.2* (*At1g29910*), *LHCB4.1* (*At5g01530*), *PSAE1* (*At4g28750*), *PSAK* (*At1g30380*), *PSAO* (*At1g08380*), *PSAD1* (*At4g02770*), *psaA* (*ATCg00350*), *rpl2.1* (AtCg00830), *rpl23.1*(AtCg00840), *rps8* (AtCg00770) and *PRPS3* (At3g07040). The following proteins were analyzed by Y2H: PRPS1, GUN1, CHLD (see above), RH50 (At3g06980), PRPS21 (At3g27160), PRPL11 (At1g32990), PRPL24 (At5g54600), PRPS17 (At1g79850).

3 Results

3.1 Replacement of the *Synechocystis* PSII core complex

3.1.1 Construction of synthetic vectors carrying an *A. thaliana* PSII core

For the introduction of the Arabidopsis PSII core complex in *Synechocystis*, two vectors containing 11 genes of the PSII core of *A. thaliana* have been designed. The first construct, called RC1 (Fig. 3.2 B), carries the plant genes *psbA* (encoding for the protein D1), the *psbDC* operon (encoding for proteins D2 and CP43) and the *psbI* gene (encoding for the low molecular weight protein I). The second one, called RC2 (Fig. 3.2 C), was designed to carry the operons *psbEFLJ* (encoding for the cytb559 α and β subunit, and the low molecular weight proteins L and J) and *psbBTH* (encoding for the antenna protein CP47 and the low molecular weight proteins T and H) (see PSII structure in Figure 3.2 A). These genes encode for the PSII core which structural composition and assembly pathway is highly conserved between plants and cyanobacteria (Nickelsen and Rengstl, 2013). To maintain the endogenous genetic regulatory elements and therefore protein stoichiometry, each of the plant coding sequences were cloned downstream the corresponding *Synechocystis*' endogenous promoters and terminators.

To ensure efficient translation, the plant coding sequences were codon optimized for *Synechocystis*, bringing the Codon Adaptation Index to a value >0.8 (see Materials and Methods).

The two constructs were synthesized by the GeneScript sequencing company (See Materials and Methods). Each construct was designed with a double selection cassette, (nptI-sacB) that allows both positive and negative selection of *Synechocystis* recombinants and enabled the generation of marker-less mutants (Cai and Wolk, 1990). To both sides of the synthetic constructs homologous regions (HR) were added to integrate each construct in a specific genomic region. As shown in Fig. 3.2B, RC1 was introduced in place of the *psbA2* coding region and RC2 in place of the *psbEFLJ* operon-coding region (Fig. 3.2 C). With this strategy, the endogenous core genes were deleted whilst the *A. thaliana* genes were introduced.

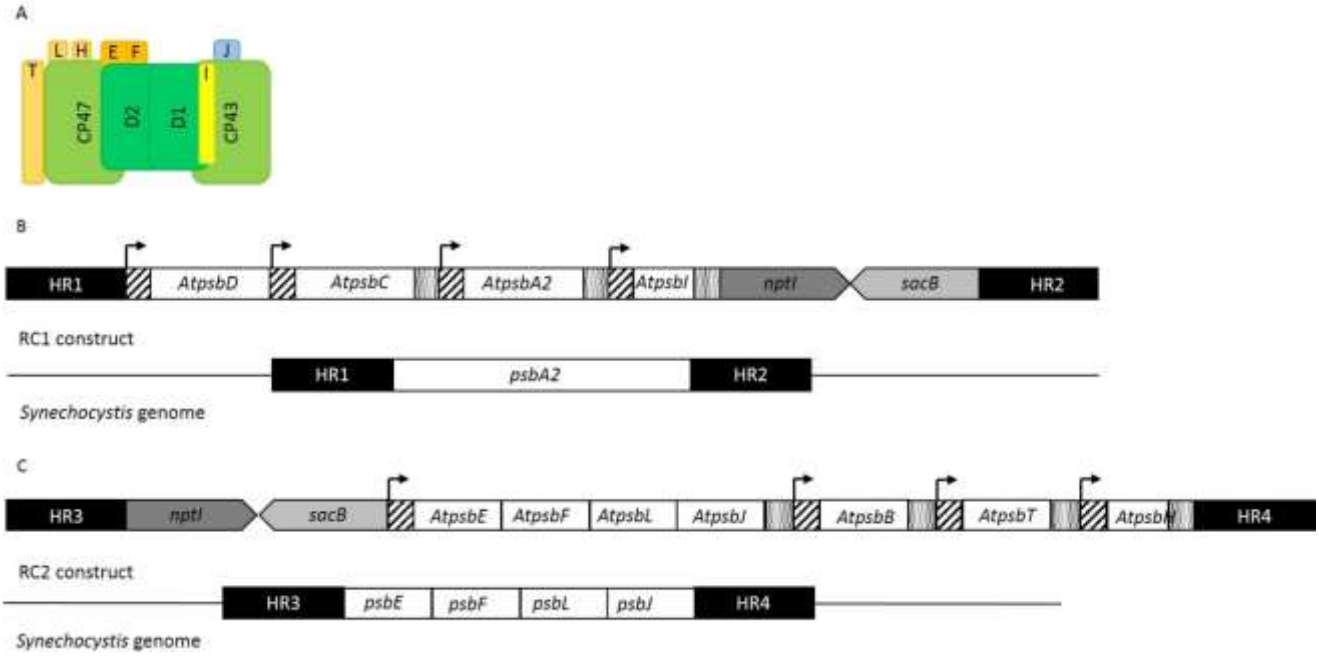

Figure 3.2: Scheme of RC1 (B) and RC2 (C) synthetic constructs and the respective regions of insertion in the *Synechocystis* genome. (A) Schematic representation of the PSII core complex encoded by RC1 and RC2 synthetic construct. **(B)** RC1 construct has been designed with HR1 and 2 that are regions homologous to upstream and downstream flanking sequences of *Synechocystis* psbA2 gene, endogenous promoter (arrow), *AtpsbD* (D2), *AtpsbC* (CP43) *AtpsbA2* (D1) and *AtpsbI* (I) coding regions of plant and double selection cassette (nptI-sacB) nptI encodes for kanamycin resistance, sacB which mediates sucrose sensibility. **(C)** RC2 construct has been designed with HR3 and 4 that are regions homologous to upstream and downstream flanking sequences of *Synechocystis psbEFLJ* operon, double selection cassette (nptI-sacB), endogenous promoter (arrow), *AtpsbEFLJ* operon ($cytb_{559}$ α and β subunit, L and J) *AtpsbB* (CP47), *AtpsbT* (T) and *AtpsbH* (H) plant coding regions.

3.1.2 Generation of *Synechocystis* RC1 mutant

To generate a *ΔpsbA2 RC1 Synechocystis* mutant strain, glucose-tolerant wild type cells were transformed with the psbA2 RC1 construct (see Table 2.2). Transformed cells were selected on kanamycin-containing BG11 plates and then sequentially plated on increasing concentration of kanamycin, to obtain complete segregation of the mutant. This is necessary, since *Synechocystis* carries multiple genome copies per cell and increasing selective pressure has to be applied in order to

substitute all wild type gene copies. Complete segregation of the mutant *ΔpsbA2 RC1-7* was confirmed by PCR (Fig. 3.3). The presence of the whole synthetic construct was also confirmed by PCR (Fig. 3.3) performed with primers designed specifically on the codon optimized plant genes (see Table 2.3).

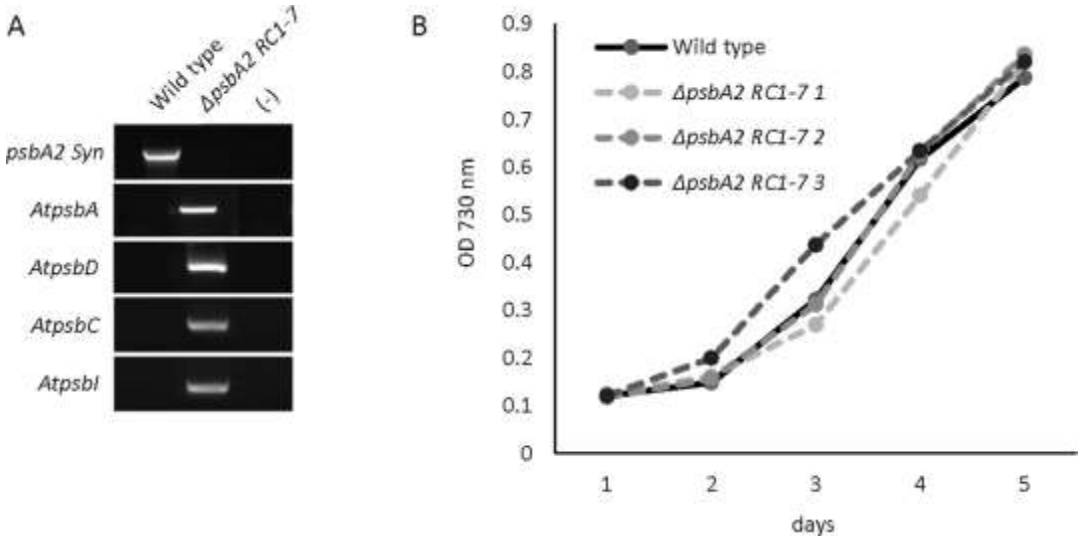

Figure3.3: Analysis of the *ΔpsbA2 RC1* mutant strain. (A) PCR analysis to test the complete segregation of the mutant *ΔpsbA2 RC1-7* and the introduction of each gene with the psbA2 RC1 synthetic construct. (-) is the negative control. Primers used psbA2 Syn FW-RV, AtpsbC FW-RV, AtpsbB FW-RV and AtpsbI FW-RV listed in Table 2.3. Fragment size: *psbA2* Syn 1772 bp, *AtpsbA* 568 bp, *AtpsbD* 708 bp, *AtpsbC* 816 bp, *AtpsbI* 91 bp. **(B)** Growth rate analysis of wild type and *psbA2 ΔRC1-7* mutant grown in photoautotrophic conditions (BG11-Glucose). Optical density at 730 nm was measured every 24 hours for 7 days and three independent cultures were used.

Growth curve analysis were performed on *Synechocystis* wild type and 3 independent *psbA2 RC1* clones (*psbA2 RC1-7 1, 2, 3*). The cultures were grown in BG11 media without glucose. Their growth was monitored every 24h for 5 days (Fig. 3.4 B). No phenotype was observed in any of the culture analyzed. To check whether the loss of *psbA2* gene would result in an inability of heterotrophic growth, psbA2 KO construct was generated (Fig. 3.5), carrying a double selection cassette (nptI-sacB) between homologous regions of psbA2 upstream and downstream region (HR1 and HR2) as for psbA2 RC1 construct. *Synechocystis* knock-out mutant of *psbA2* gene were generated by applying selective pressure with increasing concentrations of kanamycin on BG11 plates. *ΔpsbA2KO* mutant was then checked for photoautotrophic growth in BG11 media without glucose, together with *ΔpsbA2 RC1-7*

mutant and *Synechocystis* wild type. As it is shown in Fig. 3.4B, *ΔpsbA2KO* mutant was not affected in its growth. This phenotype is explained by the fact that *Synechocystis* has three genes encoding for the protein D1 (Table 1.1): *psbA2* and *psbA3*, which are expressed under normal and stress conditions and *psbA1*, which is instead induced under anaerobic conditions (Mulo et al., 2009). Therefore the KO of just one of these three genes would not affect the growth of *Synechocystis*. Since no phenotype could be observed in *ΔpsbA2 RC1-7* mutant, further investigation were necessary in order to check the accumulation of plant proteins in *Synechocystis*.

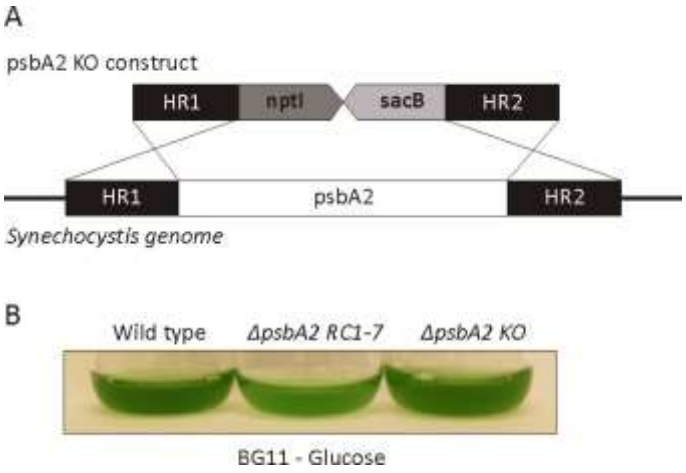

Figure 3.4: Generation of *ΔpsbA2 KO* mutant line. (A) Schematic representation of the psbA2 KO vector and of the endogenous *Synechocystis psbA2* gene target of the vector. HR1 and HR2 are the regions homologous to the upstream and downstream flanking sequences of *Synechocystis psbA2* gene and nptI-sacB is the double selection cassette. **(B)** Phenotypic analysis of *ΔpsbA2 RC1-7* and *ΔpsbA2 KO* mutant lines under normal light conditions in BG11 media without glucose.

Immunoblot analysis were performed on thylakoid proteins of *A. thaliana*, *Synechocystis* wild type and *ΔpsbA2 RC1-7* mutant, using the plant specific antibody for PsbI (Fig. 3.5 A). It has to be considered that all *Synechocystis* PSII genes were still present in both mutants, except for *psbA2*. Due to the high degree of conservation of photosynthetic complexes, few available antibodies can discriminate between plant and cyanobacterial homologs proteins, one of those being PsbI.

The western blot analysis in Fig. 5A showed that plant PsbI accumulated in the *ΔpsbA2 RC1-7* line. The Immunoblot signal was much stronger in the *A. thaliana* sample since they have been normalized on the chlorophyll content, without adjusting the PSI:PSII ratio. *Synechocystis* has indeed multiple PSI copies for each PSII (Fraser et al., 2013). The result of the western blot gave us a good indication that the plant genes introduced with the psbA2 RC1 construct can be expressed in *Synechocystis*. Lacking plant specific antibodies for D1, D2 and CP43, their transcription was confirmed through reverse transcriptase PCR (RT-PCR). As shown in Fig 5B, *AtpsbD* (D2), *AtpsbC* (CP43) and *AtpsbA2* (D1) fragments of the correct size in cDNA samples of the *ΔRC1-7* mutant line could be amplified.

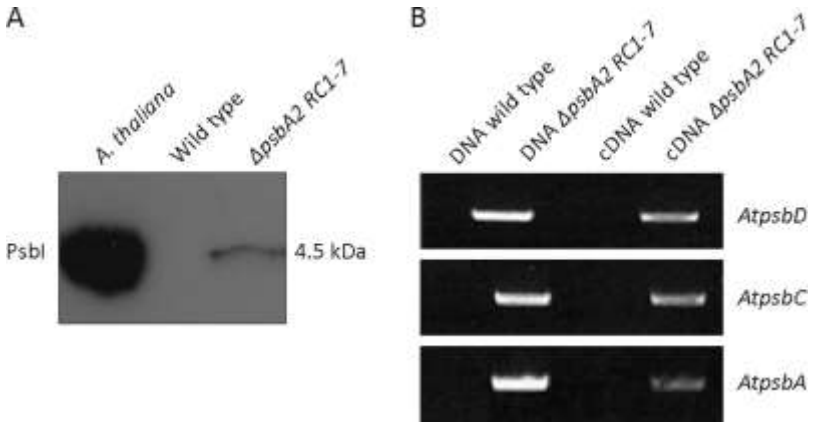

Figure 3.5: Expression analysis of *Synechocystis ΔpsbA2 RC1-7* mutant. (A) Western blot analysis of plant PsbI protein in thylakoid fractions of *A. thaliana*, *Synechocystis* wild type (Wild type) and *ΔpsbA2 RC1-7* mutant strain. 30 µg of thylakoid proteins were loaded. **(B)** PCR analysis of plant *psbD, psbC* and *psbA2* genes in DNA and cDNA samples of *Synechocystis* wild type (wild type) and *ΔpsbA2 RC1-7*. Primer used: AtpsbD FW-RV, AtpsbC FW-RV and AtpsbI FW-RV listed in table 2.3. Fragment size: *AtpsbD* 708 bp, *AtpsbC* 816 bp and *AtpsbA* 568 bp. DNA and cDNA of *Synechocystis* wild type have been used as a control for primer specificity.

3.1.3 Generation of *Synechocystis* the *RC2* mutant

To generate a *ΔpsbEFLJ RC2* mutant strain, the same procedure described for *ΔpsbA RC1-7* mutant was applied. A completely segregated *ΔpsbEFLJ RC2* mutant strain was obtained and confirmed by PCR (Fig. 3.6A). With primers specific for the *Synechocystis psbEFLJ* operon it was possible to confirm the

complete loss of the endogenous operon and the presence of the RC2 synthetic construct in the *ΔpsbEFLJ RC2* mutant (Fig 3.6 A, psbEFLJ RC2: 7800 bp). The complete construct was also amplified with specific primers (see Table 2.3) designed on the codon optimized sequences of the RC2 construct (Fig. 3.6 A).

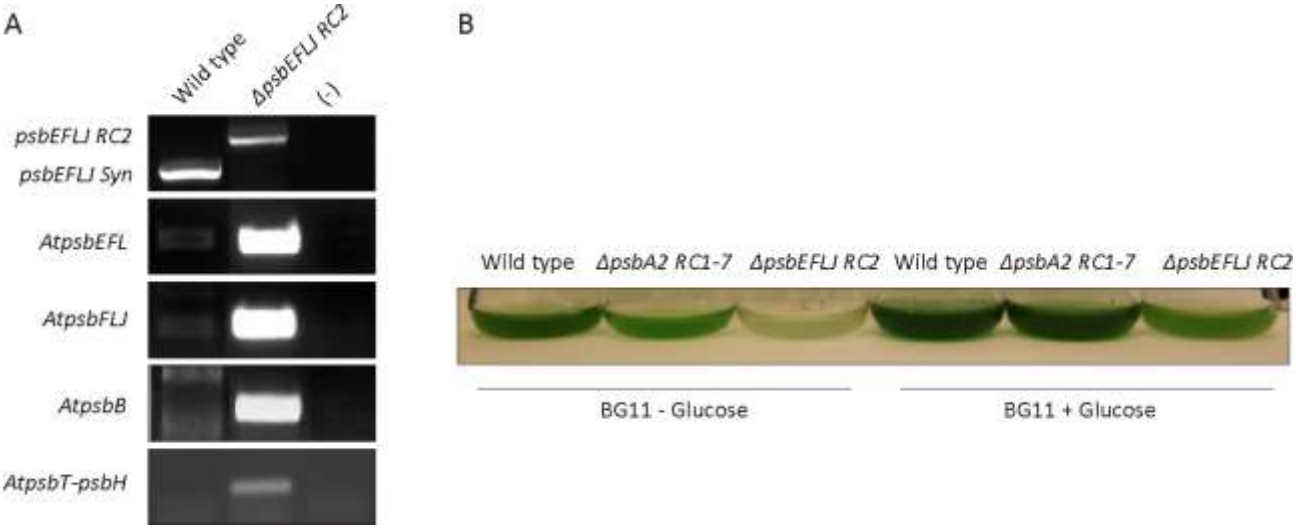

Figure 3.6: Analysis of the *ΔpsbEFLJ RC2* mutant strain. (A) PCR analysis performed on DNA extracted from *Synechocystis* wild type and *ΔpsbEFLJ RC2* mutant to check for complete segregation of the mutant and the presence of all genes introduced with the RC2 construct. (-) indicates the negative control. Primers used psbEFLJ FW-RV, AtpsbE FW-AtpsbL RV, AtpsbF FW-AtpsbJ RV, AtpsbB FW-RV and AtpsbT FW-AtpsbHRV listed in table 2.3. Fragment size: *psbEFLJ RC2* 7800 bp, *psbEFLJ Syn* 4350 bp, *AtpsbEFL* 454 bp, *AtpsbFLJ* 401 bp, *AtpsbB* 587 bp and *AtpsbT-psbH* 473 bp. **(B)** Phenotypic analysis of *ΔpsbA2 RC1-7* and *ΔpsbEFLJ RC2* mutant lines under normal light conditions in BG11 - Glucose and + Glucose.

Phenotypic analysis was performed on the mutant. *ΔpsbEFLJ RC2* was grown in BG11 media containing or lacking glucose (Fig. 3.6 B), together with *Synechocystis* wild type and *ΔpsbA2 RC1-7* mutant as control. *ΔpsbEFLJ RC2* was not able to grow photoautotrophically (BG11-Glucose) and it was growing at a slower rate than the wild type and the *ΔpsbA2 RC1-7* mutant in heterotrophic conditions (BG11+Glucose). This phenotype is in line with previously published data about the loss of the endogenous *psbEFLJ* operon (Pakrasi et al., 1988).

The *ΔpsbEFLJ RC2* mutant was further analyzed for the expression and accumulation of the newly introduced *A. thaliana* genes. As previously described in paragraph 3.1.2, only few antibodies for PSII

are available which can discriminate between plant and cyanobacterial proteins, PsbE was one of these. Immunoblot analysis was performed on thylakoid extract of *ΔpsbEFLJ RC2* mutant and of *A. thaliana* and *Synechocystis* wild type as control with PsbE antibody (Fig. 3.7 A). The western blot showed no accumulation of PsbE protein in the mutant *ΔpsbEFLJ RC2*. PCR analysis were further performed on cDNA of *ΔpsbEFLJ RC2* mutant and wild type (Fig. 3.7 B) in order to check the transcripts of *AtpsbE*, *AtpsbF, AtpsbL* and *AtpsbT* (Fig. 3.7 B). The transcripts analysis confirmed the absence of the transcripts of the genes introduced with the synthetic construct RC2.

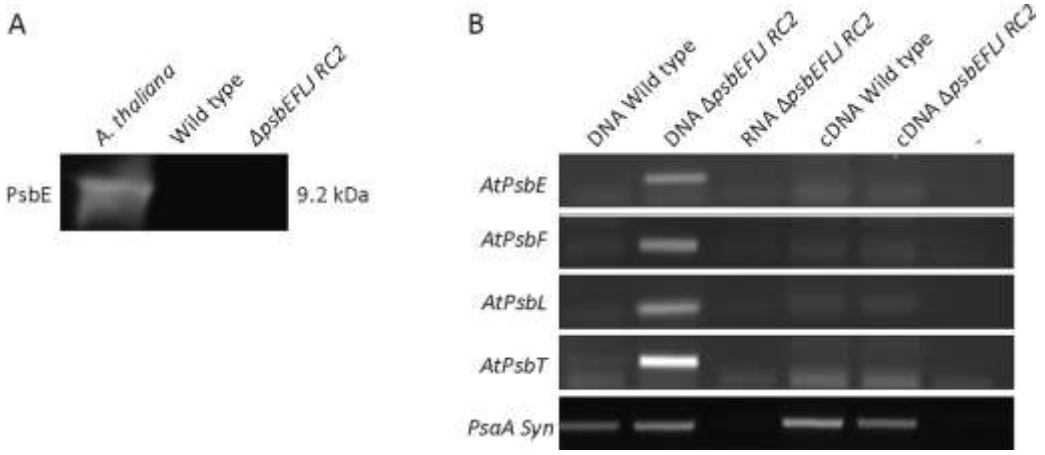

Figure 3.7: Expression analysis of *Synechocystis ΔpsbEFLJ RC2* mutant. (A) Immunoblot analysis of plant PsbE protein in thylakoid fractions of *A. thaliana*, *Synechocystis* wild type and *ΔpsbEFLJ RC2* mutant strain. **(B)** PCR analysis of plant *psbE*, *psbF*, *psbL*, *psbT* genes and *Synechocystis psaA* gene as control, in DNA and cDNA samples of *Synechocystis* wild type and *ΔpsbEFLJ RC2* and RNA of the *ΔpsbEFLJ RC2*. Primer used are AtpsbE FW-RV, AtpsbF FW-RV, AtpsbL FW-RV and AtpsbT FW-RV listed in table 2.3. Fragments size: *AtpsbE* 167 bp, *AtpsbF* 108 bp, *AtpsbL* 104 bp, At*psbT* 72 bp and *psaA 250* bp.

The fact that the transcripts could not be detected indicated a problem in mRNA synthesis or stabilization. Different causes can be ascribed for inefficient mRNA synthesis, for example rearrangement in the mRNA secondary structure due to codon bias as well as inaccessibility of Shine-Dalgarno sequence due to chromatin rearrangements (Lehmann et al., 2014).

To investigate these possible problems, RC2 synthetic construct was introduced into *Synechocystis* wild type on a self-replicative plasmid (pUR2LT) via conjugation (Fig. 3.8 A) generating the *RC2.2* mutant. In this way, the functionality of the synthetic construct could be tested independently of the genome. The expression vector *pUR2LT* has been modified in our lab from a pUR vector (Wiegard et al., 2013). The *RC2* was cloned in the expression vector downstream of an inducible promoter (*PetJ*). The successful transformation of the self-replicative plasmid carrying the synthetic construct RC2 into the *Synechocystis* wild type strain was confirmed by PCR in two independent mutant clones *RC2.2-1* and *RC2.2-2* (Fig. 3.8 B).

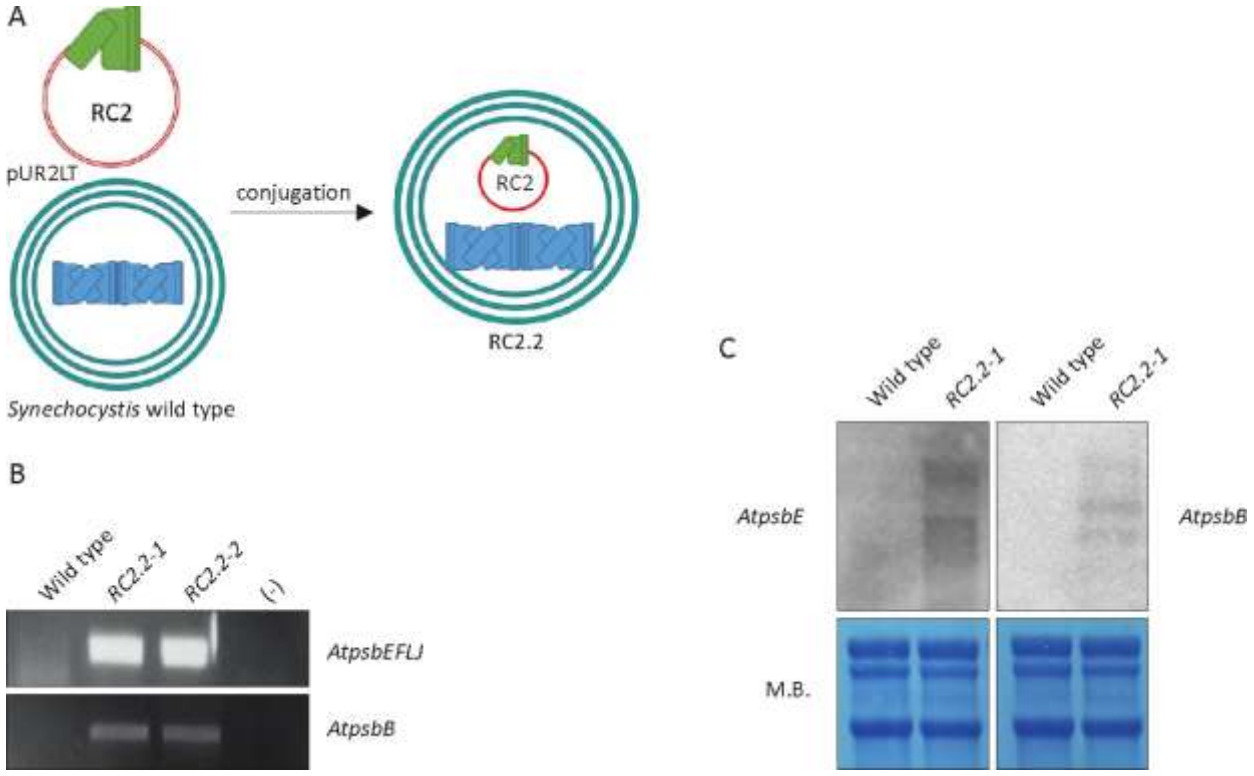

Figure 3.8: Generation and transcription analysis of the *RC2.2* mutant. (A) Schematic overview of the generation of *RC.2* mutant. The RC2 synthetic construct (represented in green) in a self-replicative vector (pUR2LT red) is introduced in *Synechocystis* wild type cells through conjugation, generating the *RC2.2* mutant. **(B)** PCR analysis performed on DNA extracted from *Synechocystis* wild type and *RC2.2* mutant to check for the presence of the synthetic construct. (-) negative control. Primer used: AtpsbE FW-AtpsbJ RV and AtpsbB FW-RV listed in table 2.3. Fragment size: *AtpsbEFLJ* 622 bp and *AtpsbB* 587 bp. **(C)** Northern blot analysis of *AtpsbE* and *AtpsbB* gene transcripts of *Synechocystis* wild type and *RC2.2* mutant. Membranes were stained with methylene blue (M.B.) as RNA loading control.

The *AtpsbEFLJ* operon and *AtpsbB* gene could be amplified in the *RC2.2* mutant but not in *Synechocystis* wild type. Northern blot analyses was then performed on *RC2.2* mutant in order to check for transcript accumulation (Fig. 3.8 C). RNA was extracted from wild type and *RC2.2-1* mutant, loaded on formaldehyde gels, blotted on nitrocellulose membrane and hybridized with radioactive probes for the synthetic *AtpsbE* and *AtpsbB* transcripts (Fig. 3.8 C). Both transcripts were detected in the *RC2.2* mutant indicating that the synthetic construct itself was correctly assembled and that there were no secondary structures blocking the transcription process.

3.1.4 Generation of a *ΔpsbA2DC RC1* mutant

The next important step for the project would be to delete the endogenous PSII genes to avoid interference between endogenous and exogenous homologous proteins and let the plant proteins assemble in *Synechocystis* thylakoids. As previously shown, the *ΔpsbA2 RC1-7* mutant already lacks the *psbA2* gene, so the next step would be to delete the *Synechocystis psbD1, psbD2, psbC* and *psbI* genes. *Synechocystis* contains two *psbD* genes coding for the D2 core protein of the PSII reaction center (Table 1.1): *psbD1* and *psbD2*. *psbD1* is cotranscribed with *psbC* whereas *psbD2* is monocistronic. In order to obtain a complete KO of the cyanobacterial D2 protein, both *psbD1C* operon and *psbD2* have to be deleted. *ΔpsbA2 RC1-7* strain would be used as background for the subsequent replacements, in order to have a final strain with none or just one marker gene. For this reason, a markerless psbA2 RC1 construct (without double selection cassette) was designed and used to transform the *ΔpsbA2 RC1-7* strain, in order to excise the nptI-sacB cassette and obtain a marker less strain. After 5 days of recovery, no transformants were able to survive on the selection plate with 5% sucrose. Longer recovery time and lower concentrations of sucrose were tested. Unfortunately, it was never possible to obtain a marker less *ΔpsbA2 RC1* mutant strain (Fig. 3.9 A). The psbDC KO construct (Fig. 3.9 B), that was firstly generated to transform the marker less *ΔpsbA2 RC1* strain, was instead used to transform *Synechocystis* wild type cells to have a control strain (Fig.3.9 A). A second psbDC KO construct was generated, carrying a single selection cassette coding for spectinomycin resistance, called psbDC KO spec construct (Fig. 3.9 B). *ΔpsbA2 RC1-7* mutant was then transformed with psbDC KO spec construct (Fig. 3.9 A). With increasing antibiotic selective pressure, two segregated mutant strains were obtained, *ΔpsbA2DC RC1* and *ΔpsbDC KO* mutants, both lacking the endogenous *psbDC* operon (Fig. 3.9 C).

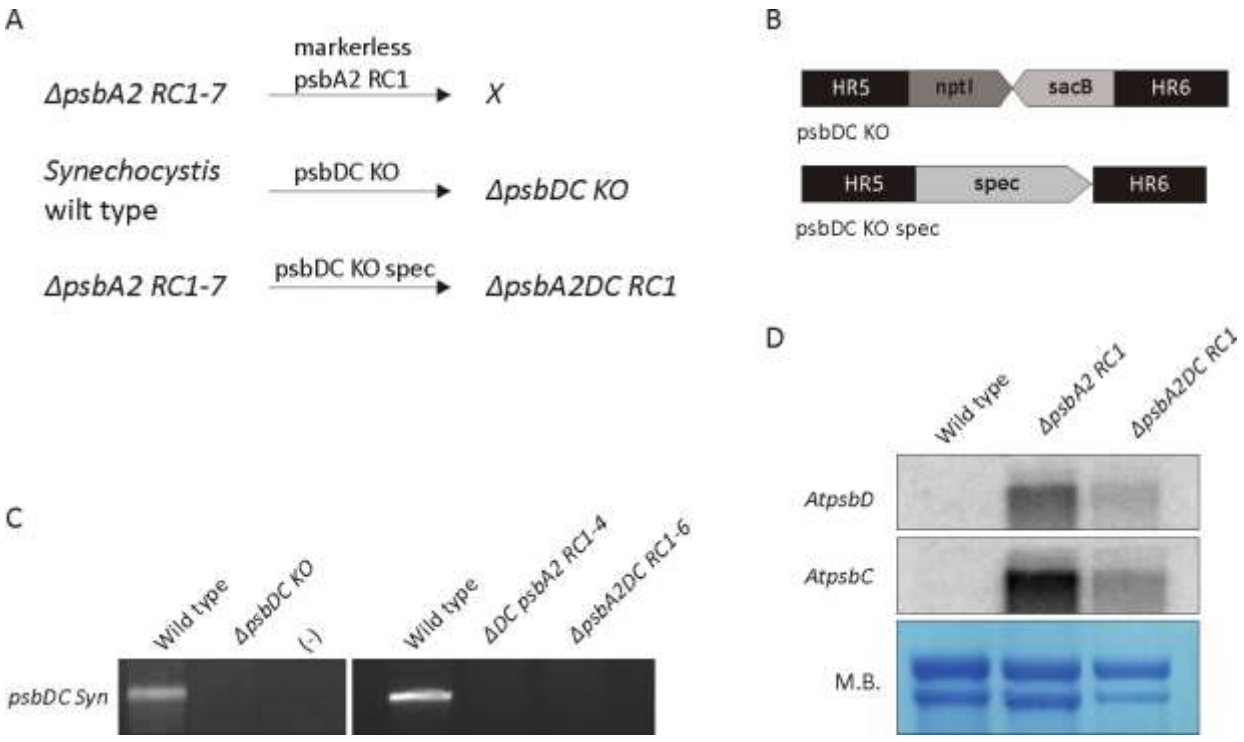

Figure 3.9: Generation of *ΔpsbDC KO* and *ΔpsbA2DC RC1* mutants. (A) Scheme of the generation of new mutant strains. Arrows indicate the transformation process. X indicates that no mutants were obtained from the transformation. **(B)** Composition of the psbDC KO vector and of the endogenous *Synechocystis psbDC* gene target of the vector. HR5 and HR6 are the regions homologous to the upstream and downstream flanking sequences of *Synechocystis psbDC* operon and nptI-sacB is the double selection cassette. **(C)** PCR analysis to test the complete segregation of the *psbDC KO* mutant and of the *ΔpsbA2DC RC1* mutant (DNA of 2 independent clones *ΔpsbA2DC RC1-4* and *-6*). (-) negative control. Primer used: psbDC Syn FW-RV listed in table 2.3. Fragment size: *psbDC Syn* 6790 bp. **(D)** Northern blot analysis of *AtpsbD* and *AtpsbC* transcripts on RNA extracted from Synechocystis wild type (wild type), *psbA2 RC1* and *ΔpsbA2DC RC1*. Transcripts size: 2.5 kb. Membranes were stained with methylene blue (M.B.) as RNA loading control.

Expression of the plant *psbD* and *psbC* genes was analyzed by Northern blot in *Synechocystis* wild type, *ΔpsbA2 RC1-7* and *ΔpsbA2DC RC1* (Fig. 3.9 D). In plant chloroplasts as well as in cyanobacteria, the *psbD* gene overlaps with the open reading frame of the *psbC gene*, and the two genes are cotranscribed generating a transcript of about 2.5 kb (Chisholm and Williams, 1988). When hybridizing the filters with radiolabelled probes of *psbD At and psbC At*, the target transcript, of about 2.5 kb, was detected only

in the two mutants carrying the synthetic construct RC1, *ΔpsbA2 RC1-7* and *ΔDC psbA2 RC1*, and not in the wild type. This confirmed the presence of the RC1 construct in both mutants and that the plant operon could be transcribed.

3.1.5 Characterization of *psbA2 RC1-7* and *ΔpsbA2DC RC1* mutant strains

The growth phenotype of the *psbA2 RC1-7* and *ΔpsbA2DC RC1* mutant strains was analyzed by growing them in liquid culture in heterotrophic (BG11+Glu) and autotrophic (BG11-Glu) conditions (see materials and Methods) (Fig. 3.10 A, B). The growth of the two mutant strains was compared with the *Synechocystis* wild type and the two KO mutant, *ΔpsbA2 KO* and *ΔpsbDC KO*, as control (Fig. 3.10 A, B). All mutants could grow in heterotrophic conditions but at slightly different rates (Fig. 3.10 A), in particular *ΔpsbDC KO* and *ΔpsbA2DC RC1* were showing a shorter exponential phase and lower maximum OD at 730 nm. A strong phenotype was observed in autotrophic conditions (Fig. 3.10 B) where the *ΔpsbDC KO* mutant was not able to grow photoautotrophically, Yu and Vermass in 1990 already described a mutant lacking PsbD-I and PsbC proteins. They showed a strong reduction of the PSII proteins which severely affected the functionality of the photosynthetic apparatus, in agreement with the phenotype observed in this study. Interestingly, *ΔpsbA2DC RC1* was able to grow photoautotrophically (Fig. 10 B), indicating that *AtpsbD* and *AtpsbC* were able to replace the function of the *Synechocystis* homologs (Yu and Vermaas, 1990).

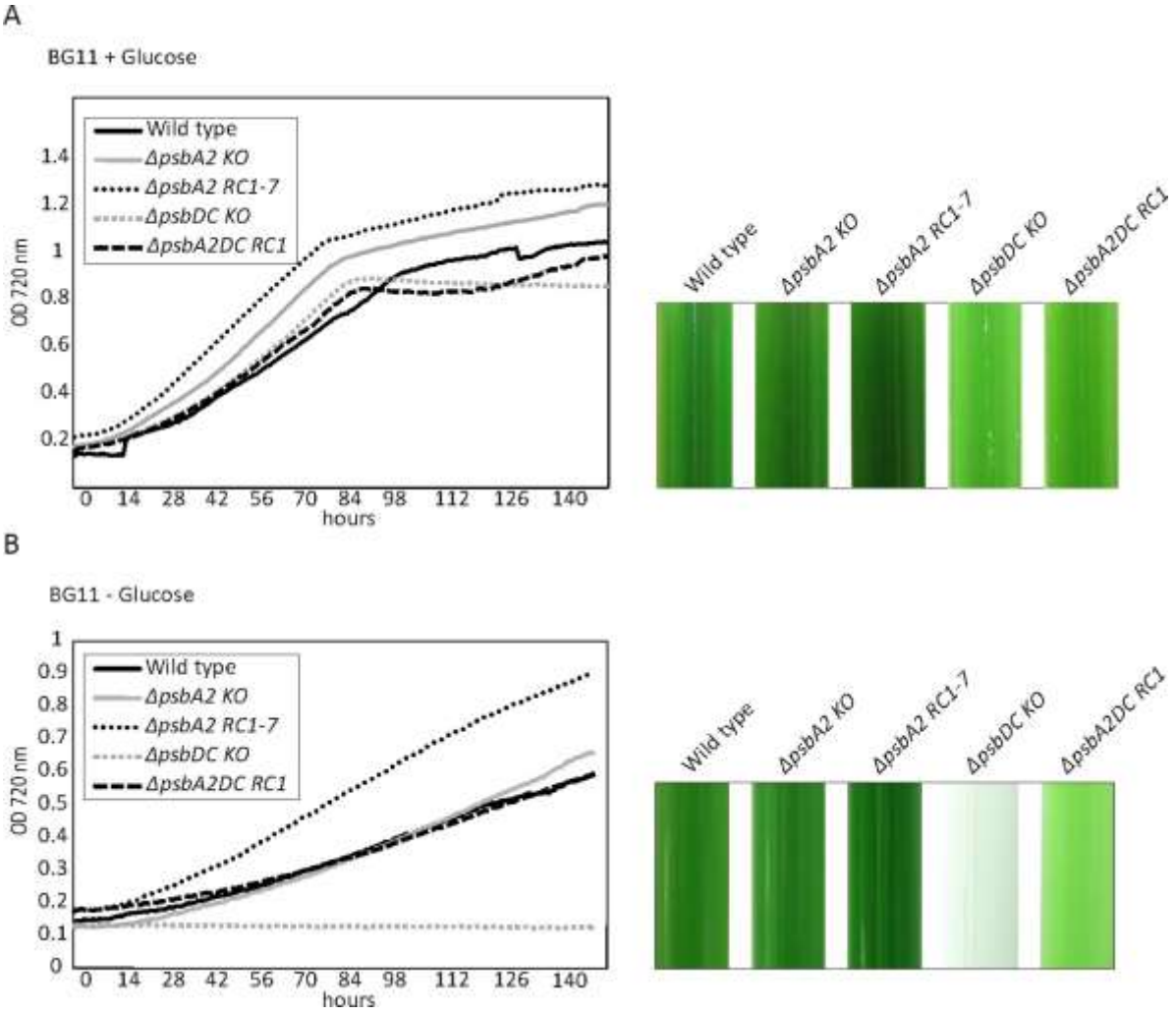

Figure 3.10: Growth rate analysis of the *ΔpsbA2DC RC1* strain. (A) Growth rate analysis of *Synechocystis* wild type (Wild type), *ΔpsbA2KO*, *ΔpsbA2 RC1-7, ΔpsbDC KO* and *ΔpsbA2DC RC1.* Cells were cultured under heterotrophic conditions (BG11 + Glucose) in a Multi-Cultivator MC1000 (see Materials and Methods) at 25°C and illuminated with 30 µmol photons m^{-2} s^{-1}. The OD was measured at 720 nm every hour for 7 days. On the right panel: phenotype of 7 days old liquid culture. **(B)** Growth rate analysis under autotrophic conditions (BG11 –Glucose).

In the attempt to detect the presence of PSII, fluorescence emission spectra of the two photosystems at low temperature (77K) were measured in cell suspensions of wild type, *ΔpsbA2 KO*, *ΔpsbA2 RC1-7*, *ΔD1* (Fig. 3.11 A), *ΔpsbDC KO* and *ΔpsbA2DC RC1* grown in BG11 media containing glucose. Chlorophyll *a* was excited with light at 435 nm and the recorded fluorescence emission was double normalized at 600 nm (Fig. 3.11 A) or at 680 nm (Fig. 3.11 B) and to the PSI emission peak at 730 nm. Three main peaks could be observed in the wild type sample; two originating from PSII, at 685 and 695 nm (CP43 and CP47 antenna) and one at 730 nm which corresponds to PSI. As expected, PSI fluorescence at 730 nm was higher than PSII fluorescence at 695 nm, because the PSI/PSII ratio varies from about 1 to almost 4 in *Synechocystis* depending on the growth light conditions (Murakami et al., 1997). *ΔD1* mutant (Prof. Nixon, Imperial College, London), lacking all three genes encoding for D1, has been used in this analyses as control for the complete loss of PSII. The emission spectra of *ΔpsbA2 KO,* lacking *psbA2* endogenous gene*,* and *ΔpsbA2 RC1-7* mutant, lacking *psbA2* endogenous gene and carrying the RC1 construct, showed a wild type PSII emission spectra (Fig. 3.11 A). Loss of only one of the three genes encoding for D1 did not affect the PSII assembly and accumulation (Mulo et al., 2009). The emission spectra of *ΔpsbDC KO,* lacking *psbDC* endogenous operon, showed a reduction in PSII (Fig. 3.11 B) with respect to the wild type. The same was observed for the *ΔpsbA2DC RC1* mutant, lacking *psbA2* and *psbDC* endogenous genes and carrying the synthetic construct RC1*.* Both *ΔpsbDC KO* and *ΔpsbA2DC RC1* displayed an additional peak at 665 nm, which indicate an accumulation of allophycocyanin, (Yu et al., 1999) not observed in the wild type.

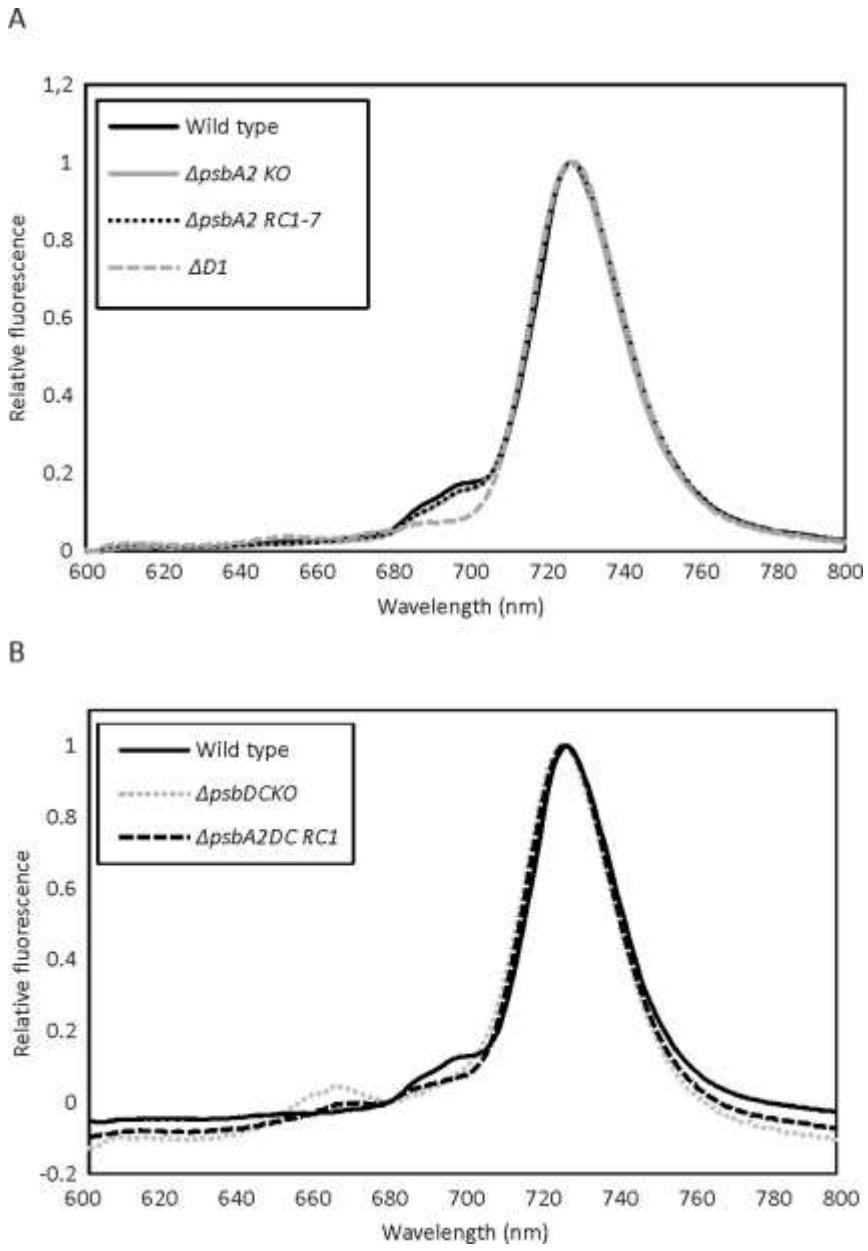

Figure 3.11: PSII characterization. (A) Steady-state fluorescence emission spectra at 77 K of cell of *Synechocystis* wild type, *ΔpsbA2 KO*, *ΔpsbA2 RC1-7* and *ΔD1*. Cell suspensions were adjusted to an OD_{720} of 1.5 and dark-adapted for 10 min prior to freezing. Fluorescence emission spectra were measured by exciting cells at 435 nm and were double normalized at 680 nm and at the PSI emission peak at 730 nm. The curves are representative of 3 repetitions. **(B)** Steady-state fluorescence emission spectra at 77 K of cell of *Synechocystis* wild type, *ΔpsbDC KO* and *ΔpsbA2DC RC1*. Fluorescence emission spectra were double normalized at 680 nm and at the PSI emission peak at 730 nm. The curves are representative of 3 repetitions.

These data indicated that no improvement in the accumulation of functional plant PSII reaction center was observed in *ΔpsbA2DC RC1* mutant. This was in contrast with the phenotype observed in autotrophic conditions for *ΔpsbA2DC RC1* (Fig. 3.10 B). Western blot analysis were further performed on total protein of wild type (100% and 50%), *ΔpsbA2 KO*, *ΔpsbA2 RC1-7*, *ΔD1*, *ΔpsbDC KO*, *ΔpsbA2DC RC1* and *A. thaliana* with CP43 and D2 antibody (Fig. 3.12). CP43 and D2 antibody both recognize plant and cyanobacterial proteins in particular the *A. thaliana* D2 protein runs slightly faster than the cyanobacterial one Fig. 3.12 (different apparent weight). This allows us to understand weather the plant proteins are indeed expressed in *Synechocystis*. The Immunoblot (Fig. 3.12) confirmed that *ΔpsbDC KO* mutant is a complete KO, since at the protein level there is no accumulation of CP43 and D2. *ΔD1* showed very low amount of D2 and of CP43 in accordance with loss of PSII previously observed at the 77K emission spectra (Fig. 3.11 A). *ΔpsbA2 KO* and *ΔpsbA2 RC1-7* mutants showed wild type level of CP43 and D2 proteins. In *ΔpsbA2DC RC1* both CP43 and D2 proteins were detected at very low level. Moreover, the D2 protein had the same apparent weight as the one of *Synechocystis*.

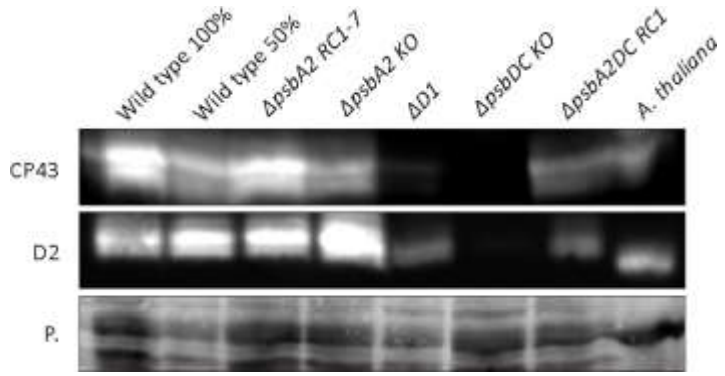

Figure 3.12: Immunoblot analysis of CP43 and D2 proteins. Total proteins were extracted from *Synechocystis* wild type, *ΔpsbA2 RC1-7 (*lacking the endogenous *psbA2* and carrying the synthetic construct RC1), *ΔpsbA2 KO (*lacking the endogenous *psbA2)*, *ΔD1 (*lacking the endogenous *pbsA1,-2 and -3)*, *ΔpsbDC KO (*lacking the endogenous *psbDC)*, *ΔpsbA2DC RC1* (lacking the endogenous *psbA2*, *psbDC* genes and carrying the synthetic construct RC1) and *A. thaliana*. Signals were detected for CP43 and D2 proteins. 30 µg of total proteins were loaded and fractionated on SDS-PAGE. Wild type 100%= 30 µg, wild type 50%= 15 µg. Membrane was stained with Ponceau (P.) and used as protein loading control.

3.2 Characterization of the DEAD-box RNA helicase RH50

3.2.1 *RH50* is co-expressed with the *GUN1* regulon

In order to identify genes with a tentative role in plastid protein homeostasis and plastid signaling a guilt-by-association approach was employed. With the help of this approach, poorly characterized DEAD-box RNA helicase (DBRH) gene, in our case *RH50*, was revealed. Expression data of all predicted plastid-located *A. thaliana* DBRHs were compared with the *GUN1* co-expression cluster (Tadini et al., 2016), which includes the plastid ribosomal protein S1 (*PRPS1*), two tetrapyrrole biosynthesis enzymes genes (the protoporphyrinogen oxidase (*PPOX*) and the D subunit of the Magnesium-chelatase (*CHLD*), as well as a set of proteins involved in plastid protein homeostasis. This comparison identified *RH50* as the DBRH that was most co-regulated with *GUN1*, *PPOX* and *CHLD*. Moreover, *RH50* also showed a high co-expression score with *RH58* (Figure 3.13), whose homologues in tobacco (*VDL*) and maize (*RH58*) were shown to be involved in plastid differentiation (Wang et al., 2000) and in rRNA metabolism (Majeran et al., 2012), respectively. A second co-expression cluster is formed by *RH17*, *RH22* and *RH26*. RH22 interacts with the 50S ribosome subunit and facilitates its assembly by processing the 23S rRNA (Chi et al., 2012). The function of RH17, RH26, RH11, and RH52 is still elusive. RH3, RH33 and RH41, which are also predicted to be plastid localized, could not be included in the co-expression cluster due to the fact that they are not represented on the ATH1 Affimetrix Array.

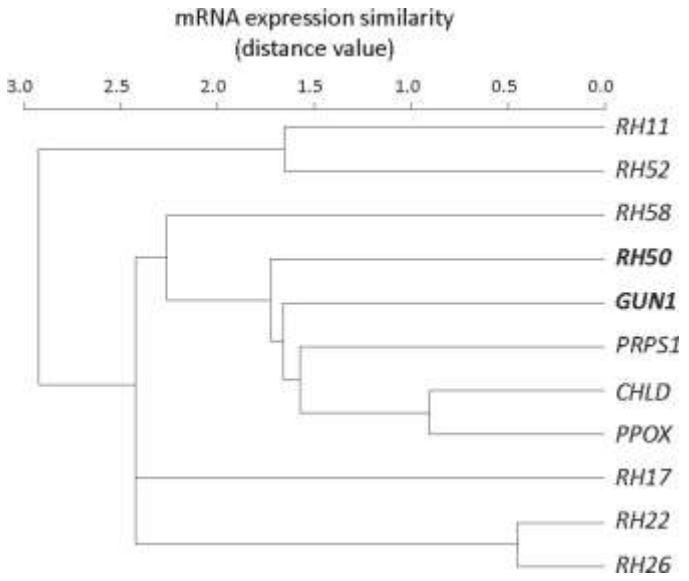

Figure 3.13: RH50 is co-expressed with the GUN1 regulon. Within the set of genes coding for chloroplast-localized DBRHs, *RH50* shows the highest co-expression score with *GUN1*. The degree of co-expression was measured with mutual rank (MR). Low distance values indicate high co-expression. Full names and accession numbers of corresponding proteins encoded are provided in Materials and Methods (paragraph 2.2.15). All gene products are predicted or experimentally confirmed chloroplast proteins. Performed by Dr. Tatjana Kleine.

3.2.2 RH50 is a subunit of the GUN1-containing subdomain of pTAC-complexes

The *RH50* gene is highly co-regulated with *GUN1*, which was shown to be located inside the nucleoids in the pTACs (Koussevitzky et al., 2007). Although mass spectrometry analyses failed to detect GUN1 so far, most likely due to its very low abundance, RH50 was identified previously in pTAC complexes together with several other DBRHs and components of the protein expression machinery (Olinares et al., 2010). To confirm the co-localization of RH50 and GUN1, transient expression of GUN1-RFP and RH50-GFP protein fusions was performed in *A. thaliana* protoplasts (see Paragraph 2.2.4). GFP and RFP signals could be clearly detected as overlapping fluorescence foci inside chloroplasts (Figure 3.14), indicating that RH50 and GUN1 belong to the same subcompartment.

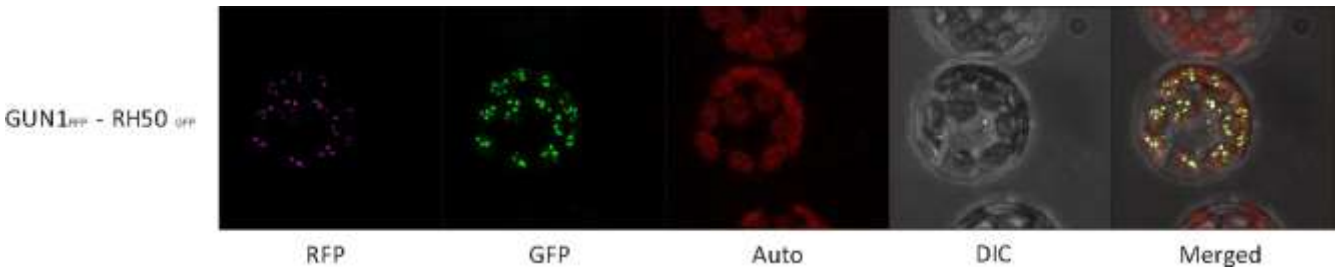

Figure 3.14: RH50 and GUN1 co-localize in chloroplasts. Protoplasts isolated from 2 week-old *A.thaliana* cotyledons and transiently cotransfected with GUN1-RFP and RH50-GFP fusion proteins. The RFP signal (red fluorescence) clearly co-localizes with the GFP signal (green fluorescence) within the chloroplast. Fluorescence was imaged by confocal microscopy.

3.2.3 The *rh50* mutation suppresses transcriptional downregulation of PhANGs

RH50 and GUN1 are co-regulated at the mRNA level and located in the same cellular sub-compartment, for this reason we investigated whether RH50 does also play a role in retrograde signaling and plastid protein homeostasis, as it was demonstrated for GUN1**.** Two independent loss-of-function *RH50* alleles (*rh50-1* and *rh50-2*, Figure 3.15 A) were isolated. In *rh50-1* mutant plants, the mutation is caused by a T-DNA insertion, whereas in *rh50-2* a transposon is inserted in the *RH50* gene locus. Both insertions are located in the second exon and completely suppress the accumulation of RH50 protein (Figure 3.15 B). The involvement of RH50 in GUN1-mediated retrograde signaling was analyzed by testing *rh50* plants for the *genome uncoupled* (*gun*) phenotype in terms of *LHCB1* expression in the presence of norflurazon (NF) or lincomycin (Lin) (Figure 3.15 C). Both, NF, which is an inhibitor of carotenoids biosynthesis and Lin, an inhibitor of chloroplast protein synthesis, block the expression of photosynthesis-associated nuclear genes (PhANGs) like *LHCB1*, in wild type plants. In contrast, *gun* mutants can express PhANGs after NF and Lin treatment. Similar to the wild type, *LHCB1* expression was strongly reduced in the *rh50-1* single mutant after Lin and NF treatments, while *gun1-102* control plants displayed de-repressed *LHCB1* expression, as expected for *gun* mutants. Moreover, *rh50-1 gun1-102* double mutant did not show a significant additive phenotype in comparison to *gun1-102*.

To further investigate the involvement of RH50 in plastid gene expression (PGE)-mediated retrograde signaling, *rh50-1* was crossed into the *prors1-1* genetic background and the expression of PhANGs was examined (Figure 3.15 D).

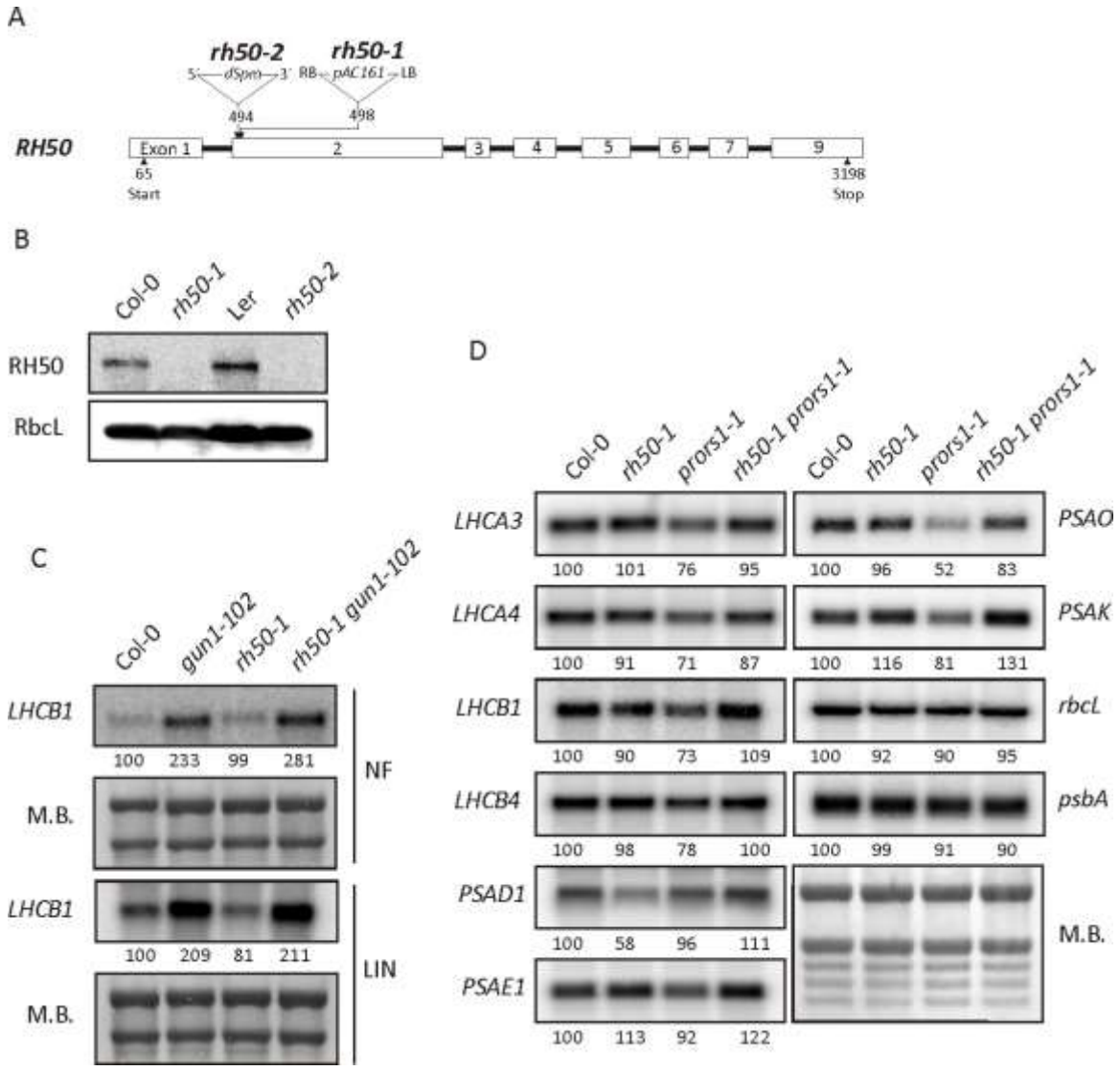

Figure 3.15: The *rh50* mutant is not a *gun* mutant but is involved in PRORS1-triggered retrograde signaling. **(A)** Schematic representation of the *RH50* locus and its mutant alleles. The *rh50-1* and *rh50-2* mutations are due to the insertion of a T-DNA and a transposon, respectively. Left (LB) and right (RB) borders indicate the orientation of the T-DNA, 5' and 3' the one of the transposon. Numbered boxes symbolize the exons and black lines the introns. Start and stop codons are indicated. **(B)** Immunoblot analysis of total protein extracted from wild type (Col-0 and Ler), *rh50-1* and *rh50-2* plants with an antibody specific for RH50 or, as control, for RbcL. **(C)** RNA gel blot analyses of *LHCB1.2* transcript levels on total RNA isolated from seedlings of wild type (Col-0) and mutant (*gun1-102*, *rh50-1*, *rh50-1 gun1-102*) plants grown for 10 days in the presence of norflurazon (NF) or lincomycin (Lin). **(D)** RNA gel blot analysis of transcripts of nuclear- (*LHCA3*, *LHCA4*, *LHCB1*, *LHCB4*, *PSAD1*, *PSAE1*, *PSAO* and *PSAK*) and plastid- (*rbcL* and *psbA*) encoded photosynthetic genes light-adapted wild type (Col-0), *rh50-*

1, *prors1-1* and *rh50-1 prors1-1* plants. Blots were stained with methylene blue (M.B.) as RNA loading control. Quantification of signals (by ImageJ) relative to Col-0 (=100%) is provided below each panel.

The *prors1-1* mutation causes the downregulation of the proline tRNA synthetase1 (PRORS1), creating a perturbation in the PGE (Pesaresi et al., 2006). Interestingly, the expression of *LHCA3*, *LHCA4*, *LHCB1*, *PSAO* and *PSAK* genes, which is downregulated by about 20-30% in *prors1-1* mutant, was restored to wild type-like levels in *rh50-1 prors1-1* mutant, similarly to what was observed before in the *gun1-102 prors1-1* mutant (Tadini et al., 2016). This implies that, like GUN1, RH50 is capable to modulate the chloroplast-to-nucleus communication when the PGE-machinery is mildly affected as in case of *prors1-1*. However, under more severe conditions, as the NF or Lin treatment, only GUN1 can trigger plastid signaling.

3.2.4 *RH50* genetically interacts with components of the 50S plastid ribosomal subunit

When the *gun1* mutation was introduced into genetic backgrounds carrying mutations for plastid ribosomal proteins, over-additive (*gun1 prpl11*) or suppressor (*gun1 prps1*) phenotype was observed, pointing to a functional link between GUN1 and plastid ribosomes (Tadini et al., 2016). Therefore, double mutants combining the *rh50* mutation, *gun1* or several other mutations (*prors1-1*, *prpl11-1*, *prps1-1*, *prps21-1*, *prps17-1* and *prpl24-1*) were generated and characterized (Figure 3.16 A-D). In contrast to *A. thaliana* plants defective for RH3, 22 or 39 with arrested embryo development (Asakura et al., 2012; Chi et al., 2012; Nishimura et al., 2010), both *rh50* mutant alleles behaved like the wild type with respect to growth and photosynthetic performance (Φ_{II}) under standard growth conditions (Figure 3.16 A,D). Interestingly, the *gun1-102 rh50-1* double mutant displayed a clear reduction in size (50% of the wild type at 26 d.a.p.) compared to the wild type-like parental single mutants, supporting the idea of a functional interaction between *GUN1* and *RH50*. However, the photosynthetic performance of adult *gun1-102 rh50-1* double mutant plants was unaffected.

In terms of PhANG expression, *rh50-1* phenocopied *gun1-102* in the *prors1-1* genetic background (see Figure 3.15 D). Moreover, the restoration of PhANG expression observed in both *rh50-1 prors1-1* and *gun1-102 prors1-1* double mutants had a positive impact on growth and photosynthetic performance (0.73 ± 0.02 for both double mutants versus 0.68 ± 0.02 in *prors1-1*) (Figure 3.16 A).

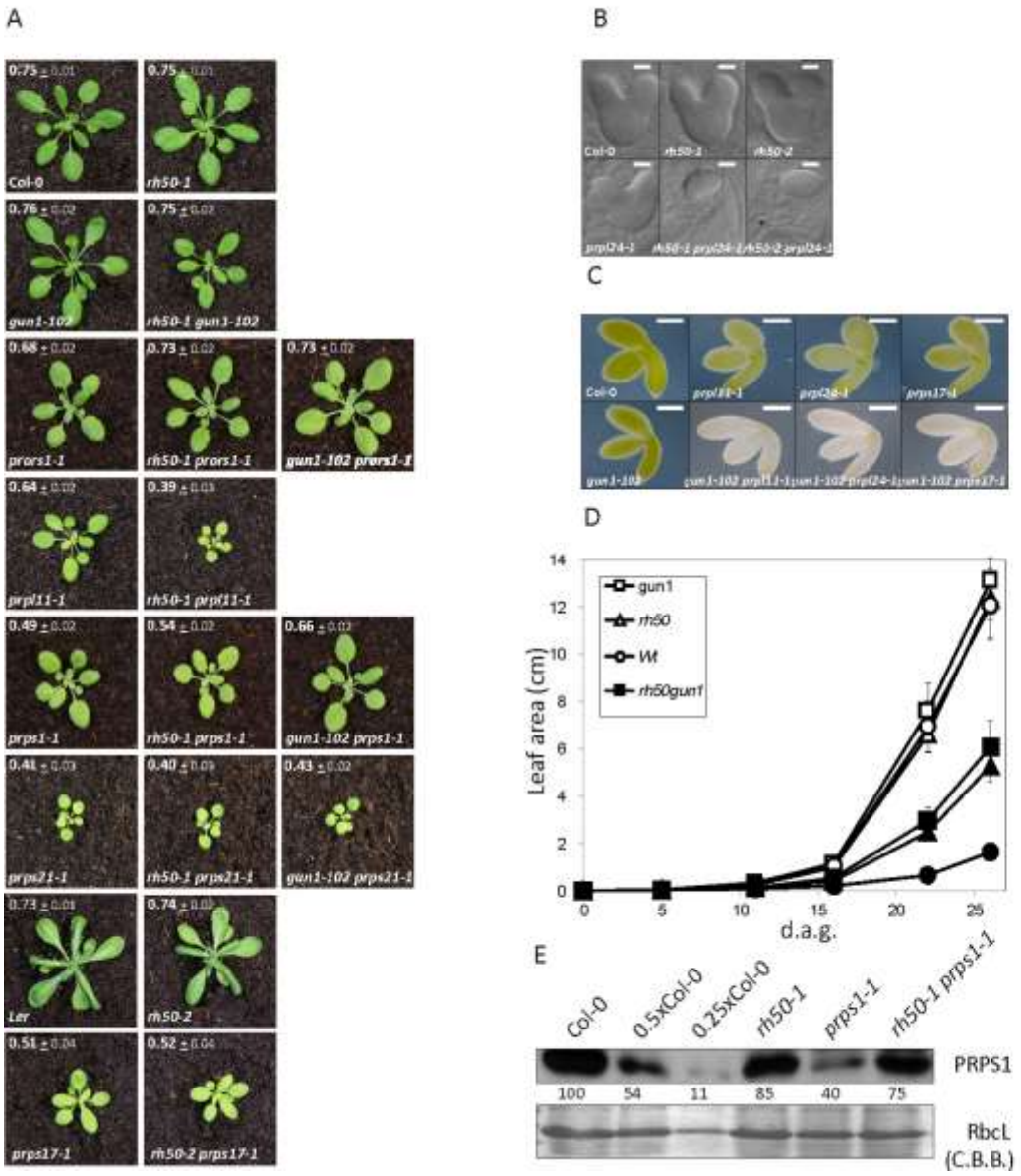

Figure 3.16: Genetic interaction between *rh50*, *gun1* and several mutation (*prors1-1, prpl11-1, prps1-1, prps21-1, prps17-1* and *prpl24-1*) affecting plastid gene expression (PGE). (A) Phenotypes of 26 day old wild type (Col-0 and *Landsberg erecta* "Ler"), single (*rh50-1*, *gun1-102*, *prors1-1*, *prpl11-1*, *prps1-1*, *prps21-1*, *rh50-2 (Ler background)*, *prps17-1*) and double (*rh50-1 gun1-102*, *rh50-1 prors1-1*, *gun1-102 prors1-1*, *rh50-1 prpl11-1*, *rh50-1 prps1-1*, *gun1-102 prps1-1*, *rh50-1 prps21-1*, *gun1-102 prps21-1*, *rh50-2 prps17-1*) mutant plants grown in a climate chamber under long day condition and light intensity of 80 µmol photons $m^{-2}s^{-1}$. The effective quantum yield of photosystem II (Φ_{II}) was determined for each genotype (average ± SD; n≥ 12) as described in Materials and Methods. **(B)** Characterization of embryo development in wild type (Col-0), single (*rh50-1*, *rh50-2*, *prps24-1*)

and double (*rh50-1 prps24-1, rh50-2 prps24-1*) mutant plants. Bars = 20 µm. **(C)** Images of fully mature embryos (bent cotyledon stage) from wild type (Col-0), single (*prpl11-1, prpl24-1, prpl17-1, gun1-102*) and double (*gun1-102 prpl11-1, gun1-102 prpl24-1, gun1-102 prpl17-1*) mutant plants. Bars = 200 µm. **(D)** Growth kinetics of the different plant lines was measured from 5 to 26 days after germination (d.a.g.). For each time point, the average leaf area was measured (n≥ 15). **(E)** Immunoblot analysis of PRPS1 ribosomal protein performed on the wild type (Col-0), *rh50-1*, *prps1-1* and *rh50-1 prps1-1* double mutants using a PRPS1-specific antibody. C.B.B. is used as loading control and quantification of signals (by ImageJ) relative to the wild type (100%) is provided. A-E done by Dr. Luca Tadini, Dr. Paolo Pesaresi and Roberto Ferrari.

The *rh50* and *gun1* alleles were also combined with mutations affecting the 30S (*prps1-1, prps17-1* and *prps21-1*) and 50S (*prpl11-1* and *prpl24-1*) subunit of the plastid ribosome. Unlike *gun1-102* (Tadini et al., 2016), the *rh50-1* mutation did not recover *prps1-1* growth phenotype in the corresponding double mutant. However, also in *rh50-1 prps1-1* the photosynthetic performance was slightly improved, if compared to *prps1-1*, as in *gun1-102 prps1-1* (*prps1-1*, 0.49 ± 0.02; *gun1-102 prps1-1,* 0.66± 0.02*; rh50-1 prps1-1*, 0.54 ± 0.02) (Figure 3.16 A). The improvement of photosynthetic parameters in the *rh50-1 prps1-1* double mutant was due to the partial de-repression of PRPS1 protein accumulation, from 40% of the wild type level in *prps1-1* single mutant to 75% in *rh50-1 prps1-1* mutant background (Figure 3.16 E)**.** A similar effect was previously observed in the *gun1-102 prps1-1* double mutant, where loss of GUN1 induced the accumulation of PRPS1 protein to wild type-like levels (Tadini et al., 2016). The *rh50-1 prps21-1* and *gun1-102 prps21-1* double mutants resembled the *prps21-1* single mutant in terms of growth rate and photosynthetic efficiency (Figure 3.16 A). Moreover, the *rh50-2* mutation had no effect in *prps17-1* genetic background, the single *prps17-1* mutant (Romani et al., 2012) and the *rh50-2 prps17-1* double mutant showed a similar phenotype, whereas *gun1-102* led to albino seedling lethality in combination with *prps17-1* (Figure 3.16 B). More severe effects were observed when *rh50-1* was crossed into *prpl11-1* and *prpl24-1* backgrounds. The *rh50-1 prpl11-1* double mutant was stronger affected compared to *prpl11-1* single mutant in terms of growth rate and photosynthesis (Figure 3.16 A,B), whereas the combination of *gun1-102* and *prpl11-1* mutations caused seedling lethality (Tadini et al., 2016). At last, the combination of *rh50-1* with *prpl24-1* resulted into embryo lethality (Figure 3.16 D), a phenotype that is more severe than *gun1-102 prpl24-1* phenotype, which similar to *gun1-102 prpl11-1* and *gun1-102 prps17-1* resulted in albino-lethal seedlings (Figure 3.16 C). In particular 25% of embryos from *RH50/rh50-1 prpl24-1/prpl24-1* and *RH50/rh50-2 prpl24-1/prpl24-1* siliques stopped

developing and remained arrested at a disordered globular stage. The arrested embryo development at the globular stage observed also in *rh50-1 prpl24-1* double mutants, has been reported for several ribosomal mutants (such as *prps20, prpl1, prpl4, prpl21, prpl27 or prpl35*) that were severely affected in plastid protein translation (Romani et al., 2012; Yin et al., 2012). Taken together, these genetic analyses suggest that the loss of RH50, similarly to GUN1, has an impact on plastid ribosomes and translation. Furthermore, *rh50* and *gun1* mutations often showed a similar phenotypic trend in the mutant background of genes encoding plastid ribosomal proteins (as in case of *prors1*, *prps1*, *prps21*, *prpl11* and *prpl24*).

3.2.5 RH50 interacts with the plastid ribosomal large subunit

As described above, *RH50* specifically interacts genetically with mutants lacking proteins of the large plastid ribosomal subunit (Figure 3.16). In order to study the structural integrity of the ribosomes in the absence of RH50-1, we analyzed the response of the mutant and wild type to the antibiotics chloramphenicol, lincomycin and erythromycin known to target the prokaryotic-like large ribosomal subunit (Wilson, 2009). Chloramphenicol and lincomycin are known to prevent peptide bond formation (Monro and Marcker, 1967; Tompkins, 1970), while erythromycin inhibits the entrance of the nascent peptide into the ribosome exit tunnel (Lovmar et al., 2004; Tenson et al., 2003).

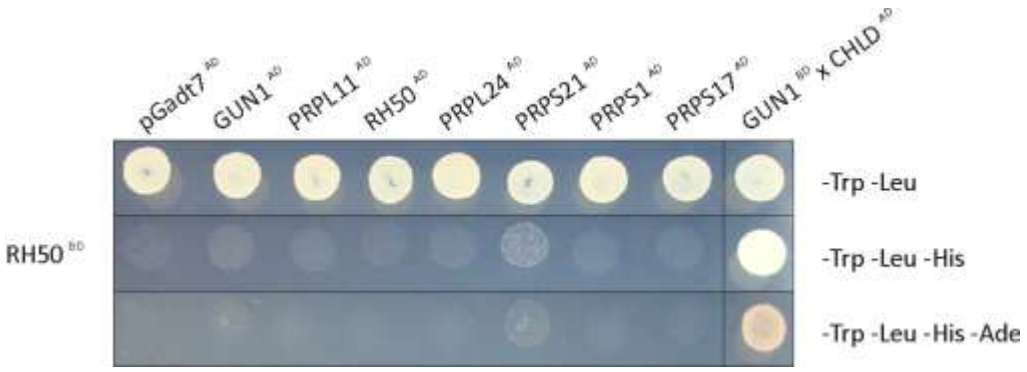

Figure 3.17: Investigation of protein-protein interactions via Yeast-2-Hybrid assay. Yeast cells were co-transformed with a plasmid expressing mature RH50 lacking the chloroplast signal peptide (cTP) as bait protein and plasmids expressing potential interaction partners as pray proteins. Cells were grown on permissive (-Trp -Leu) and selective (-Trp -Leu -His, -Trp -Leu - His - Ade) medium (which reveal interactions).

Although the mutant showed no visible phenotype when treated with lincomycin and chloramphenicol (data not shown), *rh50-1* showed higher sensitivity to erythromycin in respect to the wild type, as seedlings were smaller and paler and exhibited reduced photosynthetic efficiency (Figure 3.18 A), indicating that ribosome stability was affected. This effect points to a role of RH50 in the biogenesis of the 50S ribosomal subunit.

To further investigate whether physical interactions between RH50 and plastid ribosomal proteins occur, yeast two hybrid (Y2H) assays were performed. RH50 was exploited as bait (Bd vector) and tested for interaction with GUN1, RPL11, RPL24, RPS1, RPS17 and RPS21 as preys (Ad vectors). Besides the previously described $GUN1^{BD}$-$CHLD^{AD}$ interaction, used as positive control, no interaction was detected (Fig. 3.17).

In order to study a possible association of RH50 with ribosomes in vivo, size exclusion chromatography of chloroplast soluble fraction (stroma) was conducted. RH50 was identified in megadalton complexes (with a main peak in fractions 5 – 7) containing ribosomal proteins, as demonstrated by immunodetection using RH50-, PRPL11- and PRPS5-specific antibodies (Figure 3.18 B). Moreover, when extracts were treated with RNase A, RH50 accumulation was lost in fraction 5 - 7, indicating that RH50 is associated with RNA-containing RNAse-sensitive particles. Similar trend was observed for proteins of the large and small ribosomal subunit, pointing to the association of RH50 with immature ribosome that are more accessible for RNAses than their mature form found in fractions 3 and 4. The co-migration with ribosomes has also been documented for other plastid-localized and well-characterized DBRHs, such as RH22 (Chi et al., 2012).

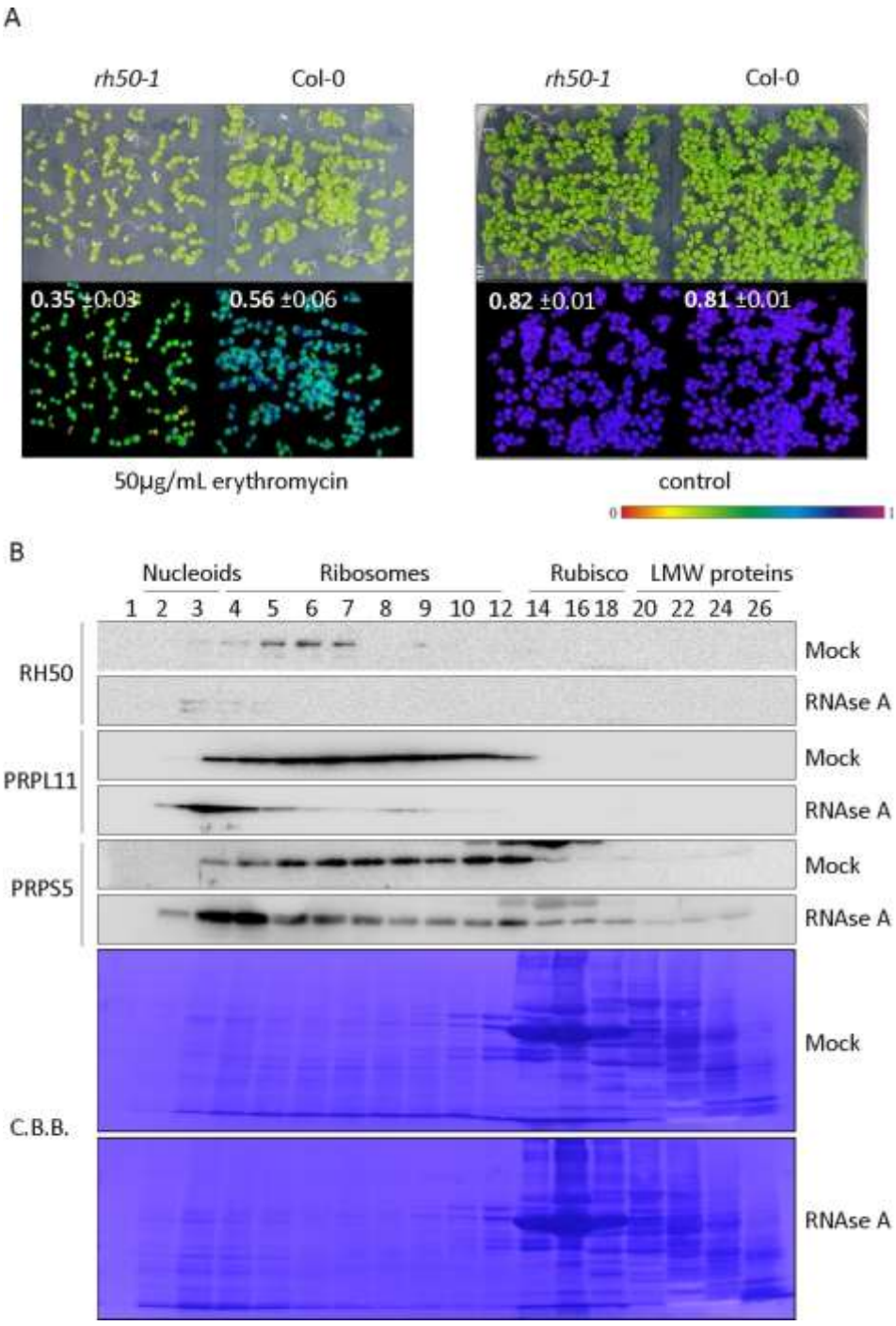

Figure 3.18: RH50 is associated with chloroplast ribosomes.

(A) *rh50-1* is sensible to erythromycin. 10 day-old wild type and *rh50-1* seedlings germinated on MS containing 50 µg/mL erythromycin (left panel) or MS plates without antibiotic, as control (right panel). The maximum quantum yield of photosystem II (F_V/F_M) was determined for each condition (average ±SD; n≥12). The color scale at the bottom indicates the signals intensities. **(B)** Size exclusion chromatography of RNAse-treated and untreated wild type stroma. Protein fractions were precipitated, transferred onto PVDF membranes and

immunodecorated with antibodies against RH50, RPL11 and RPS5. Equal loading is demonstrated by Coomassie Brilliant Blue (C.B.B.) staining of the membrane. Fractions are indicated at the top. LMW (Low Molecular Weight). Performed by Dr. Nikolay Manavski.

3.2.6 RH50 is required for cold stress acclimation

Several DBRHs have been reported to be involved in cold stress adaptation response. RH7, which plays a role in pre-18S rRNA processing and small ribosome subunit biogenesis, participates in plant growth development under low temperature conditions (Huang et al., 2016a; Liu et al., 2016); the cytosolic RH5, RH9 and RH25 helicases are involved in the response to both salt and cold stresses (Kant et al., 2007; Kim et al., 2008); the plastid located RH3, required for intron splicing, mediates salt and cold stress responses, as well (Gu et al., 2014; Larkin et al., 2003).

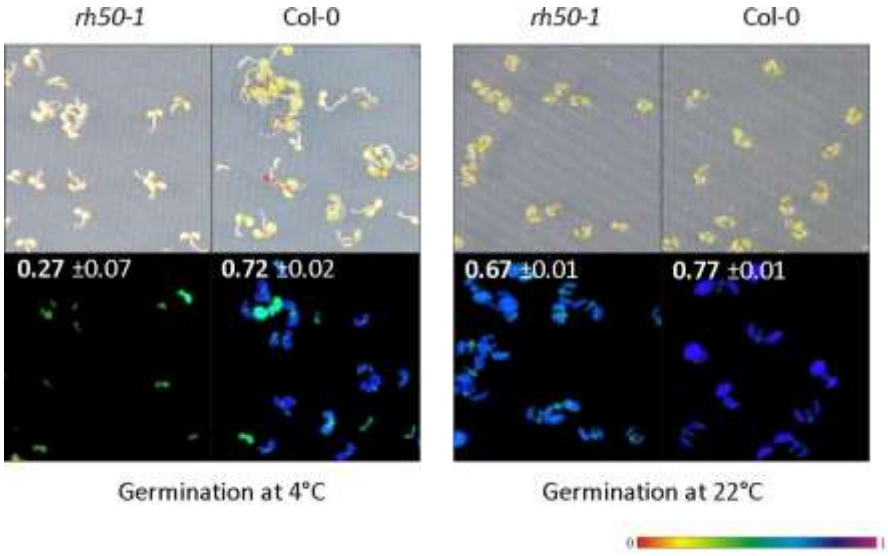

Figure 3.19: The *rh50-1* mutant is cold-stress sensitive.

rh50-1 and Col-0 seedlings were germinated at 4°C (left panel) and 22°C (right panel) and transferred at 22°C for 1 week. The maximum quantum yield of photosystem II (F_V/F_M) was determined for each condition (average ±SD; n≥12). The color scale at the bottom indicates the signals intensities.

Under standard growth conditions, 7-day-old *rh50-1* mutant seedlings showed a slight reduction in maximum quantum yield of PSII compared to the wild type (F_V/F_M 0.67 ± 0.01 *versus* 0.77 ± 0.01,

respectively) (Figure 3.19), a phenotype which is lost already with the appearance of the first true leaves (10 day old seedling Figure 3.18 A).

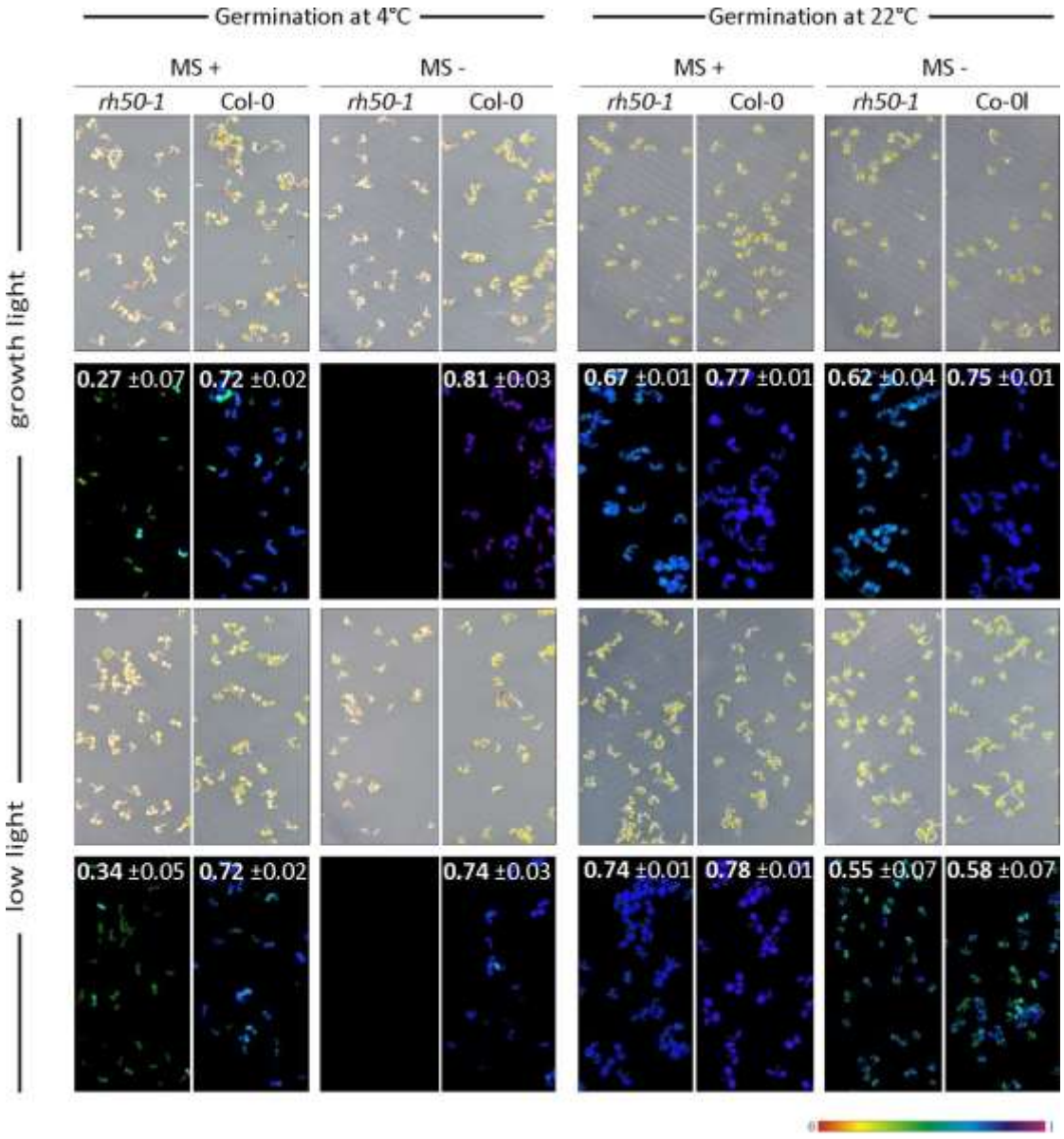

Figure 3.20: The *rh50-1* mutant is sensitive to cold stress. Seedlings of *rh50-1* and Col-0 germinated at 4°C (left panel) and 22°C (right panel) on Murashige and Skoog (MS) media with or without 1% sucrose (+ and – respectively). Seedlings germinated at 4°C were then transferred to 22°C for 1 week and cultivated under growth light (100 µmol photons $m^{-2}s^{-1}$) or low light (30 µmol photons $m^{-2}s^{-1}$). The maximum quantum yield of photosystem II (F_V/F_M) was determined for each condition (average ±SD; n≥12).

Intriguingly, *rh50* mutants displayed impaired cold-stress tolerance since *rh50-1* seedlings, germinated and grown on MS medium supplemented with 1% sucrose for 6 weeks at 4°C, and then transferred to 22°C for 1 week, showed reduced growth, chlorophyll accumulation and maximum quantum yield of PSII (F_V/F_M 0.07 ± 0.07 *versus* 0.72 ± 0.02) compared to the wild type (Figure 3.19). In the absence of sucrose, this phenotype was enhanced and *rh50-1* mutants failed completely to accumulate chlorophyll, thus causing seedling lethality (Fig. 3.20). Reducing the light intensity to decrease oxidative stress, failed to rescue the lethality of *rh50-1* seedlings (Fig. 3.20). The pale phenotype of the cold-stressed seedlings is likely to result from translational impairments, as it has been reported for other mutants involved in biogenesis of ribosomal subunits (RPL33, RPS5 and RBD1) (Rogalski et al., 2008; Wang et al., 2016; Zhang et al., 2016). To test this hypothesis, polysome loading experiments were performed with cold-treated wild type and *rh50-1* seedlings (Figure 3.21 A).

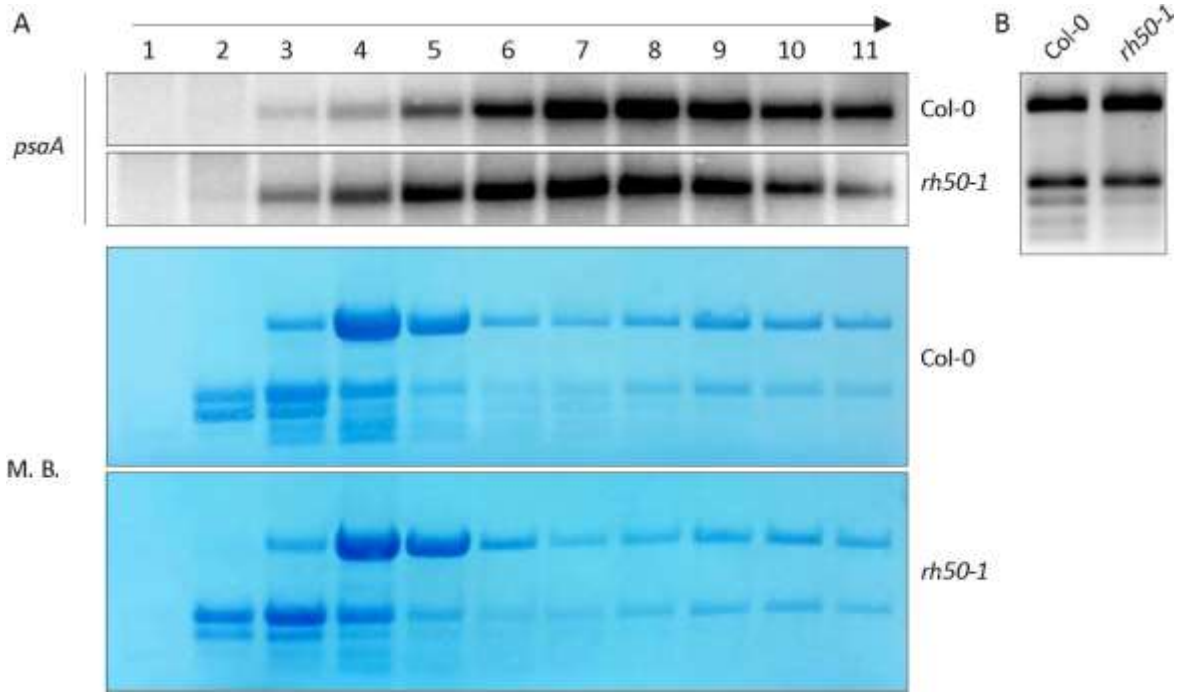

Figure 3.21: *rh50-1* shows translation impairments. (A) RNA gel blot analysis of *psaA* transcripts in polysome fractions (1 to 11) collected from sucrose gradient of cold-treated wild type and *rh50-1* extracts. **(B)** EtBr staining of total RNA from cold-treated *rh50-1* and wild type plants. Performed by Dr. Nikolay Manavski.

The *psaA* mRNA, which is efficiently loaded on polysomes hence migrates deep into the sucrose gradient, was chosen as example (Amann et al., 2004; Manavski et al., 2015). In *rh50-1* mutant plants, the *psaA* transcripts shifted towards the low molecular weight fractions, indicating that *psaA* was less efficiently loaded with polysomes as compared to the wild type control, suggesting a reduced translation rates. This was further supported by the reduced levels of plastid ribosomal RNAs in the mutant (Figure 3.21 B).

Table 3.1: RNA-seq analysis

Locus ID	Gene	Log_2 (fold change)	fold change	p-value
GL2 (Glabra2)	AT1G79840	1,6603	2,448	0,00023
GD2 (glutamate decarboxylase 2)	AT1G65960	1,6208	1,7676	0,0004
Hypothetical protein	AT3G16525	1,4392	1,7254	0,0186
Antisense long non coding RNA	AT5G07885	1,4219	1,666	0,03465
F-box family protein	AT5G10340	1,2916	1,6603	2,44804
PKS4 (phytochrome kinase substrate 4)	AT5G04190	0,8218	1,6208	1,76756
Protein of unknown function	AT5G07940	0,7869	1,551	1,72542
RecA1	AT1G79050	0,7364	1,4392	1,66603
RNA polymerase II fifth largest subunit, E	AT3G54490	0,7058	1,4219	0,04789
Calcium-binding EF hand family protein	AT4G27790	0,6789	0,7058	0,04807
Protein of unknown function	AT4G18215	0,6667	0,6789	0,03984
MET1	AT1G55480	0,6658	0,6667	0,0133
ATMRD1 (mto 1 responding down 1)	AT1G53480	0,6594	0,6658	0,0365
TRNG.1	ATCG00100	0,6466	0,6594	0,00067
LHCB4.1	AT5G01530	0,6453	0,6466	0,03645
TRNT.2	ATCG00390	0,6332	0,6453	1,55099
PSBK	ATCG00070	0,6304	0,6304	0,00045
Protein of unknown function	AT1G50710	0,6303	0,6303	0,04351
Protein phosphatase 2C family protein	AT1G09160	0,6288	0,6288	0,0499
Reticulon family protein	AT3G54120	0,6235	0,6235	0,04805
DPE1 (disproportionating enzyme)	AT5G64860	0,5981	0,5981	0,01593
Protein of unknown function	AT1G74440	0,5526	0,5526	0,01858
ABCI15 TGD2 (trigalactosyldiacylglycerol2)	AT3G20320	0,5412	0,5412	0,01771
RH50	AT3G06980	0,0038	0,0038	3,12E-180

3.2.7 RH50 is involved in plastid RNA metabolism

As suggested by the severe phenotype observed in *rh50-1 prpl11-1* and *rh50-1 prpl24-1*, *RH50* shows a genetic interaction with genes encoding proteins of the large plastid ribosomal subunit. RNA helicase activity has been shown *in vitro* for RH50 homolog protein in rice (Li et al., 2008), suggesting that RH50 might be able to bind RNA *in vivo*. To investigate the role of RH50 in chloroplast RNA metabolism, RNA-seq analyses was performed on total RNA extracted from wild type and *rh50-1* three-week-old plants. No obvious changes in gene expression were detected in the nuclear transcriptome of *rh50-1* when compared to the wild type control (Table 3.1). A closer look at the chloroplast gene expression, however, revealed a strong accumulation of the 23S-4.5S intergenic region in the mutant (Figure 3.22). In several genetic backgrounds, *RH50* showed a similar phenotypic behavior as *GUN1* (as seen for *prors1-1*, *prps1*, *prps21*, *prpl11* and *prpl24*), suggesting functional similarities.

To further characterize the role of RH50 in ribosome biogenesis and to validate the RNA-seq data, plastid rRNAs in wild type (Col-0), *gun1*, *rh50-1*, *gun1 rh50-1* plants were investigated via RNA gel blot analyses. The plastid rRNA gene cluster is transcribed as one RNA molecule and further processed by different nucleases, generating, as intermediate products, 16S precursor, 23S-4.5S bicistronic precursor and 5S precursor (Shajani et al., 2011). The 23S and 4.5S rRNAs precursor (3.2 kb) undergoes endonucleolytic cleavage to produce 4.5S and a 23S fragments (2.9 kb).

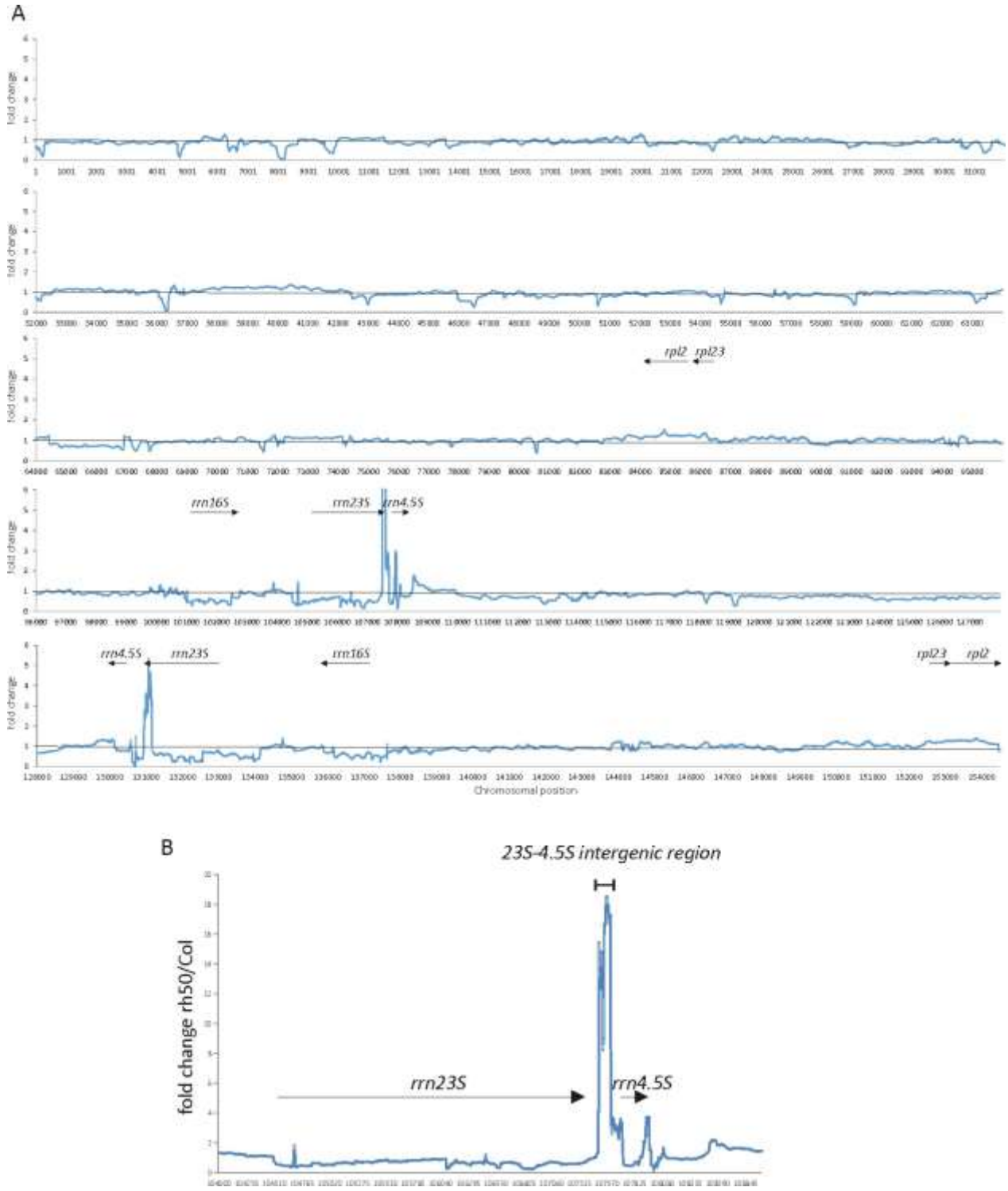

Figure 3.22: Differential enrichment of plastid-encoded genes. (A) Fold change of the read coverage of three *rh50-1* and wild type RNA-seq replicates in the chloroplast genome. Differentially regulated loci are indicated by an arrow carrying the respective name. **(B)** Fold change of read coverage between *rh50-1* mutant and wild type (Col-0) in the 23S and 4.5S rRNA genomic region. Gene names and positions are indicated by the arrows.

The 23S precursor is further processed and eventually generates three mature transcripts species of 1.3 kb, 1.1 kb and 0.5 kb which lead the assembly of 50S subunit (Bollenbach et al., 2005). To determine whether RH50 plays a role in such mechanisms, 16S, 23S, 4.5S and 5S rRNA transcripts were investigated in *gun1-102*, *rh50-1* and *rh50-1 gun1-102* genetic background (probe a, b, d and e in Figure 3.23 A). RNA gel blot analyses revealed that 16S and 5S rRNA transcripts (probe a and e, respectively; Figure 3.23 A) accumulated to the same level as in the wild type and in all the mutant backgrounds analyzed (Figure 3.23 B). However, RNA blots hybridized with specific probes for 23S (b) and 4.5S (d) revealed processing defects of 23S and 4.5S rRNA transcripts in the absence of RH50. In *rh50-1* and *rh50-1 gun1-102,* mature 23S and 4.5S transcripts appeared slightly reduced while unprocessed transcripts were accumulating as compared to wild type and *gun1.* Hybridization with a probe specific for 23S-4.5S intergenic region (c) showed seven times stronger accumulation of this region in *rh50-1* and *gun1-102 rh50-1* mutants as compared with the wild type and *gun1* (Figure 3.23 B). These findings strongly suggest the involvement of RH50 in processing of the 23S-4.5S intergenic region. In such a scenario, RH50 could promote the maturation of 23S and 4.5S rRNAs, as RNA helicase, by unravelling the 23S-4.5S intergenic region and facilitating the cut of a sequence-specific endonuclease. No additional effect could be detected in *gun1-102 rh50-1* samples, compared to *rh50-1*, implying that GUN1 plays no role in this pathway.

Several other plastid transcripts were checked but only insignificant differences were observed, suggesting that those might be secondary effects resulting from translation impairments as it was shown previously for other mutants defective in plastid translation (Fristedt et al., 2014; Tiller et al., 2012; Yu et al., 2008).

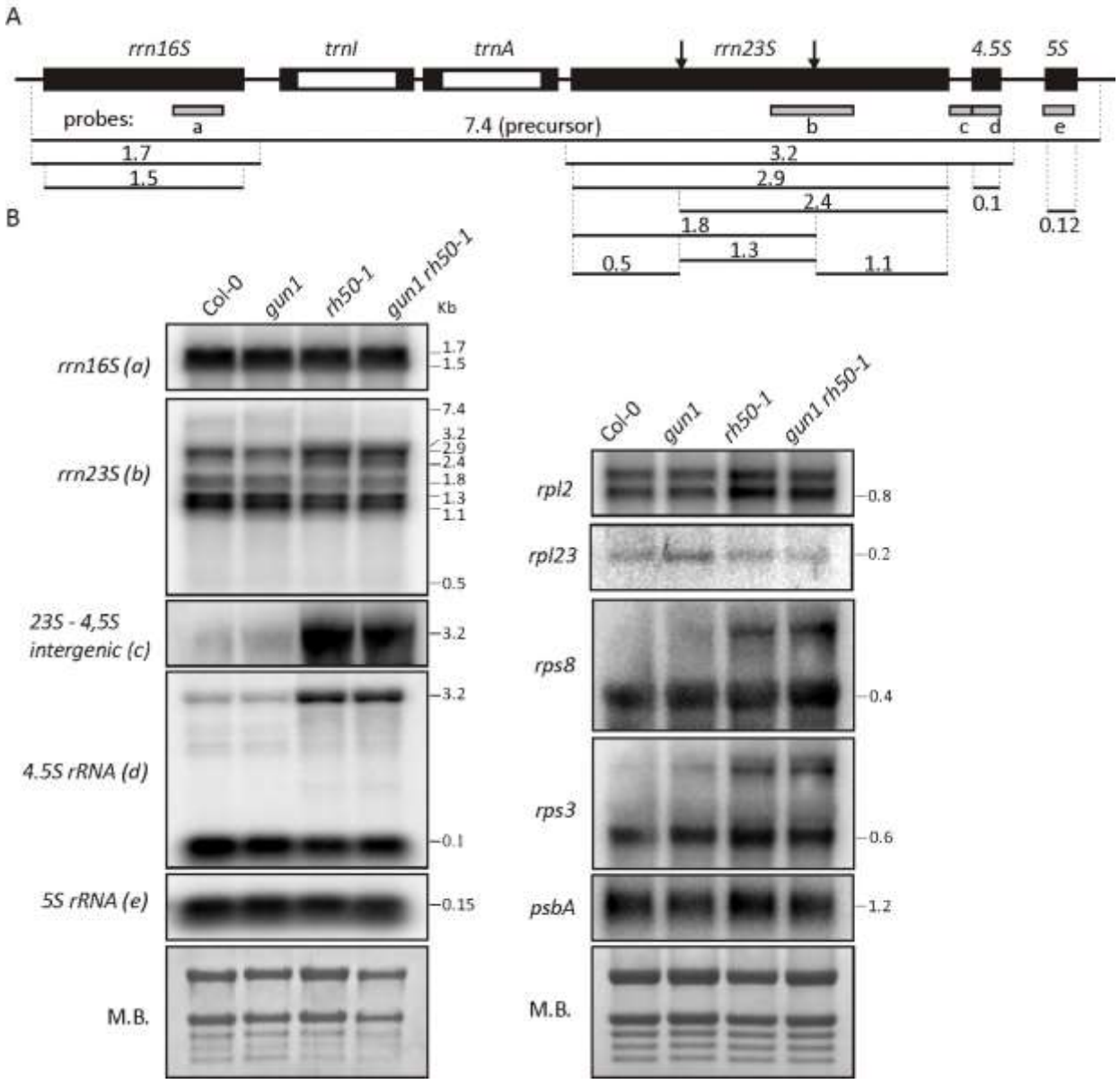

Figure 3.23: RH50 is required for the processing of the 23S-4.5S rRNA polycistronic transcript. (A) Schematic representation of chloroplast rRNA gene cluster in *Arabidopsis*, position of the probes (a-e) used for the RNA gel blot analysis is indicated. All precursors, intermediates and mature forms with their respective dimension in kilo-nucleotides (knt) are shown. The arrows indicate the position of the hidden breaks. **(B)** RNA gel blot analysis with probes specific for plastid rRNAs (16S, 5S, 23S, 4.5S, 23S-4.5S intergenic region, *rpl2*, *rpl23*, *rps8*, *rps3* and *psbA*) in total RNA from wild type (Col-0) and mutant (*gun1-102, rh50-1, gun1-102 rh50-1*) plants.

3.2.8 Lack of RH50 affects plastid translation in the *prpl11* genetic background

As previously observed, lack of RH50 in *prpl24-1* and *prpl11-1* genetic background (mutants affected in large plastid ribosomal subunit) led to the exacerbation of the single mutant phenotypes (Figure 3.16 A, B), causing embryo-lethality in *prpl24-1* and enhancing the *prpl11-1* phenotype. *rh50-1 prpl11-1* double mutant plants showed indeed a severe, but viable, phenotype. To determine whether the additivity of *rh50-1 prpl11-1* double mutant phenotype can be related to a synergistic impairment of the plastid protein synthesis, *in vivo* labelling assays were performed. To this end, the rate of incorporated ^{35}[S] methionine into plastid proteins in young leaves of wild type (Col-0), *rh50-1*, *prpl11-1*, and *rh50-1 prpl11-1* mutant plants was monitored after 5, 10 and 15 min of light exposure (Figure 3.24).

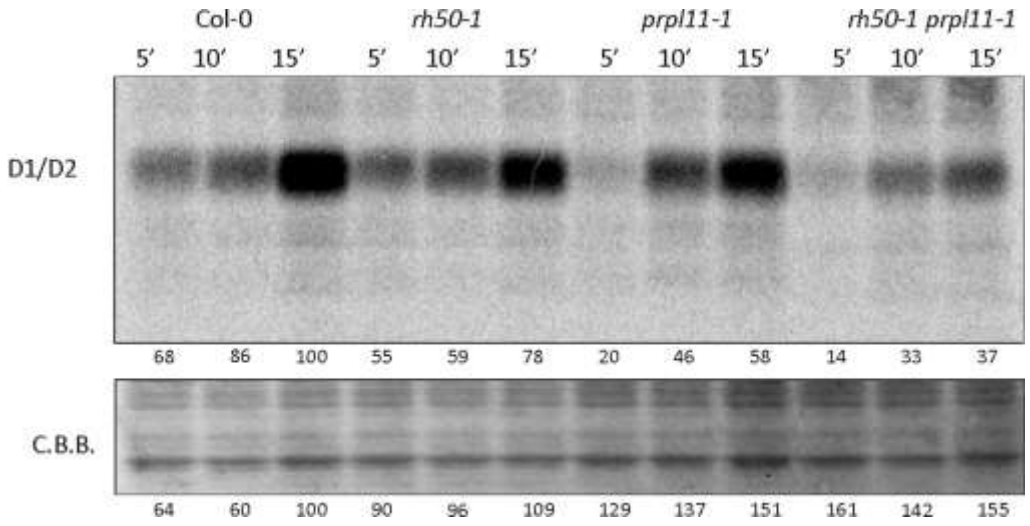

Figure 3.24: The *rh50-1* mutation impairs plastid translation in *prpl11-1* genetic background. Leaves isolated from 6-leaf-rosette plants were pulse-labeled with [^{35}S]methionine under low-light illumination (20 µmol photons m^{-2} s^{-1}) for 5, 10, and 15 min in the presence of cycloheximide to inhibit cytosolic protein synthesis. Total leaf proteins were then isolated, fractionated by SDS-PAGE and detected by autoradiography. A portion of the SDS-PAGE stained with Coomassie Brilliant Blue (C.B.B.), corresponding to the RbcL migration region, was exploited as internal standard for loading normalization. Quantification of signals (by ImageJ) relative to Col-0 15' (=100%) is provided below each panel.

The synthesis rates observed were slightly reduced in *rh50-1* and *prpl11-1* single mutants in respect to the wild type. The double mutant *rh50-1 prpl11-1* showed strongly reduced synthesis rates at all three time points, when compared to wild type and *prpl11-1*. At the end point of 15 minutes the D1/D2 synthesis reached 37% in respect to the wild type control (Figure 3.24). The phenotype of *rh50-1 prpl11-1* double mutant suggests a synergistic effect on the 50S ribosomal subunit biogenesis. According to these observations, it was suggest that the lack of PRPL11 generates instability in the 50S subunit (Pesaresi et al., 2001), while the accumulation of 23S-4.5S rRNA and reduction of their mature forms additionally impairs the translation rate.

3.2.9 RH50 associates with 23S-4.5S intergenic region

The enriched accumulation of the 23S-4.5S intergenic region (Figure 3.22 B and Figure 3.23 B) in *rh50* mutant plants suggests an involvement of RH50 in its processing. For this reason, we investigated the interaction of RH50 with the 23S-4.5S intergenic region *in vivo*. Immunoprecipitation (IP) experiments were performed using RH50-specific antibodies and pre-serum as control on wild type stroma extracts (Figure 3.25 A).

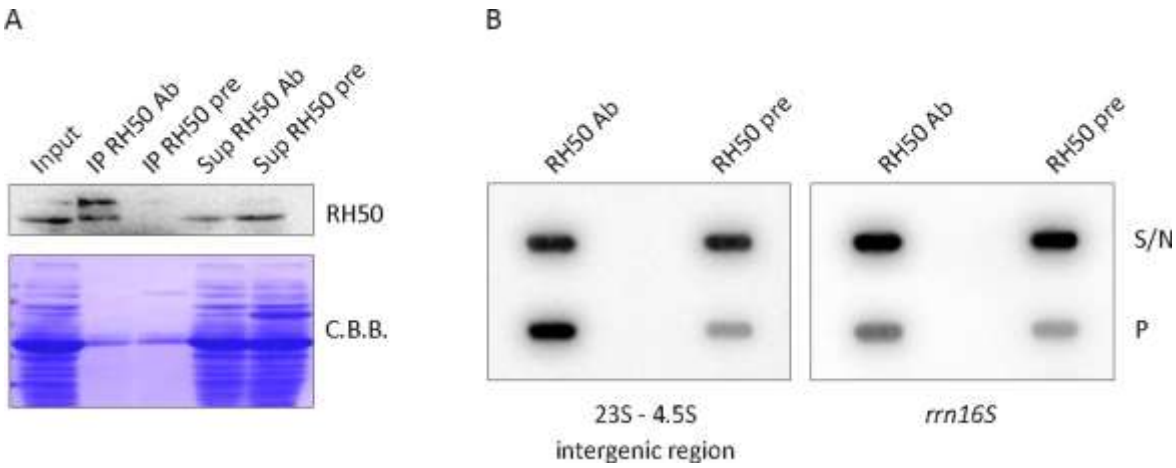

Figure 3.25: RH50 is associated with the 23S-4.5S intergenic region in vivo. (A) Western blot analysis on immunoprecipitated RH50. **(B)** Slot-blot analysis of co-immunoprecipitated RNAs. RNAs recovered from supernatant (S/N) or immunoprecipitation pellets (P) were applied to a nylon membrane using a slot blots manifold and hybridized with probes specific for 23S-4.5S intergenic region and *rrn16S* as control. A and B performed by Dr. Manavski.

As expected, the 23S-4.5S intergenic region was specifically enriched in the IP (Pellet) fraction, whereas 16S control rRNA was not enriched to the same extend, as demonstrated by slot-blot analysis (Figure 3.25 B). As this interaction might indirect, an electrophoretic mobility shift assay (EMSA) was performed utilizing purified recombinant RH50 proteins and radio-labelled RNA probe covering the 23S-4.5S intergenic region (Figure 3.26 A and 3.26 B). RH50 was able to bind the 23S-4.5S intergenic region (Figure 3.26 B), whereas no binding was observed with the 23S rRNA probe that was used as control. This observation indicates that RH50 itself is capable of binding the 23S-4.5S intergenic region. An intrinsic RNA-binding properties were also reported for other RNA helicases such as RH22 (Chi et al., 2012) and RH39 (Nishimura et al., 2010).

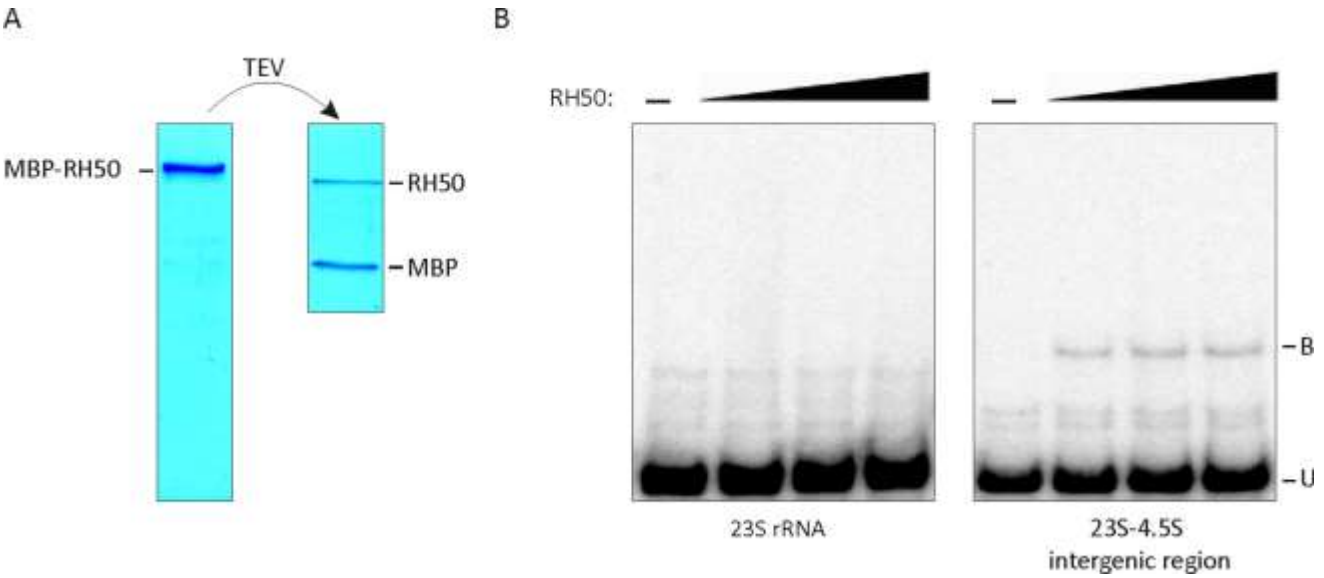

Figure 3.26: RH50 binds to the 23S-4.5S intergenic region in vitro. (A) Affinity purification of MBP-RH50 proteins before and after AcTEV cleavage. Purified proteins were stained with Coomassie Brilliant Blue. **(B)** The RNA-binding capacity of RH50 was analyzed by EMSA using radiolabelled RNA probes of the 23S rRNA and 23S-4.5S intergenic region as indicated. Increasing concentrations of the purified RH50 protein (black triangles) were used. B; bound, U; unbound. A and B performed in collaboration with Dr. Manavski.

4 Discussion

4.1 Introduction of a plant photosystem II into the cyanobacterium *Synechocystis*

Aim of the project was to replace the endogenous PSII of *Synechocystis* with the one of *A. thaliana*. Two synthetic construct carrying 11 genes encoding for the PSII core proteins of *A. thaliana:* RC1 (D1, D2, CP43 and I) and RC2 (cytb_{559} α and β subunit, L, J, CP47, T and H), were independently introduced in S*ynechocystis.* In previous studies several attempts to express PSII genes of higher plants in *Synechocystis* were performed. The *psbA* gene from *Poa annua*, encoding for D1 protein, was introduced in a *Synechocystis* mutant strain lacking all three D1 genes (*psbA1, 2 and 3*). They could show that the chimeric strain was able to grow photoautotrophically and that the hybrid PSII core reaction center could assemble and function in the mutant (Nixon et al., 1991). Attempts in replacing the CP43 from *Synechocystis* with the homologous one from spinach have been made. However, despite the high amino acid sequence identity between the two proteins (85%), CP43 of spinach seemed to be unable to incorporate in the PSII complex of *Synechocystis* (Carpenter et al., 1993). Only when the 3' half of the spinach protein was replaced with the endogenous cyanobacterial one, PSII complex could be assembled, indicating that the C-terminus of CP43 is necessary for its stability (Carpenter et al., 1993).

The replacement of *psbA2* of *Synechocystis* with the codon-optimized synthetic construct RC1, in the generated *psbA2 RC1-7* strain, resulted in the complete loss of the endogenous *psbA2* gene and in the accumulation of the plant PsbI protein (Fig. 3.5A). The expression of the *AtpsbA*, *AtpsbD* and *AtpsbC* plant genes was confirmed via RT-PCR (Fig. 3.5B). The further knock-out of the *psbDC* operon in the *ΔpsbA2 RC1-7*, produced the strain *ΔpsbA2DC RC1*. Loss of *psbD* and *psbC* in *Synechocystis* has been shown to cause decreased levels of D1, D2 and CP47 proteins that together with the lack of CP43 which leads to the formation of an unstable PSII complex and a mutant which is unable to grow photoautotrophically (Yu and Vermaas, 1990). In contrast, the *ΔpsbA2DC RC1* mutant showed a partial rescue and was able to grow photoautotrophically but with slow growth rate (Fig. 3.10). The fact that the mutant showed only a partial rescue could not be traced back to a lack of transcripts, since all plants genes were proven to be transcribed (Fig. 3.5B and 3.9C). However, it could be due to a lack of accumulation of the plant protein D2 (Fig. 12). The Immunoblot showed the accumulation of the

Synechocystis D2, instead of the plant one. It is important to consider that *Synechocystis* has two *psbD* genes, *psbD1* and *psbD2*, encoding for the D2 core protein of PSII reaction center and three *psbA* genes, *psbA2*, *psbA3 and psbA1* (Mulo et al., 2009), encoding for the PSII core complex protein D1 (See also Table 1.1). Inactivation of *psbA2* or *psbA3* or of one of the two *psbD* genes up-regulates the expression of the other gene to wild type levels indicating that cells carrying just either gene alone is able to grow photoautotrophically (Mulo et al., 2009). The *ΔpsbA2DC RC1* mutant generated so far still contains *psbD2*, *psbA1* and *psbA3*. The presence of two copies of the same gene (endogenous and synthetic genes) could indeed reduce the PSII activity by sequestering an increased amount of post-transcriptional and transcriptional factors that are required for the expression of the other genes and operons (Gimpel et al., 2016). It is also possible to speculate that several combinations of chimeric PSII might form or coexist. Therefore, it is unclear whether the newly introduced plants subunits are assembled in a functional stable structure or whether they transiently interact to be subsequently unassembled and degraded. Mass spectrometry analysis would help to understand more precisely if the plants proteins are actually assembling or not. Further experiments as the measurement of the activity of PSII in *ΔpsbA2DC RC1* mutant and the analysis of the composition of the PSII complex with Blue Native PAGE would help to better understand the life cycle of the plant subunits and identify the limiting step in the assembly of the chimeric PSII.

The successful replacement of the *Synechocystis psbEFLJ* operon with the RC2 construct resulted in generation of the mutant strain *psbEFLJ RC2*. The mutant was confirmed to be completely KO for the endogenous *psbEFLJ* operon and to carry all plant genes introduced with the RC2 construct (Fig. 3.6). The *psbEFLJ RC2* mutant was not able to grow photoautotrophically, this phenotype was proven to be related to the lack of transcripts accumulation of the plants genes introduced with the construct (Fig. 3.7). As already reported in previous studies, KO of the *psbEFLJ* operon prevents PSII accumulation. The *psbEFLJ* mutant could not grow photoautotrophically and it was growing three times slower than the wild type in heterotrophic conditions (Pakrasi et al., 1988). Absence of cytb_{559} is inhibiting the production of D2 protein, whereas D1, CP43 and CP47 synthesis is independent of the presence of the cytb_{559} (Komenda et al., 2004). This behavior has been previously described for the cyt b_6f assembly in *Chlamydomonas,* where the absence of the subunit IV of the cytochrome b_6f complex downregulated the synthesis of the cytochrome f protein (Choquet et al., 2001). This epistatic synthesis regulation may

prevent the waste of energy for the synthesis of proteins that cannot be assembled (Komenda et al., 2004). The fact that the genes introduced with the RC2 construct were not expressed was investigated by introducing the RC2 synthetic construct in *Synechocystis* wild type strain on a self-replicative plasmid, in order to avoid the simultaneous disruption of the *psbEFLJ* operon. The *RC2.2* mutant strain accumulated the transcripts of at least *psbE* and *psbB* plant genes (Fig. 3.8C). These results led to the conclusion that the position of the RC2 construct in the genome, in the *psbEFLJ Synechocystis* operon specifically, was inhibiting its transcription. Transcription could be affected by rearrangements of the DNA secondary structure or by the activation of transcriptional regulatory mechanism. Efficient transcription is one of the major concern when heterologous proteins are expressed in cyanobacteria and different components like, the cyanobacterial RNA polymerase, sigma factors, promoters, chromatin rearrangement or activation of protection mechanism against foreign DNA may have an impact on it (Lehmann et al., 2014; Stensjo et al., 2017; Vasu and Nagaraja, 2013).

Bacterial genomes show a periodic bias in nucleotide frequencies, every 11 bp in cyanobacteria, which is related to the DNA structure (Herzel et al., 1999; Mrazek, 2010). This “signal” correlated indeed with the curvature of the DNA double helix (Rohs et al., 2009). Loss of the periodicity, due to introduction of synthetic genes, might lead to structural DNA changes and inefficient transcription process. The expression of the construct outside of the genomic context, on the pUR2LT plasmid could help in overcoming genome accessibility problems; moreover, the presence of the *petJ* promoter at the 5’ of the RC2 construct could facilitate the recruiting of the ribosomes and induce efficient translation. To avoid the interference with possible regulatory elements present on the genome another possible solution could be to integrate the synthetic construct in one of the few neutral site of *Synechocystis* genome recently published (Ng et al., 2015; Pinto et al., 2015; Stensjo et al., 2017).

Several protecting systems are known in bacteria: (1) restriction-modification (R-M) systems, which uses the activity of a methyltransferase (MTase) to discriminate between self and non-self DNA and a restriction endonuclease (REase) that recognize and cleaves foreign DNA (Bickle and Kruger, 1993); (2) CRISPRs systems, which along with their associated genes (*cas* genes) are involved in immunity against phages (Barrangou et al., 2007; Brouns et al., 2008); (3) RecBCD system, distinguish the host genome which is carrying a cis element (Chi sequence) from the phage DNA (Dillingham and Kowalczykowski, 2008); (4) transcriptional silencing, where a transcription termination factor and nucleoid-associated

proteins selectively bind to xenogenic DNA with AT content higher than the that of the genome and silence it (Gordon et al., 2010). One of these systems might be involved in the inactivation or silencing of the synthetic construct psbEFLJ RC2.

The assembly of a chimeric PSII is not straightforward. Gene and protein similarities are not sufficient to predict the outcome of subunits replacement. This was also a conclusion of the work of Gimpel and coworker (Gimpel et al., 2016) on a mutant of *Chlamydomonas reinhardtii* lacking six genes of the PSII core. The complementation of this KO mutant with the core PSII gene of two different green algae resulted in partial reconstitution of PSII activity, which was however far from wild type levels (Gimpel et al., 2016). These data together with our results indicate that the replacement of PSII with the one of different species and its use as a synthetic biology module is possible but many limiting steps are still present. First, probably there are still many unknown assembly factors and accessory proteins involved in PSII assembly and repair that might be necessary for the correct assembly of all PSII. Second, as previously described, the bacterial protection systems against foreign DNA can interfere with the expression of the exogenous synthetic genes and synthetic circuits. The generation of well-characterized regulatory systems, like for example the introduction of short-regulatory RNAs (antisense RNAs) for the control of the endogenous protection systems (Higo et al., 2017) would be a useful tool for the progress of genetic engineering.

In this work, in line with the study of Viola (Viola, 2014), Vamvaka (Vamvaka, 2016) and Gandini (Gandini, 2017), *Synechocystis* has been used as platform for the identification and functional characterization of plant photosynthesis-related proteins. *Synechocystis* is becoming a prominent synthetic biological chassis to study and exploit photosynthesis thanks to the combination of its simple cellular organization and the development of new genetic and molecular biological tools. Fine-tuning and further progress in new synthetic biology strategy is a necessary step in order to help the scientific community in the dissection of complex biological processes as plant photosynthesis.

4.2 Characterization of the DEAD-box RNA helicase RH50

4.2.1 RH50 is involved in PGE-triggered plastid-to-nucleus retrograde signaling and shows comparable genetic interaction with GUN1

Organelle gene expression is regulated mainly at posttranscriptional levels through RNA processing, intron splicing, RNA editing and translational control (del Campo, 2009). Many proteins are encoded in the nucleus and are subsequently transported into the chloroplast where they play essential roles in posttranscriptional RNA metabolism (del Campo, 2009; Nott et al., 2006; Pesaresi et al., 2007). It is therefore clear that the fine-tuning of the anterograde and retrograde signaling pathway is necessary for organelle gene expression and function. It has recently been shown that RNA binding proteins play a central role in plant development and stress response (Lee and Kang, 2016). Among RNA binding proteins are the DEAD-box RNA helicase that can assist the formation of functional mRNA in chloroplasts and mitochondria (Cordin et al., 2006). DBRHs consist of 8 conserved motifs Q, Ia, Ib, II, III, IV, V and VI (Caruthers and McKay, 2002). Motif II is the so called “DEAD” (Asp-Glu-Ala-Asp) box, motif III is required for NPTase and helicase activity, it performs the unwinding of the RNA (Pause and Sonenberg, 1992). Motifs Ib, IV and V are probably involved in RNA binding (Rocak and Linder, 2004).

In *A. thaliana,* 120 RNA helicases member have been predicted by the TAIR database of which 58 have been identified as DBRH. Among them, 7 have been predicted to be plastid localized (RH3, 22, 26, 39, 47, 50 and 58) and only RH3, RH22 and RH39 have been so far functionally characterized (Asakura et al., 2012; Chi et al., 2012; Nishimura et al., 2010). Phylogenetic analyses cluster RH22, -39, -47, -50, -58 in one clade, separate from RH3 and RH26 (Asakura et al., 2012). Our expression data indicate for *RH50* a high co-regulation score with *RH58,* as well as with *GUN1*, *PRPS1*, *PPOX* and *CHLD*, previously identified as highly co-expressed gene cluster (Figure 3.13) (Tadini et al., 2016). Similar to GUN1, RH50 is located in plastid nucleoids, megadalton complexes responsible for plastid encoded protein synthesis (Koussevitzky et al., 2007; Olinares et al., 2010). GUN1 protein, known as the master regulator of chloroplast-to-nucleus retrograde signaling, physically interacts with proteins involved in plastid protein homeostasis, like chaperones, proteases, ribosomal proteins and DBRHs (Koussevitzky et al., 2007; Tadini et al., 2016). However, the function of GUN1-containing complex is still elusive and the signaling molecules, which the signaling relies on, are still under discussion. It has been suggested that

the accumulation of unprocessed plastid transcripts might trigger plastid signaling, in order to regulate gene expression of nuclear photosynthesis genes (Sun et al., 2016). The *rh50* mutants did not display any *gun* phenotype in presence of either NF or Lin, conditions in which the chloroplast is severely impaired. The *rh50-1* mutant was also analyzed in the *prors1-1* genetic background. The *prors1-1* mutation represents a milder PGE-defective condition, which does not severely affect the chloroplast physiology but mimics, nevertheless, the effect of Lin-treatment. Interestingly, the *rh50-1 prors1-1* double mutant revealed the restoration of PhANGs to a wild type level, as observed before for the *gun1 prors1-1* (Figure 3.15C) (Tadini et al., 2016). Moreover, *rh50* mutation does not alter the *gun* phenotype in *gun1* seedlings in which PhANGs are not repressed (Figure 3.15C). Such findings suggest the involvement of RH50 in PRORS1-triggered plastid-to-nucleus retrograde signaling as PhANGs repressor in GUN1-like manner. Moreover, RH50 also suppresses the accumulation of the chloroplast ribosomal protein PRPS1 like GUN1 (Fig. 3.16E). GUN1 can genetically and physically interact with PRPS1 and, only genetically, with PRPL11 (Tadini et al., 2016).

In this study, mutations for *rh50* and *gun1* genes were introduced into genetic backgrounds defective for 30S (*prps1-1, prps17-1* and *prps21-1*) and 50S (*prpl11-1* and *prpl24-1*) subunits of the plastid ribosome (Figure 3.16A-D). The additive (in combination with *prpl11* and *prpl24*) or suppressor (in combination with *prps1* and *prors1*) effect was stronger in the *gun1*-containing double mutants, except for *prpl24* where the *rh50*-containing double mutant was embryo lethal while *gun1 prpl24* was seedling lethal. In the case of *prps17,* the introduction of the *rh50* mutation had no additive effect whereas *gun1 prps17* was seedling lethal (Fig. 3.16C). Such findings are consistent with the previous observation that several RNA helicases interact with ribosomal proteins as described for RH3, RH39 and RH22 (Nishimura et al., 2010; Asakura et al., 2012; Chi et al., 2012).

Altogether, our data suggest that both RH50 and GUN1 are functionally connected with the plastid physiology but the role of GUN1 has broader functions. Since GUN1 has been proposed to be the integrator of both, the tetrapyrrole biosynthesis and the plastid gene expression pathway and RH50 shows a functional interaction only with the OGE pathway, we hypothesize that RH50 might function downstream of GUN1 in a plastid gene expression specific pathway.

4.2.2 RH50 promotes the biogenesis of the plastid ribosome large subunit by assisting in the 23S-4.5S rRNA processing

Ribosome biogenesis is a complex and fine-tuned process, that involves events like the transcription of the ribosomal gene cluster, rRNA processing and ribosome assembly (Kaczanowska and Rydén-Aulin, 2007). Several proteins involved in plastid ribosome biogenesis have been described. RHON1, as an example, was identified to bind the inter-cistronic region on the 23S-4.5S rRNA precursor and to confer sequence specificity to the *A. thaliana* endonuclease RNAseE (Stoppel et al., 2012). SUPPRESSOR OF THYLAKOID FORMATION1 (SOT1), a plastid localized pentatricopeptide repeat protein, is required for the correct processing of 23S-4.5S rRNA precursor (Wu et al., 2016). RAP, an octotricopeptide repeat protein, binds to the 5' region of 16S rRNA precursor and assists its maturation (Kleinknecht et al., 2014). The chloroplast DEAD-box RNA helicase RH39 plays an important role in the introduction of the hidden-brake in the 23S rRNA together with an unknown endonuclease (Nishimura et al., 2010). A second plastid localized DBRH, RH22 is also involved in 50S ribosomal subunit biogenesis by assisting in the processing of 23S rRNA and, at the same time, binding the ribosomal protein RPL24 (Chi et al., 2012). DBRHs not only play an important role in rRNA metabolism but they seem to have a pivotal role in plant stress responses (Kant et al., 2007; Liu et al., 2002; Owttrim, 2006; Vashisht and Tuteja, 2006). Several studies show that chloroplasts function as temperature sensor, by perceiving the changes in membrane plasticity, enzyme activity and inhibition of the photosynthetic performance (Crosatti et al., 2013; Kindgren et al., 2015; Svensson et al., 2006). The role of RNA helicases in cold conditions relies on their ability to unwind RNA, which, at low temperatures, tends to form stable non-functional secondary structure. Several DBRHs have been identified so far to be involved in both cold stress response and rRNA metabolism. The cytosolic RH7, involved in pre-18S rRNA processing and small ribosome subunit biogenesis, participates in plant growth development under low temperature (Huang et al., 2016b; Liu et al., 2016). RH5, RH9 and RH25 helicases are involved in the response to salt and cold stresses (Kant et al., 2007; Kim et al., 2008) as well as the plastid located RH3, required for intron splicing (Gu et al., 2014).

In this study, were collected several evidences in favor of a role of RH50 in the rRNA metabolism. As previously described, plants mutated in *RH50* and genes encoding for proteins of the large ribosomal

subunit, *rh50 prpl11* and *rh50 prpl24*, showed severely impaired growth rate and photosynthetic efficiency (Fig. 3.16 A, C), indicating genetic interaction of *RH50* with genes encoding proteins of the 50S ribosomal subunit. In addition, the *rh50* mutant resulted to be more sensitive to erythromycin and cold-stress suggesting ribosomal instability and a possible translational impairment. *rh50* seedlings treated with erythromycin (Fig. 3.18A) or germinated at low temperatures (4 °C) and then transferred to normal temperature condition (22 °C) (Fig. 3.19), displayed a smaller and paler phenotype respect to the wild type and a reduced photosynthetic efficiency. Accordingly, polysome-loading experiments performed with cold treated wild type and *rh50* mutant seedlings (Fig. 3.21A) proved aberrant polysome loading and reduced translation efficiency in the absence of *RH50*. Moreover, RH50 co-migrated with the ribosomal particle when size exclusion chromatography of chloroplast soluble fraction was performed (Fig. 3.18B). Finally, RNA gel blot of *rh50* and *rh50 gun1* mutants revealed accumulation of unprocessed 23S and 4.5S rRNA transcripts whereas their mature form appeared to be slightly reduced (Fig. 3.23B). Strong accumulation of the specific 23S-4.5S intergenic region was also observed in these mutants (Fig. 3.23B), indicating a processing impairment in this specific region. Confirming this result, accumulation of the 23S-4.5S intergenic region was also clearly observed in RNA seq data performed on *rh50* total RNA (Fig. 3.22). The association of RH50 with the 23S-4.5S intergenic region was finally proved both in vivo with Co-Immunoprecipitation experiments (Fig. 3. 25B) and in vitro with EMSA experiments (Fig. 3.26 B). Such findings, all strongly suggest a role of RH50 in the biogenesis of the large 50S ribosomal subunit in general, and in the correct processing of the 23S-4.5S intergenic region in particular.

Appendix

Optimized coding regions are indicated in capital letters, promoter and terminator regions in small letters. BsaI restriction site are indicated in bold.

Complete sequence of the synthetic construct RC1

Optimized coding sequences of *A. thaliana AtpsbA*, *AtpsbD*, *AtpsbC* and *AtpsbI* genes are indicated in capital letters.

ttt**ggtctc**tacccataagaaaatggcatcaggagaacaaatattgttccaccgacaggccgcatttgggttttggccaaccgctataccccggcggtgtagtttc
caatcgtctcgtcttattagagaatggagtctaaatgg

cataacccaaattacaaaagcctcctttagaaattcttgcctttgatgctagctacgcaagaggatttgcatttATGACTATTGCCCTGGGAAAATTTA
CTAAAGACGAAAAAGACTTGTTTGACATTATGGATGATTGGTTACGCCGTGATCGGTTTGTGTTTGTGGGGTGGAGCGGA
TTGTTACTGTTTCCCTGTGCCTATTTTGCTTTAGGCGGTTGGTTTACCGGGACCACTTTTGTTACCTCCTGGTATACTCATGG
ATTGGCCTCCAGTTACTTAGAAGGCTGCAATTTTCTGACCGCCGCTGTGAGTACTCCCGCCAACAGCCTGGCTCACTCTTTG
TTACTGTTGTGGGGACCCGAAGCCCAAGGCGATTTTACCCGTTGGTGTCAGCTGGGGGGATTGTGGGCCTTTGTTGCTTTA
CATGGTGCCTTTGCTCTGATTGGGTTTATGTTGCGGCAATTTGAATTAGCCCGGTCCGTGCAGTTGCGCCCCTATAATGCCA
TTGCTTTTAGCGGCCCCATTGCCGTGTTTGTTTCTGTGTTTTTAATTTACCCCCTGGGCCAATCCGGTTGGTTTTTCGCCCCC
AGTTTTGGTGTTGCCGCTATTTTTCGCTTTATTTTGTTTTTCCAGGGGTTTCATAACTGGACTTTGAACCCCTTTCACATGATG
GGGGTTGCCGGAGTGTTAGGCGCCGCTTTACTGTGCGCCATTCATGGTGCTACCGTGGAAAATACTTTGTTTGAAGATGG
CGACGGTGCCAATACCTTTCGTGCTTTTAACCCCACCCAAGCCGAAGAAACTTACAGTATGGTTACCGCTAATCGCTTTTGG
TCCCAGATTTTTGGAGTGGCCTTTAGTAACAAACGTTGGCTGCATTTCTTTATGTTGTTTGTTCCCGTGACCGGCTTATGGA
TGAGCGCCCTGGGTGTGGTTGGGCTGGCCTTGAATTTACGTGCTTATGATTTTGTGTCTCAAGAAATTCGGGCCGCTGAAG
ATCCCGAATTTGAAACCTTTTACACTAAAAACATTTTGTTAAACGAAGGTATTCGTGCTTGGATGGCTGCTCAAGACCAGCC
CCACGAAAATTTGATTTTTCCCGAAGAAGTGTTGCCCCGCGGGAACGCCTTATAAacccataagaaaatggcatcaggagaacaaat
attgttccaccgacaggccgcatttgggttttggccaaccgctataccccggcggtgtagtttccaatcgtctcgtcttattagagaatggagtctaaatggcataa
cccaaattacaaaagcctcctttagaaattcttgcctttgatgctagctacgcaagaggatttgcatttATGAAAACTTTGTATTCTTTACGCCGCTTT
TATCACGTTGAAACTTTATTTAATGGGACTCTGGCCTTGGCTGGTCGGGATCAGGAAACCACTGGTTTTGCCTGGTGGGCT
GGGAATGCCCGCTTGATTAACTTATCCGGGAAATTGTTAGGAGCCCATGTGGCCCACGCTGGGTTAATTGTGTTTTGGGCC
GGAGCTATGAATTTGTTTGAAGTGGCCCATTTTGTTCCCGAAAAACCCATGTATGAACAAGGCTTGATTCTGTTGCCCCACC
TGGCTACCTTGGGATGGGGAGTGGGTCCCGGCGGTGAAGTTATTGATACTTTTCCCTACTTTGTGTCCGGTGTTTTGCATTT
AATTTCCAGTGCCGTGCTGGGGTTTGGGGGAATTTATCACGCCTTACTGGGCCCCGAAACCTTAGAAGAAAGTTTTCCCTT
TTTCGGCTACGTGTGGAAAGATCGTAACAAAATGACCACTATTCTGGGTATTCATCTGATTTTGCTGGGGGTGGGAGCTTT
TCTGTTGGTTTTTAAAGCCTTGTACTTTGGTGGTGTGTACGATACCTGGGCTCCCGGGGGAGGCGACGTTCGTAAAATTAC
CAACCTGACTTTGAGCCCCTCTGTGATTTTTGGTTATTTACTGAAATCCCCCTTTGGTGGGGAAGGGTGGATTGTGAGTGTT
GATGACTTGGAAGATATTATTGGAGGCCATGTGTGGTTAGGCAGTATTTGTATTTTTGGTGGGATTTGGCACATTTTAACC
AAACCCTTTGCCTGGGCTCGTCGGGCTCTGGTGTGGTCCGGAGAAGCTTATTTGTCCTACAGTTTAGCCGCTCTGAGTGTG
TGCGGTTTTATTGCCTGTTGCTTTGTTTGGTTTAATAACACCGCCTATCCCAGCGAATTTTACGGGCCCACTGGACCCGAAG
CCTCTCAAGCCCAGGCTTTTACCTTTTTGGTGCGGGATCAACGCTTAGGCGCTAATGTTGGTAGCGCTCAGGGACCCACTG
GCTTGGGTAAATATTTAATGCGTTCTCCCACCGGCGAAGTGATTTTTGGAGGCGAAACTATGCGTTTTTGGGACTTGCGTG
CTCCCTGGTTGGAACCCTTACGTGGCCCCAATGGTTTAGATCTGAGCCGTTTGAAAAAAGACATTCAACCCTGGCAGGAAC
GTCGGAGTGCTGAATATATGACCCATGCCCCCCTGGGTTCCTTGAACAGTGTGGGTGGGGTTGCTACTGAAATTAATGCC
GTGAACTACGTTAGCCCCCGGTCTTGGTTGAGCACCTCTCATTTTGTGCTGGGCTTTTTCTTGTTTGTTGGCCATTTATGGCA

CGCTGGTCGTGCTCGTGCTGCTGCTGCTGGATTTGAAAAAGGCATTGATCGCGACTTTGAACCCGTGTTATCCATGACCCC
CCTGAATTAAattgagacttttctgattttgcaaaggttttgctttagttaaacccaattgattagtgtcccctgcccatttggtgggggattattatttttaagat
aatcctatttttttggagtgaggccagttacctattagacgcgcgactcgaaagtcgttcaggggagttggaacggcttccaaaaaccttttcccgctggtgtttttg
gttataattccttatgtatttgtcgatgttcagattggaactgactaaacttagtctaaaggattaatgagagttttgtaaagctttgtaacaggaagttaatataca
cgaagcttatagatgacataagttttactttcttgtaattgtcgttttttccatgggATGACTGCTATTCTGGAACGGCGTGAAAGCGAAAGCCTG
TGGGGTCGGTTTTGTAACTGGATTACTTCTACTGAAAATCGGTTGTATATTGGGTGGTTTGGAGTTTTGATGATTCCCACCT
TGTTAACCGCTACTTCCGTGTTTATTATTGCCTTTATTGCCGCTCCCCCCGTTGATATTGACGGCATTCGGGAACCCGTGAGC
GGCTCTCTGTTGTACGGTAATAACATTATTTCCGGGGCCATTATTCCCACCAGTGCCGCTATTGGACTGCATTTTTATCCCAT
TTGGGAAGCCGCTTCCGTGGATGAATGGTTGTATAATGGCGGTCCCTACGAACTGATTGTTTTGCATTTTCTGCTGGGGGT
GGCCTGTTACATGGGACGCGAATGGGAATTAAGCTTTCGGCTGGGTATGCGCCCCTGGATTGCTGTGGCCTACTCTGCTCC
CGTTGCTGCTGCTACCGCTGTGTTTTTAATTTATCCCATTGGCCAAGGTTCCTTTAGTGACGGGATGCCCCTGGGCATTAGT
GGTACTTTTAACTTTATGATTGTGTTTCAGGCCGAACATAACATTTTAATGCATCCCTTTCACATGCTGGGGGTGGCCGGAG
TTTTTGGGGGATCCTTGTTTAGTGCCATGCACGGTTCCCTGGTTACCTCCAGTTTGATTCGCGAAACCACTGAAAATGAAAG
TGCCAACGAAGGGTATCGTTTTGGACAAGAAGAAGAAACCTACAACATTGTGGCTGCCCATGGCTACTTTGGTCGTTTAAT
TTTTCAGTACGCCAGCTTTAACAACAGCCGGTCCTTGCATTTCTTTTTGGCTGCCTGGCCCGTGGTTGGCATTTGGTTTACC
GCTTTGGGTATTAGTACTATGGCCTTTAACCTGAACGGCTTTAACTTTAACCAAAGCGTGGTTGATTCTCAGGGTCGTGTGA
TTAATACCTGGGCTGACATTATTAATCGGGCCAACTTAGGGATGGAAGTTATGCATGAACGCAATGCCCACAACTTTCCCT
TGGATTTAGCTGCCGTGGAAGCCCCCTCCACCAATGGCTAAttccttggtgtaatgccaactgaataatctgcaaattgcactctccttcaatgg
ggggtgctttttgcttgactgagtaatcttctgattgctgatcttgattgccatcgatcgccggggagtccggggcagttaccattagagagtctagagaattaatc
catcttcgatagaggaattctccccaaagcctagaccgaaatggggtaaagtaggcaaggtagaatggtttctgcgcccggatttttacccaaattaagctttgc
acgcctttgcatttaactaaggagaatttATGTTGACCCTGAAACTGTTTGTGTACACTGTGGTTATTTTCTTTGTTTCCTTGTTTATTTT
TGGCTTTTTGAGTAACGATCCCGGCCGGAACCCCGGTCGCGAAGAATAAgctttagcccaaaattcttccttctctccctagactaattttg
gtgccaagggtagattggaacctgattactctcccccaccggagagttttttgtcactggcgtta**gagacc**aaa

Complete sequence of the synthetic construct RC2

Optimized coding sequences of *A. thaliana AtpsbEFLJ, AtpsbB, AtpsbT* and *AtpsbH* genes are indicated in capital letters.

ttt**ggtctc**ttatggcggctcacaaaatagtagactagactctacttgctttgcatttgtcagtcaatgttgttttgaaaaattgaaggagaacacaaaATGTCT
GGGTCCACTGGGGAACGGTCTTTTGCCGATATTATTACCTCCATTCGCTACTGGGTTATTCACAGCATTACTATTCCCTCTCT
GTTTATTGCCGGGTGGTTGTTTGTGAGCACCGGATTAGCTTATGATGTTTTTGGTTCTCCCCGGCCCAATGAATACTTTACC
GAAAGTCGCCAAGGCATTCCCCTGATTACTGGTCGTTTTGATCCCTTGGAACAGTTAGACGAATTTTCCCGGAGTTTTTAAa
acatttaattgttctttttagttggtaattaacaATGACTATTGACCGCACTTATCCCATTTTTACTGTTCGCTGGTTGGCTGTTCACGGG
CTGGCTGTTCCCACTGTTTCCTTTTTAGGGTCCATTAGTGCCATGCAATTTATTCAGCGGTAAgagtttttcATGACTCAATCCA
ATCCCAATGAACAATCTGTGGAACTGAACCGCACCTCTTTATACTGGGGTCTGCTGTTAATTTTTGTTTTAGCCGTGTTGTTT
TCCAATTATTTCTTTAACTAAacttttttaatacgcaatttaggaggcatggtATGGCCGATACCACTGGGCGGATTCCCTTGTGGGTGA
TTGGCACCGTTGCTGGTATTTTGGTGATTGGGTTAATTGGAATTTTCTTTTATGGTAGCTACTCCGGCCTGGGTTCCAGTTT
GTAAtcgagggctagccgccacacaatatcatggtacagcttgcagaaatcctggccgctcgttacaatccttcaaaatattctcactttgtaagggataatgg
ataaaacttgactctgtctgtcttgttcggttaacacaacctatagacaagggttttatttacccaacgcagaataaaaattaaaacgtctttaagacacaaaaca
ctattcgttactagaaggagcgtcaATGGGATTGCCCTGGTATCGCGTTCACACCGTGGTTTTAAATGACCCCGGACGTTTGCTGGC
TGTTCACATTATGCACACCGCCCTGGTGGCCGGGTGGGCTGGATCTATGGCCTTGTATGAATTAGCTGTTTTTGACCCCTCC
GATCCCGTGCTGGATCCCATGTGGCGCCAAGGGATGTTTGTGATTCCCTTTATGACCCGTTTGGGCATTACTAATAGTTGG
GGCGGTTGGAACATTACCGGGGGAACCATTACTAATCCCGGTTTATGGAGTTATGAAGGCGTTGCCGGTGCTCATATTGT

GTTTAGCGGGCTGTGTTTTCTGGCCGCTATTTGGCACTGGGTGTACTGGGACTTGGAAATCTTTTGTGATGAACGGACCGG
CAAACCCTCTCTGGATTTGCCCAAAATTTTTGGCATTCATTTATTTCTGTCCGGTGTTGCCTGTTTTGGGTTTGGAGCTTTTC
ACGTGACCGGTCTGTATGGCCCCGGTATTTGGGTTTCCGACCCCTACGGGTTGACTGGAAAAGTTCAACCCGTGAATCCCG
CCTGGGGCGTTGAAGGTTTTGATCCCTTTGTGCCCGGCGGTATTGCCAGTCATCACATTGCCGCTGGGACCTTAGGAATTC
TGGCCGGCTTGTTTCATTTAAGCGTGCGTCCCCCCCAGCGGCTGTATAAAGGGTTGCGGATGGGAAACATTGAAACCGTTT
TATCCAGTAGCATTGCCGCTGTGTTTTTCGCCGCTTTTGTGGTTGCCGGCACCATGTGGTACGGTAGTGCCACCACTCCCAT
TGAATTGTTTGGGCCCACTCGCTATCAATGGGATCAGGGATACTTTCAACAGGAAATTTATCGGCGCGTGTCCGCCGGCTT
GGCTGAAAATCAAAGTTTAAGCGAAGCCTGGGCTAAAATTCCCGAAAAATTGGCCTTTTACGATTACATTGGTAATAACCC
CGCCAAAGGGGGATTATTTCGTGCTGGGAGTATGGACAATGGGGATGGAATTGCCGTTGGCTGGTTAGGTCATCCCGTGT
TTCGTAACAAAGAAGGTCGGGAACTGTTTGTGCGTCGGATGCCCACCTTTTTCGAAACTTTTCCCGTGGTTTTAGTTGATGG
CGACGGTATTGTTCGGGCCGACGTGCCCTTTCGCCGTGCTGAAAGTAAATATAGCGTGGAACAAGTGGGCGTTACCGTGG
AATTTTACGGCGGTGAATTAAACGGTGTTTCTTATTCCGATCCCGCCACTGTGAAAAAATACGCCCGTCGGGCTCAGCTGG
GGGAAATTTTTGAATTAGACCGCGCCACCCTGAAATCTGATGGCGTGTTTCGCTCTTCCCCCCGTGGGTGGTTTACTTTTGG
ACACGCCAGCTTTGCTTTGTTGTTTTTCTTTGGCCATATTTGGCACGGTGCTCGTACCCTGTTTCGTGACGTGTTTGCCGGTA
TTGATCCCGACTTGGATGCCCAAGTTGAATTTGGGGCTTTTCAGAAATTAGGAGATCCCACCACTAAACGTCAAGCCGTGT
AAgtgcttcttgcacagcttttaaccacagcttaagagcgtgtttgaaaagcctccctggtcacccaagtttgggggggaaactaagtcaaagtcccccagcatcg
ggagatttagggagcagagtcagactttacaaacaggttctaagtcttgggagttatccctcataattcgagcccgcagtgtttggttcttggccaagtcggtcta
gttgtcaggggacaggggaatgtatagattagtgtgtaaggataaacttttaggaatttttttagattATGGAAGCCCTGGTGTATACCTTTTTGTTA
GTTTCCACTTTGGGCATTATTTTCTTTGCTATTTTCTTTCGGGAACCCCCCAAAATTAGTACCAAAAAATAAtccaattaaagggt
ctttttttccaggtgtttttttgcctggacactcccttaaaaccccagtttttacctctgtttcaaccgtgggctagcttgactttgactggggtaagattgatagttgtttc
tgttgtcttatattattacagaacattacaaaaactcatttagtcatttttacgggaagtctATGGCTACTCAGACCGTTGAAGATTCCTCTCGCAG
CGGCCCCCGTTCTACTACCGTTGGCAAACTGTTGAAACCCTTAAACTCCGAATATGGGAAAGTGGCCCCCGGCTGGGGTAC
CACTCCCTTAATGGGAGTGGCCATGGCTCTGTTTGCTGTTTTTCTGAGCATTATTTTGGAAATTTACAACTCCAGTGTGTTGT
TAGATGGTATTTCCGTTAACTAAtgggggggttgttgacatattcctgacccaatttaatcccaacttaattttggttaactttctttagatcccgccccgcc
gggatttttttgtcttatggagcataggggggccacaaactgtcattggctagtcagggtta**gagacc**aaa

Bibliography

Allen, J.F., de Paula, W.B.M., Puthiyaveetil, S., Nield, J., 2011. A structural phylogenetic map for chloroplast photosynthesis. Trends Plant Sci. 16, 645–655. doi:10.1016/j.tplants.2011.10.004

Amann, K., Lezhneva, L., Wanner, G., Herrmann, R.G., Meurer, J., 2004. ACCUMULATION OF PHOTOSYSTEM ONE1, a member of a novel gene family, is required for accumulation of [4Fe-4S] cluster-containing chloroplast complexes and antenna proteins. Plant Cell 16, 3084–3097. doi:10.1105/tpc.104.024935

Armbruster, U., Zühlke, J., Rengstl, B., Kreller, R., Makarenko, E., Rühle, T., Schünemann, D., Jahns, P., Weisshaar, B., Nickelsen, J., Leister, D., 2010. The Arabidopsis thylakoid protein PAM68 is required for efficient D1 biogenesis and photosystem II assembly. Plant Cell 22, 3439–60. doi:10.1105/tpc.110.077453

Aro, E.-M., Suorsa, M., Rokka, A., Allahverdiyeva, Y., Paakkarinen, V., Saleem, A., Battchikova, N., Rintamäki, E., 2005. Dynamics of photosystem II: a proteomic approach to thylakoid protein complexes. J. Exp. Bot. 56, 347–56. doi:10.1093/jxb/eri041

Aro, E.-M., Virgin, I., Andersson, B., 1993. Photoinhibition of Photosystem II. Inactivation, protein damage and turnover. Biochim. Biophys. Acta - Bioenerg. 1143, 113–134. doi:10.1016/0005-2728(93)90134-2

Asakura, Y., Galarneau, E., Watkins, K.P., Barkan, A., van Wijk, K.J., 2012. Chloroplast RH3 DEAD Box RNA Helicases in Maize and Arabidopsis Function in Splicing of Specific Group II Introns and Affect Chloroplast Ribosome Biogenesis. PLANT Physiol. 159, 961–974. doi:10.1104/pp.112.197525

Barber, J., Andersson, B., 1992. Too much of a good thing: light can be bad for photosynthesis. Trends Biochem. Sci. 17, 61–66.

Barkan, A., 1993. Nuclear Mutants of Maize with Defects in Chloroplast Polysome Assembly Have Altered Chloroplast RNA Metabolism. Plant Cell 5, 389 LP-402.

Barrangou, R., Fremaux, C., Deveau, H., Richards, M., Boyaval, P., Moineau, S., Romero, D.A., Horvath, P., 2007. CRISPR provides acquired resistance against viruses in prokaryotes. Science 315, 1709–1712. doi:10.1126/science.1138140

Bentley, F.K., Zurbriggen, A., Melis, A., 2014. Heterologous expression of the mevalonic acid pathway in cyanobacteria enhances endogenous carbon partitioning to isoprene. Mol. Plant 7, 71–86. doi:10.1093/mp/sst134

Bertani, G., 2004. Lysogeny at Mid-Twentieth Century: P1, P2, and Other Experimental Systems. J. Bacteriol. 186, 595–600. doi:10.1128/JB.186.3.595-600.2004

Bickle, T.A., Kruger, D.H., 1993. Biology of DNA restriction. Microbiol. Rev. 57, 434–450.

Blankenship, R.E., Tiede, D.M., Barber, J., Brudvig, G.W., Fleming, G., Ghirardi, M., Gunner, M.R., Junge, W., Kramer, D.M., Melis, A., Moore, T.A., Moser, C.C., Nocera, D.G., Nozik, A.J., Ort, D.R., Parson, W.W., Prince, R.C., Sayre, R.T., 2011. Comparing photosynthetic and photovoltaic efficiencies and recognizing the potential for improvement. Science 332, 805–9. doi:10.1126/science.1200165

Boehm, M., Romero, E., Reisinger, V., Yu, J., Komenda, J., Eichacker, L. a., Dekker, J.P., Nixon, P.J., 2011. Investigating the Early Stages of Photosystem II Assembly in *Synechocystis* sp. PCC 6803. J. Biol. Chem. 286, 14812–14819. doi:10.1074/jbc.M110.207944

Boehm, M., Yu, J., Reisinger, V., Beckova, M., Eichacker, L. a., Schlodder, E., Komenda, J., Nixon, P.J., 2012. Subunit

composition of CP43-less photosystem II complexes of Synechocystis sp. PCC 6803: implications for the assembly and repair of photosystem II. Philos. Trans. R. Soc. B Biol. Sci. 367, 3444–3454. doi:10.1098/rstb.2012.0066

Bolger, A.M., Lohse, M., Usadel, B., 2014. Trimmomatic: A flexible trimmer for Illumina sequence data. Bioinformatics 30, 2114–2120. doi:10.1093/bioinformatics/btu170

Bollenbach, T.J., Lange, H., Gutierrez, R., Erhardt, M., Stern, D.B., Gagliardi, D., 2005. RNR1, a 3'-5' exoribonuclease belonging to the RNR superfamily, catalyzes 3' maturation of chloroplast ribosomal RNAs in Arabidopsis thaliana. Nucleic Acids Res. 33, 2751–63. doi:10.1093/nar/gki576

Bricker, T.M., Roose, J.L., Fagerlund, R.D., Frankel, L.K., Eaton-Rye, J.J., 2012. The extrinsic proteins of Photosystem II. Biochim. Biophys. Acta - Bioenerg. 1817, 121–142. doi:10.1016/j.bbabio.2011.07.006

Brouns, S.J.J., Jore, M.M., Lundgren, M., Westra, E.R., Slijkhuis, R.J.H., Snijders, A.P.L., Dickman, M.J., Makarova, K.S., Koonin, E. V, van der Oost, J., 2008. Small CRISPR RNAs guide antiviral defense in prokaryotes. Science 321, 960–964. doi:10.1126/science.1159689

Cai, Y.P., Wolk, C.P., 1990. Use of a conditionally lethal gene in Anabaena sp. strain PCC 7120 to select for double recombinants and to entrap insertion sequences. J. Bacteriol. 172, 3138–3145.

Carpenter, S.D., Ohad, I., Vermaas, W.F., 1993. Analysis of chimeric spinach/cyanobacterial CP43 mutants of Synechocystis sp. PCC 6803: the chlorophyll-protein CP43 affects the water-splitting system of Photosystem II. Biochim. Biophys. Acta 1144, 204–212.

Caruthers, J.M., McKay, D.B., 2002. Helicase structure and mechanism. Curr. Opin. Struct. Biol. 12, 123–133. doi:10.1016/S0959-440X(02)00298-1

Chi, W., He, B., Mao, J., Li, Q., Ma, J., Ji, D., Zou, M., Zhang, L., 2012. The Function of RH22, a DEAD RNA Helicase, in the Biogenesis of the 50S Ribosomal Subunits of Arabidopsis Chloroplasts. PLANT Physiol. 158, 693–707. doi:10.1104/pp.111.186775

Chiaramonte, S., Giacometti, G.M., Bergantino, E., 1999. Construction and characterization of a functional mutant of Synechocystis 6803 harbouring a eukaryotic PSII-H subunit. Eur. J. Biochem. 260, 833–843.

Chisholm, D., Williams, J.G., 1988. Nucleotide sequence of psbC, the gene encoding the CP-43 chlorophyll a-binding protein of Photosystem II, in the cyanobacterium Synechocystis 6803. Plant Mol. Biol. 10, 293–301. doi:10.1007/BF00029879

Choquet, Y., Wostrikoff, K., Rimbault, B., Zito, F., Girard-Bascou, J., Drapier, D., Wollman, F.A., 2001. Assembly-controlled regulation of chloroplast gene translation. Biochem. Soc. Trans. 29, 421–426.

Christian, M., Qi, Y., Zhang, Y., Voytas, D.F., 2013. Targeted mutagenesis of Arabidopsis thaliana using engineered TAL effector nucleases. G3 (Bethesda). 3, 1697–1705. doi:10.1534/g3.113.007104

Cordin, O., Banroques, J., Tanner, N.K., Linder, P., 2006. The DEAD-box protein family of RNA helicases. Gene 367, 17–37. doi:10.1016/j.gene.2005.10.019

Crosatti, C., Rizza, F., Badeck, F.W., Mazzucotelli, E., Cattivelli, L., 2013. Harden the chloroplast to protect the plant. Physiol. Plant. 147, 55–63. doi:10.1111/j.1399-3054.2012.01689.x

DalCorso, G., Pesaresi, P., Masiero, S., Aseeva, E., Schünemann, D., Finazzi, G., Joliot, P., Barbato, R., Leister, D., 2008. A Complex Containing PGRL1 and PGR5 Is Involved in the Switch between Linear and Cyclic Electron Flow in Arabidopsis. Cell 132, 273–285. doi:10.1016/j.cell.2007.12.028

Dasgupta, J., Ananyev, G.M., Dismukes, G.C., 2008. Photoassembly of the Water-Oxidizing Complex in Photosystem II. Coord. Chem. Rev. 252, 347–360. doi:10.1016/j.ccr.2007.08.022

De Las Rivas, J., Barber, J., 2004. Analysis of the Structure of the PsbO Protein and its Implications. Photosynth. Res. 81, 329–343. doi:10.1023/B:PRES.0000036889.44048.e4

del Campo, E.M., 2009. Post-transcriptional control of chloroplast gene expression. Gene Regul. Syst. Bio. 3, 31–47.

Dillingham, M.S., Kowalczykowski, S.C., 2008. RecBCD enzyme and the repair of double-stranded DNA breaks. Microbiol. Mol. Biol. Rev. 72, 642–71, Table of Contents. doi:10.1128/MMBR.00020-08

Dovzhenko, A., Dal Bosco, C., Meurer, J., Koop, H.U., 2003. Efficient regeneration from cotyledon protoplasts in Arabidopsis thaliana. Protoplasma 222, 107–11. doi:10.1007/s00709-003-0011-9

Engler, C., Kandzia, R., Marillonnet, S., 2008. A one pot, one step, precision cloning method with high throughput capability. PLoS One 3, e3647. doi:10.1371/journal.pone.0003647

Estavillo, G.M., Crisp, P.A., Pornsiriwong, W., Wirtz, M., Collinge, D., Carrie, C., Giraud, E., Whelan, J., David, P., Javot, H., Brearley, C., Hell, R., Marin, E., Pogson, B.J., 2011. Evidence for a SAL1-PAP chloroplast retrograde pathway that functions in drought and high light signaling in Arabidopsis. Plant Cell 23, 3992–4012. doi:10.1105/tpc.111.091033

Feng, Z., Zhang, B., Ding, W., Liu, X., Yang, D.-L., Wei, P., Cao, F., Zhu, S., Zhang, F., Mao, Y., Zhu, J.-K., 2013. Efficient genome editing in plants using a CRISPR/Cas system. Cell Res. doi:10.1038/cr.2013.114

Ferreira, K.N., 2004. Architecture of the Photosynthetic Oxygen-Evolving Center. Science (80-.). 303, 1831–1838. doi:10.1126/science.1093087

Fraser, J.M., Tulk, S.E., Jeans, J.A., Campbell, D.A., Bibby, T.S., Cockshutt, A.M., 2013. Photophysiological and photosynthetic complex changes during iron starvation in Synechocystis sp. PCC 6803 and Synechococcus elongatus PCC 7942. PLoS One 8, e59861. doi:10.1371/journal.pone.0059861

Fristedt, R., Scharff, L.B., Clarke, C.A., Wang, Q., Lin, C., Merchant, S.S., Bock, R., 2014. RBF1, a plant homolog of the bacterial ribosome-binding factor RbfA, acts in processing of the chloroplast 16S ribosomal RNA. Plant Physiol. 164, 201–15. doi:10.1104/pp.113.228338

Gandini, C., 2017. Exploring Synechocystis PCC 6803 as a synthetic biology platform to study plant photosynthesis. LMU.

Giardine, B., Riemer, C., Hardison, R., Burthans, R., Elnitski, L., Shah, F., Zhang, Y., Blankenberg, D., Albert, I., Taylor, J., Miller, W., Kent, W., Nekrutenko, A., 2005. Galaxy: a platform for interactive large-scale genome analysis. Genome Res. 15, 1451–5.

Gimpel, J.A., Nour-Eldin, H.H., Scranton, M.A., Li, D., Mayfield, S.P., 2016. Refactoring the Six-Gene Photosystem II Core in the Chloroplast of the Green Algae Chlamydomonas reinhardtii. ACS Synth. Biol. 5, 589–596. doi:10.1021/acssynbio.5b00076

Gimpel, J. a., Nour-Eldin, H.H., Scranton, M. a., Li, D., Mayfield, S.P., 2015. Refactoring the Six-Gene Photosystem II Core in the Chloroplast of the Green Algae *Chlamydomonas reinhardtii*. ACS Synth. Biol. 150807083206003. doi:10.1021/acssynbio.5b00076

Gordon, B.R.G., Li, Y., Wang, L., Sintsova, A., van Bakel, H., Tian, S., Navarre, W.W., Xia, B., Liu, J., 2010. Lsr2 is a nucleoid-associated protein that targets AT-rich sequences and virulence genes in Mycobacterium

tuberculosis. Proc. Natl. Acad. Sci. U. S. A. 107, 5154–5159. doi:10.1073/pnas.0913551107

Green M.R. and Sambrook J., 2001. Molecular Cloning A LABORATORY MANUAL.

Gu, L., Xu, T., Lee, K., Lee, K.H., Kang, H., 2014. A chloroplast-localized DEAD-box RNA helicaseAtRH3 is essential for intron splicing and plays an important role in the growth and stress response in Arabidopsis thaliana. Plant Physiol. Biochem. PPB / Société Fr. Physiol. végétale 82, 309–18. doi:10.1016/j.plaphy.2014.07.006

Hajdukiewicz, P.T., Allison, L.A., Maliga, P., 1997. The two RNA polymerases encoded by the nuclear and the plastid compartments transcribe distinct groups of genes in tobacco plastids. EMBO J. 16, 4041–4048. doi:10.1093/emboj/16.13.4041

He, Q., Schlich, T., Paulsen, H., Vermaas, W., 1999. Expression of a higher plant light-harvesting chlorophyll a/b-binding protein in Synechocystis sp. PCC 6803. Eur. J. Biochem. 263, 561–570.

Herzel, H., Weiss, O., Trifonov, E.N., 1999. 10-11 bp periodicities in complete genomes reflect protein structure and DNA folding. Bioinformatics 15, 187–193.

Higo, A., Isu, A., Fukaya, Y., Hisabori, T., 2017. Designing Synthetic Flexible Gene Regulation Networks Using RNA Devices in Cyanobacteria. ACS Synth. Biol. 6, 55–61. doi:10.1021/acssynbio.6b00201

Huang, C.-K., Shen, Y.-L., Huang, L.-F., Wu, S.-J., Yeh, C.-H., Lu, C.-A., 2016a. The DEAD-Box RNA Helicase AtRH7/PRH75 Participates in Pre-rRNA Processing, Plant Development and Cold Tolerance in Arabidopsis. Plant Cell Physiol. 57, 174–91. doi:10.1093/pcp/pcv188

Huang, C.-K., Shen, Y.-L., Huang, L.-F., Wu, S.-J., Yeh, C.-H., Lu, C.-A., 2016b. The DEAD-Box RNA Helicase AtRH7/PRH75 Participates in Pre-rRNA Processing, Plant Development and Cold Tolerance in Arabidopsis. Plant Cell Physiol. 57, 174–91. doi:10.1093/pcp/pcv188

Ihnatowicz, A., Pesaresi, P., Varotto, C., Richly, E., Schneider, A., Jahns, P., Salamini, F., Leister, D., 2004. Mutants for photosystem I subunit D of Arabidopsis thaliana: effects on photosynthesis, photosystem I stability and expression of nuclear genes for chloroplast functions. Plant J. 37, 839–852. doi:10.1111/J.1365-313X.2004.02011.X

Jarmoskaite, I., Russell, R., 2011. DEAD-box proteins as RNA helicases and chaperones. Wiley Interdiscip. Rev. RNA 2, 135–152. doi:10.1002/wrna.50

Jarvis, P., Lopez-Juez, E., 2013. Biogenesis and homeostasis of chloroplasts and other plastids. Nat. Rev. Mol. Cell Biol. 14, 787–802. doi:10.1038/nrm3702

Jensen, P.E., Leister, D., 2014a. Cyanobacteria as an Experimental Platform for Modifying Bacterial and Plant Photosynthesis. Front. Bioeng. Biotechnol. 2, 1–4. doi:10.3389/fbioe.2014.00007

Jensen, P.E., Leister, D., 2014b. Chloroplast evolution, structure and functions. F1000Prime Rep. 6, 1–14. doi:10.12703/P6-40

Kaczanowska, M., Rydén-Aulin, M., 2007. Ribosome biogenesis and the translation process in Escherichia coli. Microbiol. Mol. Biol. Rev. 71, 477–494. doi:10.1128/MMBR.00013-07

Kakizaki, T., Matsumura, H., Nakayama, K., Che, F.-S., Terauchi, R., Inaba, T., 2009. Coordination of plastid protein import and nuclear gene expression by plastid-to-nucleus retrograde signaling. Plant Physiol. 151, 1339–1353. doi:10.1104/pp.109.145987

Kant, P., Kant, S., Gordon, M., Shaked, R., Barak, S., 2007. STRESS RESPONSE SUPPRESSOR1 and STRESS RESPONSE SUPPRESSOR2, two DEAD-box RNA helicases that attenuate Arabidopsis responses to multiple abiotic

stresses. Plant Physiol. 145, 814–830. doi:10.1104/pp.107.099895

Kim, C., Apel, K., 2013. Singlet oxygen-mediated signaling in plants: moving from flu to wild type reveals an increasing complexity. Photosynth. Res. 116, 455–464. doi:10.1007/s11120-013-9876-4

Kim, J.S., Kim, K.A., Oh, T.R., Park, C.M., Kang, H., 2008. Functional Characterization of DEAD-Box RNA Helicases in Arabidopsis thaliana under Abiotic Stress Conditions. Plant Cell Physiol. 49, 1563–1571. doi:10.1093/PCP/PCN125

Kindgren, P., Dubreuil, C., Strand, Å., 2015. The Recovery of Plastid Function Is Required for Optimal Response to Low Temperatures in Arabidopsis. PLoS One 10. doi:10.1371/journal.pone.0138010

Kleine, T., Maier, U.G., Leister, D., 2009. DNA transfer from organelles to the nucleus: the idiosyncratic genetics of endosymbiosis. Annu. Rev. Plant Biol. 60, 115–138. doi:10.1146/annurev.arplant.043008.092119

Kleinknecht, L., Wang, F., Stübe, R., Philippar, K., Nickelsen, J., Bohne, A.-V., 2014. RAP, the sole octotricopeptide repeat protein in Arabidopsis, is required for chloroplast 16S rRNA maturation. Plant Cell 26, 777–87. doi:10.1105/tpc.114.122853

Komenda, J., Reisinger, V., Müller, B.C., Dobáková, M., Granvogl, B., Eichacker, L.A., 2004. Accumulation of the D2 protein is a key regulatory step for assembly of the photosystem II reaction center complex in Synechocystis PCC 6803. J. Biol. Chem. 279, 48620–9. doi:10.1074/jbc.M405725200

Koussevitzky, S., Nott, A., Mockler, T.C., Hong, F., Sachetto-martins, G., Surpin, M., Lim, J., Mittler, R., Chory, J., 2007. Signals from Chloroplasts Converge to Regulate Nuclear Gene Expression.

Larkin, R.M., Alonso, J.M., Ecker, J.R., Chory, J., Martin, W., Herrmann, R.G., Rodermel, S., Surpin, M., Larkin, R.M., Chory, J., Mochizuki, N., Strand, Å., Reid, J.D., Hunter, C.N., Jensen, P.E., Gibson, L.C., Hunter, C.N., Shelnutt, J.A., Fidai, S., Dahl, J.A., Richards, W.R., Karger, G.A., Reid, J.D., Hunter, C.N., Guo, R., Luo, M., Weinstein, J.D., Falbel, T.G., Staehelin, L.A., Walker, C.J., Willows, R.D., Pöpperl, G., Oster, U., Rüdiger, W., Thomas, J., Weinstein, J.D., Jacobs, J.M., Jacobs, N.J., Terry, M.J., Wahleithner, J.A., Lagarias, J.C., Takamiya, K.I., Tsuchiya, T., Ohta, H., Konieczny, A., Ausubel, F.M., Goff, S.A., Emanuelsson, O., Nielsen, H., Heijne, G. von, 2003. GUN4, a regulator of chlorophyll synthesis and intracellular signaling. Science 299, 902–6. doi:10.1126/science.1079978

Lee, K., Kang, H., 2016. Emerging Roles of RNA-Binding Proteins in Plant Growth, Development, and Stress Responses. Mol. Cells 39, 179–185. doi:10.14348/molcells.2016.2359

Lehmann, R., Machne, R., Herzel, H., 2014. The structural code of cyanobacterial genomes. Nucleic Acids Res. 42, 8873–8883. doi:10.1093/nar/gku641

Leister, D., 2017. Experimental evolution in photoautotrophic microorganisms as a means of enhancing chloroplast functions. Essays Biochem. doi:10.1042/EBC20170010

Leister, D., 2012. How Can the Light Reactions of Photosynthesis be Improved in Plants? Front. Plant Sci. 3, 1–3. doi:10.3389/fpls.2012.00199

Leister, D., 2005. Origin, evolution and genetic effects of nuclear insertions of organelle DNA. Trends Genet. 21, 655–663. doi:10.1016/j.tig.2005.09.004

Li, D., Liu, H., Zhang, H., Wang, X., Song, F., 2008. OsBIRH1, a DEAD-box RNA helicase with functions in modulating defence responses against pathogen infection and oxidative stress. J. Exp. Bot. 59, 2133–46. doi:10.1093/jxb/ern072

Li, X., Henry, R., Yuan, J., Cline, K., Hoffman, N.E., 1995. A chloroplast homologue of the signal recognition particle subunit SRP54 is involved in the posttranslational integration of a protein into thylakoid membranes. Proc. Natl. Acad. Sci. U. S. A. 92, 3789–3793.

Lima, A., Lima, S., Wong, J.H., Phillips, R.S., Buchanan, B.B., Luan, S., 2006. A redox-active FKBP-type immunophilin functions in accumulation of the photosystem II supercomplex in Arabidopsis thaliana. Proc. Natl. Acad. Sci. U. S. A. 103, 12631–12636. doi:10.1073/pnas.0605452103

Liu, H.-Y., Nefsky, B.S., Walworth, N.C., 2002. The Ded1 DEAD box helicase interacts with Chk1 and Cdc2. J. Biol. Chem. 277, 2637–2643. doi:10.1074/jbc.M109016200

Liu, H., Zhang, H., Niedzwiedzki, D.M., Prado, M., He, G., Gross, M.L., Blankenship, R.E., 2013. Phycobilisomes supply excitations to both photosystems in a megacomplex in cyanobacteria. Science 342, 1104–1107. doi:10.1126/science.1242321

Liu, Y., Tabata, D., Imai, R., 2016. A Cold-Inducible DEAD-Box RNA Helicase from Arabidopsis thaliana Regulates Plant Growth and Development under Low Temperature. PLoS One 11, e0154040. doi:10.1371/journal.pone.0154040

Love, M.I., Huber, W., Anders, S., 2014. Moderated estimation of fold change and dispersion for RNA-seq data with DESeq2. Genome Biol. 15, 550. doi:10.1186/s13059-014-0550-8

Lovmar, M., Tenson, T., Ehrenberg, M., 2004. Kinetics of macrolide action: the josamycin and erythromycin cases. J. Biol. Chem. 279, 53506–53515. doi:10.1074/jbc.M401625200

Ma, J., Peng, L., Guo, J., Lu, Q., Lu, C., Zhang, L., 2007. LPA2 is required for efficient assembly of photosystem II in Arabidopsis thaliana. Plant Cell 19, 1980–1993. doi:10.1105/tpc.107.050526

Majeran, W., Friso, G., Asakura, Y., Qu, X., Huang, M., Ponnala, L., Watkins, K.P., Barkan, A., van Wijk, K.J., 2012. Nucleoid-Enriched Proteomes in Developing Plastids and Chloroplasts from Maize Leaves: A New Conceptual Framework for Nucleoid Functions. PLANT Physiol. 158, 156–189. doi:10.1104/pp.111.188474

Manavski, N., Torabi, S., Lezhneva, L., Arif, M.A., Frank, W., Meurer, J., 2015. HIGH CHLOROPHYLL FLUORESCENCE145 Binds to and Stabilizes the psaA 5' UTR via a Newly Defined Repeat Motif in Embryophyta. Plant Cell 27, 2600–2615. doi:10.1105/tpc.15.00234

Martin, W., Rujan, T., Richly, E., Hansen, A., Cornelsen, S., Lins, T., Leister, D., Stoebe, B., Hasegawa, M., Penny, D., 2002. Evolutionary analysis of Arabidopsis, cyanobacterial, and chloroplast genomes reveals plastid phylogeny and thousands of cyanobacterial genes in the nucleus. Proc. Natl. Acad. Sci. U. S. A. 99, 12246–12251. doi:10.1073/pnas.182432999

Martínez-García, J.F., Monte, E., Quail, P.H., 1999. A simple, rapid and quantitative method for preparing Arabidopsis protein extracts for immunoblot analysis. Plant J. 20, 251–257. doi:10.1046/j.1365-313x.1999.00579.x

Meurer, J., Schmid, L.-M., Stoppel, R., Leister, D., Brachmann, A., Manavski, N., 2017. PALE CRESS binds to plastid RNAs and facilitates the biogenesis of the 50S ribosomal subunit. Plant J. 92, 400–413. doi:10.1111/tpj.13662

Mingam, A., Toffano-Nioche, C., Brunaud, V., Boudet, N., Kreis, M., Lecharny, A., 2004. DEAD-box RNA helicases in Arabidopsis thaliana: establishing a link between quantitative expression, gene structure and evolution of a family of genes. Plant Biotechnol. J. 2, 401–15. doi:10.1111/j.1467-7652.2004.00084.x

Monro, R.E., Marcker, K.A., 1967. Ribosome-catalysed reaction of puromycin with a formylmethionine-

containing oligonucleotide. J. Mol. Biol. 25, 347–350.

Moore, M., Harrison, M.S., Peterson, E.C., Henry, R., 2000. Chloroplast Oxa1p homolog albino3 is required for post-translational integration of the light harvesting chlorophyll-binding protein into thylakoid membranes. J. Biol. Chem. 275, 1529–1532.

Mrazek, J., 2010. Comparative analysis of sequence periodicity among prokaryotic genomes points to differences in nucleoid structure and a relationship to gene expression. J. Bacteriol. 192, 3763–3772. doi:10.1128/JB.00149-10

Mulo, P., Sakurai, I., Aro, E.M., 2012. Strategies for psbA gene expression in cyanobacteria, green algae and higher plants: From transcription to PSII repair. Biochim. Biophys. Acta - Bioenerg. 1817, 247–257. doi:10.1016/j.bbabio.2011.04.011

Mulo, P., Sicora, C., Aro, E.-M., 2009. Cyanobacterial psbA gene family: optimization of oxygenic photosynthesis. Cell. Mol. Life Sci. 66, 3697–3710. doi:10.1007/s00018-009-0103-6

Murakami, A., Kim, S.J., Fujita, Y., 1997. Changes in photosystem stoichiometry in response to environmental conditions for cell growth observed with the cyanophyte Synechocystis PCC 6714. Plant Cell Physiol. 38, 392–397.

Ng, A.H., Berla, B.M., Pakrasi, H.B., 2015. Fine-Tuning of Photoautotrophic Protein Production by Combining Promoters and Neutral Sites in the Cyanobacterium Synechocystis sp. Strain PCC 6803. Appl. Environ. Microbiol. 81, 6857–6863. doi:10.1128/AEM.01349-15

Nickelsen, J., Rengstl, B., 2013. Photosystem II Assembly: From Cyanobacteria to Plants. Annu. Rev. Plant Biol. 64, 609–635. doi:10.1146/annurev-arplant-050312-120124

Nishimura, K., Ashida, H., Ogawa, T., Yokota, A., 2010. A DEAD box protein is required for formation of a hidden break in Arabidopsis chloroplast 23S rRNA. Plant J. 63, 766–777. doi:10.1111/j.1365-313X.2010.04276.x

Nixon, P.J., Michoux, F., Yu, J., Boehm, M., Komenda, J., 2010. Recent advances in understanding the assembly and repair of photosystem II. Ann. Bot. 106, 1–16. doi:10.1093/aob/mcq059

Nixon, P.J., Rögner, M., Diner, B. a, 1991. Expression of a higher plant psbA gene in Synechocystis 6803 yields a functional hybrid photosystem II reaction center complex. Plant Cell 3, 383–395. doi:10.1105/tpc.3.4.383

Nott, A., Jung, H.-S., Koussevitzky, S., Chory, J., 2006. Plastid-to-nucleus retrograde signaling. Annu. Rev. Plant Biol. 57, 739–759. doi:10.1146/annurev.arplant.57.032905.105310

Obayashi, T., Hayashi, S., Saeki, M., Ohta, H., Kinoshita, K., 2009. ATTED-II provides coexpressed gene networks for Arabidopsis. Nucleic Acids Res. 37, D987-91. doi:10.1093/nar/gkn807

Obayashi, T., Kinoshita, K., Nakai, K., Shibaoka, M., Hayashi, S., Saeki, M., Shibata, D., Saito, K., Ohta, H., 2007. ATTED-II: a database of co-expressed genes and cis elements for identifying co-regulated gene groups in Arabidopsis. Nucleic Acids Res. 35, D863-9. doi:10.1093/nar/gkl783

Olinares, P.D.B., Ponnala, L., van Wijk, K.J., 2010. Megadalton complexes in the chloroplast stroma of Arabidopsis thaliana characterized by size exclusion chromatography, mass spectrometry, and hierarchical clustering. Mol. Cell. Proteomics 9, 1594–615. doi:10.1074/mcp.M000038-MCP201

Ort, D.R., Merchant, S.S., Alric, J., Barkan, A., Blankenship, R.E., Bock, R., Croce, R., Hanson, M.R., Hibberd, J.M., Long, S.P., Moore, T.A., Moroney, J., Niyogi, K.K., Parry, M.A.J., Peralta-Yahya, P.P., Prince, R.C., Redding, K.E., Spalding, M.H., van Wijk, K.J., Vermaas, W.F.J., von Caemmerer, S., Weber, A.P.M., Yeates, T.O., Yuan,

J.S., Zhu, X.G., 2015. Redesigning photosynthesis to sustainably meet global food and bioenergy demand. Proc. Natl. Acad. Sci. 112, 201424031. doi:10.1073/pnas.1424031112

Owttrim, G.W., 2006. RNA helicases and abiotic stress. Nucleic Acids Res. 34, 3220–3230. doi:10.1093/nar/gkl408

Pakrasi, H.B., Williams, J.G., Arntzen, C.J., 1988. Targeted mutagenesis of the psbE and psbF genes blocks photosynthetic electron transport: evidence for a functional role of cytochrome b559 in photosystem II. EMBO J. 7, 325.

Pause, A., Sonenberg, N., 1992. Mutational analysis of a DEAD box RNA helicase: the mammalian translation initiation factor eIF-4A. EMBO J. 11, 2643–2654.

Pesaresi, P., Hertle, A., Pribil, M., Kleine, T., Wagner, R., Strissel, H., Ihnatowicz, A., Bonardi, V., Scharfenberg, M., Schneider, A., Pfannschmidt, T., Leister, D., 2009. Arabidopsis STN7 kinase provides a link between short- and long-term photosynthetic acclimation. Plant Cell 21, 2402–23. doi:10.1105/tpc.108.064964

Pesaresi, P., Masiero, S., Eubel, H., Braun, H.-P., Bhushan, S., Glaser, E., Salamini, F., Leister, D., 2006. Nuclear photosynthetic gene expression is synergistically modulated by rates of protein synthesis in chloroplasts and mitochondria. Plant Cell 18, 970–91. doi:10.1105/tpc.105.039073

Pesaresi, P., Schneider, A., Kleine, T., Leister, D., 2007. Interorganellar communication. Curr. Opin. Plant Biol. 10, 600–606. doi:10.1016/j.pbi.2007.07.007

Pesaresi, P., Varotto, C., Meurer, J., Jahns, P., Salamini, F., Leister, D., 2001. Knock-out of the plastid ribosomal protein L11 in Arabidopsis: effects on mRNA translation and photosynthesis. Plant J. 27, 179–189. doi:10.1046/j.1365-313x.2001.01076.x

Pfalz, J., Liere, K., Kandlbinder, A., Dietz, K.-J., Oelmuller, R., 2006. pTAC2, -6, and -12 are components of the transcriptionally active plastid chromosome that are required for plastid gene expression. Plant Cell 18, 176–197. doi:10.1105/tpc.105.036392

Pfannschmidt, T., Schutze, K., Fey, V., Sherameti, I., Oelmuller, R., 2003. Chloroplast redox control of nuclear gene expression--a new class of plastid signals in interorganellar communication. Antioxid. Redox Signal. 5, 95–101. doi:10.1089/152308603321223586

Pinto, F., Pacheco, C.C., Oliveira, P., Montagud, A., Landels, A., Couto, N., Wright, P.C., Urchueguia, J.F., Tamagnini, P., 2015. Improving a Synechocystis-based photoautotrophic chassis through systematic genome mapping and validation of neutral sites. DNA Res. 22, 425–437. doi:10.1093/dnares/dsv024

Pogson, B.J., Woo, N.S., Forster, B., Small, I.D., 2008. Plastid signalling to the nucleus and beyond. Trends Plant Sci. 13, 602–609. doi:10.1016/j.tplants.2008.08.008

Powikrowska, M., Oetke, S., Jensen, P.E., Krupinska, K., 2014. Dynamic composition, shaping and organization of plastid nucleoids. Front. Plant Sci. 5, 424. doi:10.3389/fpls.2014.00424

Ramel, F., Mialoundama, A.S., Havaux, M., 2013. Nonenzymic carotenoid oxidation and photooxidative stress signalling in plants. J. Exp. Bot. 64, 799–805. doi:10.1093/jxb/ers223

Rippka, R., Deruelles, J., Waterbury, J.B., Herdman, M., Stanier, R.Y., 1979. Generic assignments, strain histories and properties of pure cultures of cyano- bacteria. Journal of General Microbiology 11: 1-61. J. Gen. Microbiol. 11, 1–61.

Rocak, S., Linder, P., 2004. DEAD-box proteins: the driving forces behind RNA metabolism. Nat. Rev. Mol. Cell Biol. 5, 232–41. doi:10.1038/nrm1335

Rogalski, M., Schottler, M.A., Thiele, W., Schulze, W.X., Bock, R., 2008. Rpl33, a nonessential plastid-encoded ribosomal protein in tobacco, is required under cold stress conditions. Plant Cell 20, 2221–2237. doi:10.1105/tpc.108.060392

Rohs, R., West, S.M., Liu, P., Honig, B., 2009. Nuance in the double-helix and its role in protein-DNA recognition. Curr. Opin. Struct. Biol. 19, 171–177. doi:10.1016/j.sbi.2009.03.002

Rokka, A., Suorsa, M., Saleem, A., Battchikova, N., Aro, E.-M., 2005. Synthesis and assembly of thylakoid protein complexes: multiple assembly steps of photosystem II. Biochem. J. 388, 159–168. doi:10.1042/BJ20042098

Romani, I., Tadini, L., Rossi, F., Masiero, S., Pribil, M., Jahns, P., Kater, M., Leister, D., Pesaresi, P., 2012. Versatile roles of Arabidopsis plastid ribosomal proteins in plant growth and development. Plant J. 72, 922–934. doi:10.1111/tpj.12000

Rosso, M.G., Li, Y., Strizhov, N., Reiss, B., Dekker, K., Weisshaar, B., 2003. An Arabidopsis thaliana T-DNA mutagenized population (GABI-Kat) for flanking sequence tag-based reverse genetics. Plant Mol. Biol. 53, 247–59. doi:10.1023/B:PLAN.0000009297.37235.4a

Rühle, T., Leister, D., 2015. Photosystem II Assembly from Scratch. Front. Plant Sci. 6, 1234. doi:10.3389/fpls.2015.01234

Sakai, A., Takano, H., Kuroiwa, T., 2004. Organelle nuclei in higher plants: structure, composition, function, and evolution. Int. Rev. Cytol. 238, 59–118. doi:10.1016/S0074-7696(04)38002-2

Schagger, H., von Jagow, G., 1987. Tricine-sodium dodecyl sulfate-polyacrylamide gel electrophoresis for the separation of proteins in the range from 1 to 100 kDa. Anal. Biochem. 166, 368–379.

Shajani, Z., Sykes, M.T., Williamson, J.R., 2011. Assembly of bacterial ribosomes. Annu. Rev. Biochem. 80, 501–26. doi:10.1146/annurev-biochem-062608-160432

Silverman, E., Edwalds-Gilbert, G., Lin, R.-J., 2003. DExD/H-box proteins and their partners: helping RNA helicases unwind. Gene 312, 1–16. doi:10.1016/S0378-1119(03)00626-7

Stengel, A., Gu, I.L., Hilger, D., Rengstl, B., Jung, H., 2012. Initial Steps of Photosystem II de Novo Assembly and Preloading with Manganese Take Place in Biogenesis Centers in Synechocystis 24, 660–675. doi:10.1105/tpc.111.093914

Stensjo, K., Vavitsas, K., Tyystjarvi, T., 2017. Harnessing transcription for bioproduction in cyanobacteria. Physiol. Plant. doi:10.1111/ppl.12606

Stoppel, R., Manavski, N., Schein, A., Schuster, G., Teubner, M., Schmitz-Linneweber, C., Meurer, J., 2012. RHON1 is a novel ribonucleic acid-binding protein that supports RNase e function in the Arabidopsis chloroplast. Nucleic Acids Res. 40, 8593–8606. doi:10.1093/nar/gks613

Suck, R., Zeltz, P., Falk, J., Acker, A., Kossel, H., Krupinska, K., 1996. Transcriptionally active chromosomes (TACs) of barley chloroplasts contain the alpha-subunit of plastome-encoded RNA polymerase. Curr. Genet. 30, 515–521.

Sugimoto, I., Takahashi, Y., 2003. Evidence that the PsbK polypeptide is associated with the photosystem II core antenna complex CP43. J. Biol. Chem. 278, 45004–45010. doi:10.1074/jbc.M307537200

Sun, X., Ouyang, M., Guo, J., Ma, J., Lu, C., Adam, Z., Zhang, L., 2010. The thylakoid protease Deg1 is involved in photosystem-II assembly in Arabidopsis thaliana. Plant J. 62, 240–249. doi:10.1111/j.1365-313X.2010.04140.x

Sun, X., Xu, D., Liu, Z., Kleine, T., Leister, D., 2016. Functional relationship between mTERF4 and GUN1 in retrograde signaling. J. Exp. Bot. 67, 3909–24. doi:10.1093/jxb/erv525

Svensson, J.T., Crosatti, C., Campoli, C., Bassi, R., Stanca, A.M., Close, T.J., Cattivelli, L., 2006. Transcriptome Analysis of Cold Acclimation in Barley Albina and Xantha Mutants. Plant Physiol. 141, 257–270. doi:10.1104/PP.105.072645

Tadini, L., Pesaresi, P., Kleine, T., Rossi, F., Guljamow, A., Sommer, F., Mühlhaus, T., Schroda, M., Masiero, S., Pribil, M., Rothbart, M., Hedtke, B., Grimm, B., Leister, D., 2016. GUN1 Controls Accumulation of the Plastid Ribosomal Protein S1 at the Protein Level and Interacts with Proteins Involved in Plastid Protein Homeostasis. Plant Physiol. 170, 1817–30. doi:10.1104/pp.15.02033

Tenson, T., Lovmar, M., Ehrenberg, M., 2003. The mechanism of action of macrolides, lincosamides and streptogramin B reveals the nascent peptide exit path in the ribosome. J. Mol. Biol. 330, 1005–1014.

Tikkanen, M., Nurmi, M., Kangasjarvi, S., Aro, E.-M., 2008. Core protein phosphorylation facilitates the repair of photodamaged photosystem II at high light. Biochim. Biophys. Acta 1777, 1432–1437. doi:10.1016/j.bbabio.2008.08.004

Tiller, N., Weingartner, M., Thiele, W., Maximova, E., Schöttler, M.A., Bock, R., 2012. The plastid-specific ribosomal proteins of Arabidopsis thaliana can be divided into non-essential proteins and genuine ribosomal proteins. Plant J. 69, 302–316. doi:10.1111/j.1365-313X.2011.04791.x

Tillett, D., Neilan, B.A., 2000. XANTHOGENATE NUCLEIC ACID ISOLATION FROM CULTURED AND ENVIRONMENTAL CYANOBACTERIA 258, 251–258.

Tompkins, R.K., 1970. Sequential translation of trinucleotide codons for peptide bond formation, translocation, and termination. Proc. Natl. Acad. Sci. U. S. A. 66, 1164–1169.

Umena, Y., Kawakami, K., Shen, J.-R., Kamiya, N., 2011. Crystal structure of oxygen-evolving photosystem II at a resolution of 1.9 Å. Nature 473, 55–60. doi:10.1038/nature09913

Vamvaka, E., 2016. Metabolic engineering of Synechocystis sp. PCC6803 for plant type pigment production, and identification of new splicing factors in Arabidopsis thaliana.

Vashisht, A.A., Tuteja, N., 2006. Stress responsive DEAD-box helicases: A new pathway to engineer plant stress tolerance. J. Photochem. Photobiol. B Biol. 84, 150–160. doi:10.1016/j.jphotobiol.2006.02.010

Vasu, K., Nagaraja, V., 2013. Diverse functions of restriction-modification systems in addition to cellular defense. Microbiol. Mol. Biol. Rev. 77, 53–72. doi:10.1128/MMBR.00044-12

Vinti, G., Hills, A., Campbell, S., Bowyer, J.R., Mochizuki, N., Chory, J., López-Juez, E., 2000. Interactions between hy1 and gun mutants of Arabidopsis, and their implications for plastid/nuclear signalling. Plant J. 24, 883–94.

Viola, S., 2014. Expression of higher plant photosynthetic proteins in the cyanobacterium Synechocystis sp. PCC 6803.

Viola, S., Ruhle, T., Leister, D., 2014. A single vector-based strategy for marker-less gene replacement in Synechocystis sp. PCC 6803. Microb. Cell Fact. 13, 4. doi:10.1186/1475-2859-13-4

Wang, D., Qu, Z., Adelson, D.L., Zhu, J.-K., Timmis, J.N., 2014. Transcription of nuclear organellar DNA in a model plant system. Genome Biol. Evol. doi:10.1093/gbe/evu111

Wang, S., Bai, G., Wang, S., Yang, L., Yang, F., Wang, Y., Zhu, J.-K., Hua, J., 2016. Chloroplast RNA-Binding Protein

RBD1 Promotes Chilling Tolerance through 23S rRNA Processing in Arabidopsis. PLoS Genet. 12, e1006027. doi:10.1371/journal.pgen.1006027

Wang, Y., Duby, G., Purnelle, B., Boutry, M., 2000. Tobacco VDL gene encodes a plastid DEAD box RNA helicase and is involved in chloroplast differentiation and plant morphogenesis. Plant Cell 12, 2129–42.

Wiegard, A., Dorrich, A.K., Deinzer, H.-T., Beck, C., Wilde, A., Holtzendorff, J., Axmann, I.M., 2013. Biochemical analysis of three putative KaiC clock proteins from Synechocystis sp. PCC 6803 suggests their functional divergence. Microbiology 159, 948–958. doi:10.1099/mic.0.065425-0

Williams, J.G.K.B.T.-M. in E., 1988. [85] Construction of specific mutations in photosystem II photosynthetic reaction center by genetic engineering methods in Synechocystis 6803, in: Cyanobacteria. Academic Press, pp. 766–778. doi:https://doi.org/10.1016/0076-6879(88)67088-1

Wilson, D.N., 2009. The A-Z of bacterial translation inhibitors. Crit. Rev. Biochem. Mol. Biol. 44, 393–433. doi:10.3109/10409230903307311

Woodson, J.D., Perez-Ruiz, J.M., Chory, J., 2011. Heme synthesis by plastid ferrochelatase I regulates nuclear gene expression in plants. Curr. Biol. 21, 897–903. doi:10.1016/j.cub.2011.04.004

Woodson, J.D., Perez-Ruiz, J.M., Schmitz, R.J., Ecker, J.R., Chory, J., 2013. Sigma factor-mediated plastid retrograde signals control nuclear gene expression. Plant J. 73, 1–13. doi:10.1111/tpj.12011

Wu, W., Liu, S., Ruwe, H., Zhang, D., Melonek, J., Zhu, Y., Hu, X., Gusewski, S., Yin, P., Small, I.D., Howell, K.A., Huang, J., 2016. SOT1, a pentatricopeptide repeat protein with a small MutS-related domain, is required for correct processing of plastid 23S-4.5S rRNA precursors in *Arabidopsis thaliana*. Plant J. 85, 607–621. doi:10.1111/tpj.13126

Xiao, Y., Savchenko, T., Baidoo, E.E.K., Chehab, W.E., Hayden, D.M., Tolstikov, V., Corwin, J.A., Kliebenstein, D.J., Keasling, J.D., Dehesh, K., 2012. Retrograde signaling by the plastidial metabolite MEcPP regulates expression of nuclear stress-response genes. Cell 149, 1525–1535. doi:10.1016/j.cell.2012.04.038

Xu, H., Vavilin, D., Vermaas, W., 2001. Chlorophyll b can serve as the major pigment in functional photosystem II complexes of cyanobacteria. Proc. Natl. Acad. Sci. U. S. A. 98, 14168–14173. doi:10.1073/pnas.251530298

Yalovsky, S., Paulsen, H., Michaeli, D., Chitnis, P.R., Nechushtai, R., 1992. Involvement of a chloroplast HSP70 heat shock protein in the integration of a protein (light-harvesting complex protein precursor) into the thylakoid membrane. Proc. Natl. Acad. Sci. U. S. A. 89, 5616–5619.

Yin, T., Pan, G., Liu, H., Wu, J., Li, Y., Zhao, Z., Fu, T., Zhou, Y., 2012. The chloroplast ribosomal protein L21 gene is essential for plastid development and embryogenesis in Arabidopsis . Planta 235, 907–921. doi:10.1007/s00425-011-1547-0

Yu, F., Liu, X., Alsheikh, M., Park, S., Rodermel, S., 2008. Mutations in SUPPRESSOR OF VARIEGATION1, a factor required for normal chloroplast translation, suppress var2-mediated leaf variegation in Arabidopsis. Plant Cell 20, 1786–1804. doi:10.1105/tpc.107.054965

Yu, J., Wu, Q., Mao, H., Zhao, N., Vermaas, W.F., 1999. Effects of chlorophyll availability on phycobilisomes in Synechocystis sp. PCC 6803. IUBMB Life 48, 625–630. doi:10.1080/713803568

Yu, J.J., Vermaas, W.F.J., 1990. Transcript Levels and Synthesis of Photosystem-Ii Components in Cyanobacterial Mutants with Inactivated Photosystem-Ii Genes. Plant Cell 2, 315–322.

Yu, Q., Lutz, K.A., Maliga, P., 2017. Efficient Plastid Transformation in Arabidopsis. Plant Physiol. 175, 186–193.

doi:10.1104/pp.17.00857

Zhang, J., Yuan, H., Yang, Y., Fish, T., Lyi, S.M., Thannhauser, T.W., Zhang, L., Li, L., 2016. Plastid ribosomal protein S5 is involved in photosynthesis, plant development, and cold stress tolerance in Arabidopsis. J. Exp. Bot. 67, 2731–2744. doi:10.1093/jxb/erw106

Zhang, L., Paakkarinen, V., van Wijk, K.J., Aro, E.M., 1999. Co-translational assembly of the D1 protein into photosystem II. J. Biol. Chem. 274, 16062–16067.

Zhu, X.-G., Long, S.P., Ort, D.R., 2010. Improving Photosynthetic Efficiency for Greater Yield. Annu. Rev. Plant Biol. 61, 235–261. doi:10.1146/annurev-arplant-042809-112206

Acknowledgment

I would like to thank Prof. Dr. Dario Leister for giving me the opportunity and the funding to accomplish my Ph.D. in his research group and for involving me in this project.

I gratefully acknowledge the funding received towards my PhD from the Foundation Edmund Mach with a 4 years Ph.D. scholarship and the possibility to work in its institute for 1 year.

I would also like to thank the GRK2062, the graduate school of Synthetic Biology, for its support during the lasts years of my Ph.D. and for giving me the opportunity to get to know motivating researchers from different research field.

Thanks to Prof. Dr. Jörg Nickelsen for taking over the “Zweitgutachter”.

Thanks to Belen, Toni, Marcel, Luca, Chiara, Kayo and Thilo for the comments and corrections of my PhD thesis and my defense presentation.

Thanks to all the people in the lab, for the nice working environment, for the support in the good and in the bad moments and for the time spent together inside and outside the lab.

Thanks to Luca, for the help in the lab and with the paper and for always being ready to help and share.

Thanks to Nicola, for being a funny and supportive friend and colleague and for following me around Europe.

Thanks to Chiara, Marcel, Bennet, Simon and Lisa Marie for being great colleagues and friends. It was nice to work with you and I am happy that we are still sharing moments together outside the lab.

Thanks to my friends Erika and Cristina, for a life lasting friendship and for always being next to me even if we are far away.

I would like to thank Anne and Eugenia for the friendship, for the everyday support and for making my life here in Munich special.

Thanks to Leo for the energy, the positivity and the love that you bring every day into my life.

A special thanks to my family for everything, for being always at my side and for believing in me.

Curriculum vitae

Personal details

Name: Francesca Paieri

Date of birth: 08 June 1987

Place of birth: Milan

Nationality: Italian

Education

October 2006 – December 2010

Bachelor degree in Industrial and Environmental Biotechnology. Final grade: 101/110

Università degli studi di Milano (Milan, Italy)

October 2010 – April 2012

Master degree in Molecular Biology and Bio-Informatic Technology. Final grade: 108/110

Università degli studi di Milano (Milan, Italy)

June 2013 – June 2017

PhD Scholarship, from Fondazione S. Michele all'Adige TN, Italy

Research experience

September 2010 –December 2010

Bachelor thesis: "Isolation of Cyt P450 mutant in *Arabidopsis thaliana*"

Supervisor: Prof. Dr. Carlo Soave, Università degli studi di Milano (Milan, Italy)

January 2011 – February 2011

Internship in biology at the Royal Holloway University of London (London, United Kingdom)

Supervisor: Dr. Alessandra Devoto

June 2011 – April 2012

Master thesis: “Involvement of cytochrome P450 enzymes in the iron-deficiency response in plants”

Supervisor: Dr. Irene Murgia, Università degli studi di Milano (Milan, Italy)

July 2012 – October 2012

Internship in Molecular biology at the Ludwig-Maximilians Universität (LMU, München, Germany)

Supervisor: Dr. Tatjana Kleine

Publications

Leister D, Romani I, Mittermayr L, Paieri F, Fenino E, Kleine T. (2014) “Identification of target genes and transcription factors implicated in translation dependent retrograde signaling in Arabidopsis” Mol Plant. ; 7(7): 1228-47

 # Paieri F*, Tadini L*, Manavski N*, Kleine T, Morandini P, Pesaresi P, Meurer J and Leister D. (2018) “The DEAD-box RNA Helicase RH50 Is a 23S-4.5S rRNA Maturation Factor that Functionally Overlaps with the Plastid Signaling Factor GUN1” Plant Physiol. 176(1): 634–648

publications related to this dissertation

* authors contributed equally

Declaration / Eidesstattliche Erklärung

Ich versichere hiermit an Eides statt, dass die vorgelegte Dissertation von mir selbständig und ohne unerlaubte Hilfe angefertigt ist.

München, den 09.09.2018

Francesca Paieri

Erklärung

Hiermit erkläre ich, *

☒ dass die Dissertation nicht ganz oder in wesentlichen Teilen einer anderen Prüfungskommission vorgelegt worden ist.

☒ dass ich mich anderweitig einer Doktorprüfung ohne Erfolg nicht unterzogen habe.

☐ dass ich mich mit Erfolg der Doktorprüfung im Hauptfach ..... und in den Nebenfächern ..... bei der Fakultät für ..... der .....

(Hochschule/Universität)

unterzogen habe.

☐ dass ich ohne Erfolg versucht habe, eine Dissertation einzureichen oder mich der Doktorprüfung zu unterziehen.

München, den 09-09-2018

Francesca Paieri

*) Nichtzutreffendes streichen